Tumor targeting using $\alpha_v\beta_3$ integrin binding peptides and peptidomimetics: synthesis and biological evaluation

Ingrid Dijkgraaf

Tumor targeting using $\alpha_v\beta_3$ integrin binding peptides and peptidomimetics: synthesis and biological evaluation; thesis, Radboud University Nijmegen, The Netherlands

The work described in this thesis was performed at the Department of Nuclear Medicine (Prof. dr. F.H.M. Corstens), Radboud University Nijmegen Medical Centre, Nijmegen, The Netherlands and the Department of Medicinal Chemistry and Chemical Biology (Prof. dr. R.M.J. Liskamp), Utrecht Institute for Pharmaceutical Sciences, Utrecht University, The Netherlands.
The research was financially supported by a grant (KUN 2002-2744) from the Dutch Cancer Society (KWF Kankerbestrijding).

ISBN: 978-90-9021544-0

Coverdesign: Vasco Veenbergen
Layout: Dia Hopmans, Scriptura, Nijmegen
Printed by: Drukkerij Quickprint B.V., Nijmegen

Publication of this thesis was financially supported by the Dutch Cancer Society.

Tumor targeting using $\alpha_v\beta_3$ integrin binding peptides and peptidomimetics: synthesis and biological evaluation

Een wetenschappelijke proeve op het gebied van de Medische Wetenschappen

Proefschrift

ter verkrijging van de graad van doctor
aan de Radboud Universiteit Nijmegen
op gezag van de rector magnificus prof. dr. C.W.P.M. Blom,
volgens besluit van het College van Decanen
in het openbaar te verdedigen op
donderdag 22 maart 2007
des namiddags om 1.30 uur precies

door

Ingrid Dijkgraaf

geboren op 22 mei 1979
te Epe

Promotores:
prof. dr. F.H.M. Corstens
prof. dr. R.M.J. Liskamp (Universiteit Utrecht)
prof. dr. W.J.G. Oyen

Copromotor:
dr. O.C. Boerman

Manuscriptcommissie:
prof. dr. J.H.J.M. van Krieken
prof. dr. F.P.J.T. Rutjes
prof. dr. J.A. Schalken

Table of contents

Table of contents

Outline of the thesis

Outline of the thesis

Radiolabeled peptides have become very important in nuclear medicine for tumor diagnosis and therapy. The specific receptor binding property of the peptide can be exploited by labeling the peptide with a radionuclide and using the radiolabeled peptide as a vehicle to guide the radioactivity to the tissues expressing a particular receptor. **Chapter 1** provides an overview of peptides, receptors, and therapy.

Radiolabeled RGD peptides can be used to visualize and quantify $\alpha_v\beta_3$ expression non-invasively. The aim of this thesis was to develop improved radiolabeled ligands for $\alpha_v\beta_3$ expressing tumors. In this thesis, the in vivo targeting properties of $\alpha_v\beta_3$ binding ligands were optimized by:

Synthesis of new $\alpha_v\beta_3$ targeting analogs

In **chapter 2**, the synthesis of a cyclic RGD peptide, a cyclic peptoid-peptide hybrid in which the arginine residue is replaced by the corresponding peptoid residue, an all-peptoid in which all the amino acid residues are replaced by their corresponding peptoid residues, and a peptidomimetic $\alpha_v\beta_3$ receptor antagonist is described. After the radiolabeling of these compounds with ^{111}In, the stability, in vitro and in vivo $\alpha_v\beta_3$ binding characteristics were systematically studied.

Multimerization

To develop improved tracers for $\alpha_v\beta_3$ targeting, we aimed to increase the affinity of the peptide by multimerization. In **chapter 3**, the $\alpha_v\beta_3$ binding characteristics of an ^{111}In-labeled monomeric, dimeric, and tetrameric RGD analog were compared. In addition, **chapter 4** describes the design, synthesis and in vitro evaluation of a series of $\alpha_v\beta_3$ integrin-directed c(RGDfK) containing dendrimers.

Linker variation

The effect of modification of the linker between the dimeric RGD peptide and the DOTA chelator on the in vitro and in vivo characteristics was systematically investigated in **chapter 5**.

A new application of one of the $\alpha_v\beta_3$ binding ligands is described in **chapter 6**. In this chapter, the tumor targeting potential of an ^{111}In-labeled cyclic RGD peptide in athymic BALB/c nude mice with intraperitoneally growing NIH:OVCAR-3 ovarian carcinoma tumors was studied. In addition, the therapeutic potential of the ^{177}Lu-labeled cyclic RGD peptide was investigated.

Chapter 7 provides a summary and general discussion.

Chapter 1

General introduction

General introduction

During the past decade, radiolabeled receptor binding peptides have emerged as an important class of radiopharmaceuticals for tumor diagnosis and therapy. The specific receptor binding property of the ligand can be exploited by labeling the ligand with a radionuclide and using the radiolabeled ligand as a vehicle to guide the radioactivity to the tissues expressing a particular receptor. The concept of using radiolabeled receptor binding peptides to target receptor expressing tissues in vivo has stimulated a large body of research in nuclear medicine. Small peptides for receptor imaging and targeted radiotherapy have some advantages over proteins, antibodies, and antibody fragments. Peptides are small molecules and show rapid diffusion in target tissue. They clear rapidly from the blood and non-target tissues, resulting in high tumor-to-background ratios. Furthermore, peptides have a low toxicity and generally they are not immunogenic.

Apart from planar imaging, single photon emission computed tomography (SPECT) and positron emission tomography (PET) are the two main imaging modalities in nuclear medicine. SPECT requires compounds labeled with single photon emitters or so-called gamma emitters. Commonly used gamma emitters are: ^{123}I, ^{111}In, and ^{99m}Tc. Receptor binding peptides labeled with gamma emitters can be used to non-invasively visualize receptor expressing tissues, a technique referred to as peptide-receptor radionuclide imaging (PRRI). To date, the ^{111}In-labeled somatostatin analog octreotide (OctreoScan®) is the most successful radiopeptide for tumor imaging and has been the first that was approved for diagnostic use. ^{111}In-octreotide is considered the gold standard for imaging several types of neuroendocrine tumors. Receptor targeting with other peptides such as cholecystokinin (CCK) analogs, bombesin, substance P, neurotensin, glucagon-like peptide 1 (GLP-1), and RGD peptides are currently under development or undergoing clinical trials.

Compared to SPECT, PET has a higher spatial resolution and the possibility to more accurately quantitate the uptake in tumor and in normal organs. For PET imaging, peptides are radiolabeled with positron-emitting radionuclides such as ^{18}F, ^{68}Ga, ^{64}Cu, ^{86}Y, ^{89}Zr, and ^{124}I. Peptide-receptor radionuclide therapy (PRRT) can be used to treat cancers. For this purpose, peptides with specific affinity for tumor-associated receptors on cancer cells are radiolabeled with cytotoxic, β-emitting radionuclides like ^{131}I, ^{90}Y, ^{188}Re, and ^{177}Lu. Here we discuss the criteria for peptide ligand development, the selection of radioisotopes and of chelators, including various chemical aspects of radiopeptide development. In addition, the current state of clinical use of radiopeptides for diagnosis and therapy of tumors is discussed.

Regulatory peptides and their receptors

Regulatory peptides are potent small messenger molecules binding to specific receptors. Physiologically, these regulatory peptides are very potent molecules and usually they are not larger than 40 amino acids. Regulatory peptides are synthesized mainly in the brain and the digestive tract. Due to their relatively small size, they are able to rapidly penetrate almost any tissue, except the brain.

Because of the hydrophilicity of regulatory peptides, the blood-brain barrier is non-permeable for these peptides. Therefore, the central nervous system and the periphery (e.g., the digestive tract) form two independent regulatory systems that can use the same messenger molecules without any danger of confusing interaction of both [1, 2, 3]. All regulatory peptides bind to and act through transmembrane G-protein-coupled receptors. The signal transduction of these receptors is triggered by the binding of the respective peptide to the extracellular domain of the receptor, which in turn, activates the intracellular guanine nucleotide binding proteins (G-proteins).

Regulatory peptides influence many aspects of mammalian physiology. Their role as flexible messenger molecules requires rapid degradation in the blood to prevent prolonged action of secreted peptides. Due to ubiquitously occurring peptidases, most regulatory peptides are rapidly degraded. The application of (radio)peptides as (radio)pharmaceutical may therefore be hampered by enzymatic degradation since the half-life of most peptides is relatively short and in some cases too short to reach the target tissue in sufficient quantities. Therefore, most peptides have to be modified to prevent rapid enzymatic degradation [4, 5].

Application of peptides as radiopharmaceuticals

The ideal peptide-based radiopharmaceutical should have a high in vivo stability, high uptake in tumors, low uptake in non-target tissues, and rapid clearance from the blood preferably via the kidneys [6]. It is obvious that the peptide should preserve its receptor binding affinity and biological activity during the radiolabeling procedure. Peptide-based radiopharmaceuticals offer some advantages over antibodies and proteins, like rapid clearance from blood and non-target tissues, rapid penetration into tumor tissue, toleration of harsh conditions of chemical modifications or radiolabeling, low toxicity, and low immunogenicity. As described above, the application of peptides can be hampered by the limited in vivo stability of the peptide. To overcome the enzymatic degradation of peptides, several methods of inhibiting proteolysis of peptides have been developed. These methods commonly used include: substitution of L-amino acids by D-amino acids, substitution of peptide bonds, insertion of unusual amino acids or side chains, amidation, cyclization, and use of peptidomimetics. Cyclization of peptides results not only in resistance to enzymatic degradation, it could also lead to conformationally more constrained compounds with enhanced receptor affinity and biological activity [4, 7].

As stated above, the preferred route of clearance of a peptide-based radiopharmaceutical is via the kidneys. For rapid renal excretion, hydrophilicity is required as lipophilic peptides are cleared via the hepatobiliary route. As a result, lipophilic peptide-based radiopharmaceuticals will show a higher background activity in the abdomen and slow clearance, possibly masking tumors in the abdomen, making them less suitable for diagnostic and therapeutic purposes. The route and rate of excretion of peptides can be modified by introduction of specific hydrophilic or lipophilic amino acids into the peptide chain [8]. Peptides can also be modified by linking them to polyethylene

glycol (PEG) chains, a technique called PEGylation. PEG is a hydrophilic polymer which is non-toxic and non-immunogenic. In general, by PEGylation peptides become more hydrophilic and are less susceptible to enzymatic degradation. In addition, PEGylation could enhance the circulatory half-life of a peptide [9, 10].

Another method to improve the pharmacokinetics of a peptide is glycosylation. The attachment of carbohydrates enhances the hydrophilicity of a peptide, resulting in reduced hepatobiliary uptake, enhanced urinary excretion, and reduced non-specific binding [11]. However, modification of a peptide by for example PEGylation, glycosylation or conjugation to a chelator, could also affect the affinity of a peptide for the receptor.

Radiolabeling of peptides

For the radiolabeling of peptides, the radiolabeling procedure should not affect the receptor binding affinity of the peptide. Various techniques have been developed that enable efficient labeling of peptides with radionuclides such as ^{123}I, ^{99m}Tc, ^{111}In, ^{64}Cu, ^{18}F, and $^{66/67/68}$Ga (Table 1).

Table 1. Half-life and decay type of several radionuclides. Half-life is given in hours, unless stated otherwise.

	Isotope	Half-life (h)	Decay type
γ-emitter	^{99m}Tc	6.02	IT
	^{111}In	67.2	EC, γ
	^{123}I	13.0	EC, γ, e^-
β^+-emitter	^{18}F	1.83	β^+, EC
	^{11}C	20.4 min	β^+, EC, γ
	^{15}O	122 s	β^+,
	^{13}N	10.0 min	β^+,
	^{64}Cu	12.9	β^-, EC
	^{68}Ga	1.14	β^+, EC
	^{124}I	76.8	EC, β^+, γ
β-emitter	^{90}Y	64.1	β^-
	^{177}Lu	161	β^-
	^{186}Re	91	β^-, EC, γ
	^{188}Re	17.0	β^-
	^{131}I	192	β^-, γ, e^-
α-emitter	^{211}At	7.21	α
	^{212}Bi	1.01	β^-, α
	^{213}Bi	45.6 min	β^-, α
	^{225}Ac	10 d	α

α = alpha decay, β^- = negative beta decay, β^+ = positive beta decay, γ = gamma transition, IT = isometric transition, EC = electron capture.

Radioiodination

Radioiodination of peptides with ^{125}I, ^{123}I, or ^{131}I can be performed by either direct labeling or indirect labeling via an auxiliary group [8]. During direct radioiodination, radioactive iodine is incorporated covalently into the side chains of tyrosyl or histidyl residues in the presence of an oxidizing agent such as chloramine-T or iodogen. If no tyrosyl or histidyl residue is available, free amino groups in the peptide may be radioiodinated by auxiliary groups, including *N*-succinimidyl-3-(4-hydroxyphenyl)propionate, known as Bolton-Hunter reagent [12]. Other auxiliary groups for radioiodination of peptides are *N*-succinimidyl-3-iodobenzoate (SIB) and *N*-succinimidyl-5-iodo-3-pyridinecarboxylate (SIPC) (Figure 1) [13-15].

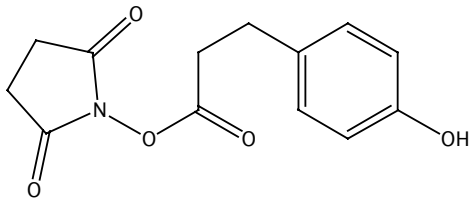

N-succinimidyl-3-(4-hydroxyphenyl)propionate
Bolton-Hunter reagent

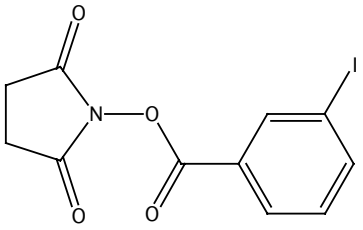

N-succinimidyl-3-iodobenzoate (SIB)

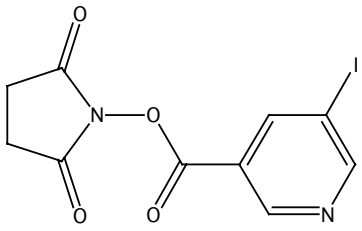

N-succinimidyl-5-iodo-3-pyridinecarboxylate (SIPC)

Figure 1. The auxiliary groups Bolton-Hunter reagent, SIB, and SIPC for the radioiodination of peptides.

A major drawback of radioiodinated peptides is that upon internalization and lysosomal degradation, the radioiodinated amino acid residues will be rapidly excreted out of the cell. This so-called non-residualizing property of iodine results in reduced tumor-to-background ratios. In contrast to radioiodinated amino acids, radiometal labeled amino acids are trapped in the lysosomes as no metabolic transport pathway exists for the processing and transport of these molecules. These residualizing labels will show enhanced retention in tumor cells following internalization. Recently, the residualizing radioiodine labels dilactitol-tyramine (DLT) and DTPA-appended peptide moieties have been developed to increase the tumor uptake of radioiodinated targeting vehicles. In nude mice with human lung tumor xenografts, antibodies labeled with these residualizing iodine labels showed superior tumor-to-non-tumor ratios. In addition, the therapeutic efficacy of these radioiodinated antibodies was significantly improved compared to the conventional ^{131}I-labeled antibody [16, 17, 18]. To our knowledge, this concept has not been applied to receptor binding peptides yet.

Labeling of peptides with radiometals

Radiolabeling of peptides with metals such as ^{111}In or ^{177}Lu is performed by conjugating peptides with bifunctional chelators (BFCs) that complex free metal ions. Several acyclic and cyclic bifunctional chelators have been developed for both diagnostic and therapeutic applications (Figure 2). The most widely used chelators are diethylenetriaminepentaacetic acid (DTPA) and 1,4,7,10-tetraazacyclododecane-N',N'',N''',N''''-tetraacetic acid (DOTA) or derivatives thereof. For diagnostic purposes, DTPA chelates ^{111}In with sufficient stability. This DTPA chelator is used in the commercially available somatostatin analog OctreoScan®. For therapeutic purposes, the DTPA chelator is not suited as the ^{90}Y- and ^{177}Lu-DTPA complex is not stable in vivo over longer time. Some substituted DTPA analogs such as 2-(4-Isothiocyanatobenzyl)-diethylenetriaminepentaacetic acid (*p*-SCN-Bn-DTPA) have been synthesized showing improved in vivo stability [19]. In contrast, the macrocyclic chelator DOTA provides sufficient stability for a broad range of metallic radionuclides, like ^{90}Y, $^{67/68}$Ga, ^{177}Lu, or ^{212}Pb [20, 21]. A stable radiometal-chelator complex is particularly required for therapeutic applications. The macrocyclic DOTA chelator is the most frequently used chelator for peptide-receptor radionuclide therapy (PRRT). A major drawback of the use of DOTA is that high labeling efficiencies require heating during the labeling procedure, which could affect the structure and receptor binding properties of the peptide.

Other chelators such as 1,4,7-triazacyclononane-N,N',N''-triacetic acid (NOTA) and 1,4,8,11-tetraazacyclotetradecane-1,4,8,11-tetraacetic acid (TETA) and derivatives of these have been developed. For example, Prata et al. demonstrated the high in vivo stability of NOTA and its derivative 1,4,7-triazacyclononane-N,N',N'''-tris(methylenephosphonate-monoethylester) (NOTPME) complexed with $^{67}Ga^{3+}$ [22]. In addition, for copper radionuclides TETA has been extensively used. However, Anderson et al. showed the dissociation of ^{64}Cu from TETA-D-Phe^{1}-octreotide resulting in subsequent binding of ^{64}Cu to superoxide dismutase (SOD) [23]. Furthermore, DeNardo and coworkers reported the transfer of ^{67}Cu from a TETA derivative to ceruloplasmin [24]. To overcome

this problem, Boswell et al. developed a "cross-bridged" TETA derivative, which proved to have significant potential for labeling copper radionuclides to biological molecules for diagnostic imaging and targeted radiotherapy [25].

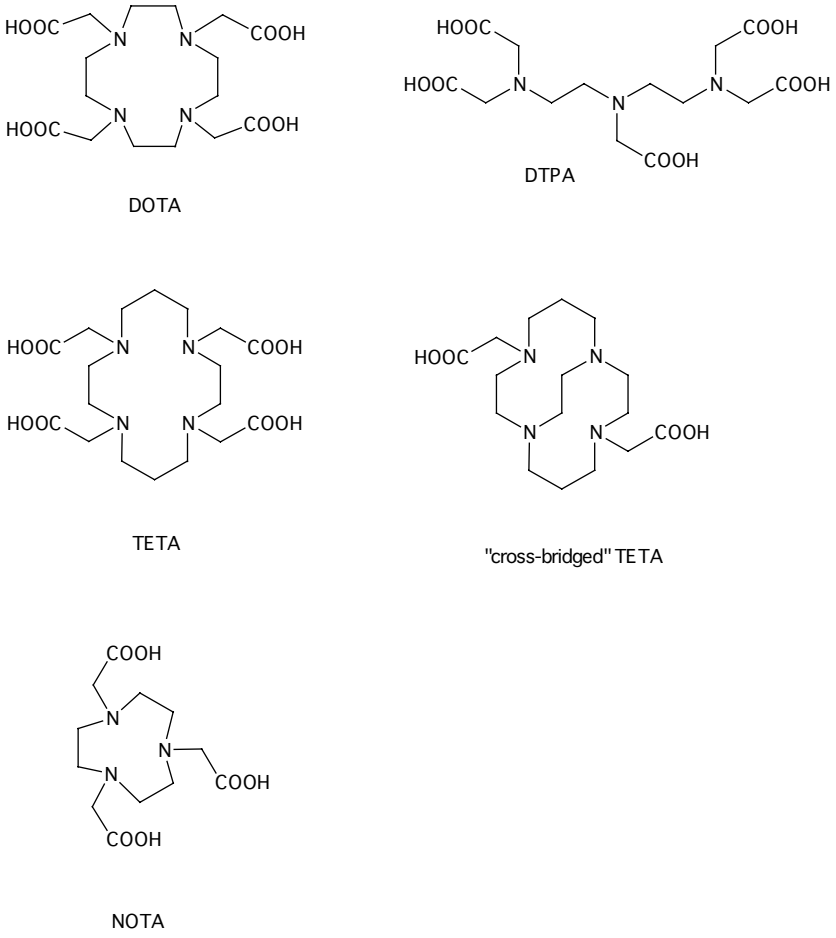

Figure 2. Structural formula of different chelators for radiolabeling of peptides.

Radiolabeling of peptides with ^{99m}Tc

Nowadays there is considerable interest in labeling peptides with ^{99m}Tc for nuclear medicine imaging because of the excellent chemical and imaging characteristics of this radionuclide. Three main methods for radiolabeling peptides with ^{99m}Tc can be distinguished: (I) direct labeling, (II) preformed chelate approach, and (III) indirect labeling using a bifunctional coupling agent (BCA) [26, 27]. The direct labeling approach uses a reducing agent to convert the cystine disulfide bridges of a peptide into free cysteine thiols, which are able to efficiently bind ^{99m}Tc. However, this method applies only to peptides and proteins with disulfide bonds. More importantly, these bonds are

often critical for maintaining the biological and receptor binding properties of the peptide. In the preformed chelate approach, first a complex of ^{99m}Tc with a BCA is formed. In a second step the ^{99m}Tc-BCA complex is conjugated to a peptide. However, a two-step radiochemical synthesis is not optimal for routine clinical applications. In the indirect labeling approach, first the BCA is attached to the peptide to form a BCA-peptide conjugate. Secondly, the conjugate is labeled with ^{99m}Tc either by reduction of $^{99m}TcO_4^-$ or indirectly by ligand exchange with an intermediate ^{99m}Tc-complex, such as ^{99m}Tc-glucoheptonate, ^{99m}Tc-diphosphonate, or ^{99m}Tc-tricine. A variety of BCAs has been developed including MAG_3 [28, 29, 30], MAG_2 [31], HYNIC [32, 33], DADT [34], EC [35], and tetraamine [36]. Succinimidyl-hydrazinonicotinamide (S-HYNIC) as developed by Abrams and coworkers [37] appears to be an ideal BCA for ^{99m}Tc-labeling, because it allows rapid and efficient labeling of peptides and proteins even at room temperature. In addition, the HYNIC-^{99m}Tc complex is very stable in vivo, especially when used in combination with the proper coligands such as ethylenediaminediacetic acid (EDDA), tricine, and nicotinic acid.

Radiolabeling of peptides with ^{18}F

For radiolabeling of peptides with ^{18}F, an auxiliary group is necessary. *N*-succinimidyl-4-^{18}F fluorobenzoate ([^{18}F]SFB) is a very suitable ^{18}F-labeling agent (Figure 3). However, the efficiency of the labeling is low. Several improvements in the synthesis of [^{18}F]SFB have been achieved, including reduced synthesis time and increased radiochemical yield [38, 39, 40, 41, 42]. Recently, a high-yield two-step radiohalogenation method via chemoselective oxime formation between an aminooxy-functionalized peptide and a radiohalogenated aldehyde or ketone was developed. This method offers new perspectives for large-scale radiofluorination of bioactive peptides [43, 44].

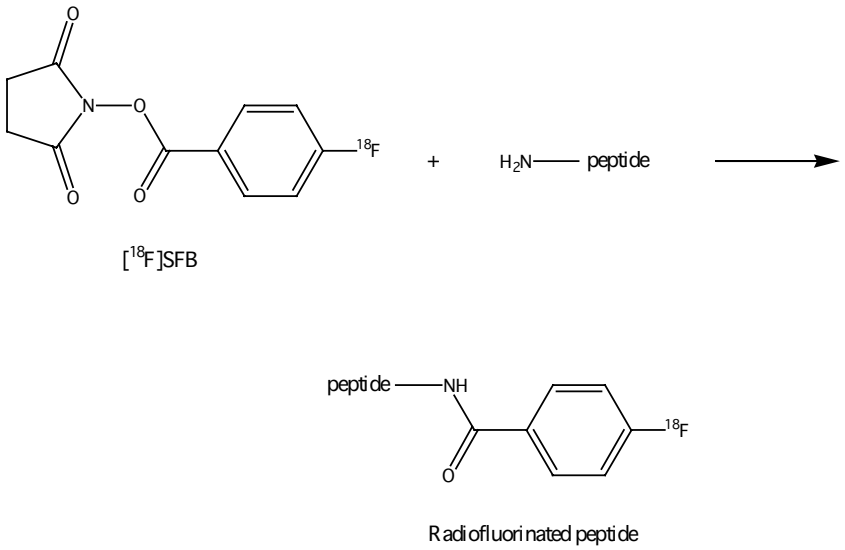

Figure 3. Radiolabeling of peptides with ^{18}F using [^{18}F]SFB.

Peptides for peptide receptor radionuclide imaging and therapy

Somatostatins

Natural somatostatin is a cyclic 14 amino acid, which was discovered in 1973. The amino acids 7-11 and the cyclic structure of this peptide are required for receptor binding. In the central nervous system, somatostatin acts as a neurotransmitter and this peptide can inhibit the release of growth hormone, insulin, glucagon, and gastrin [45]. Somatostatin receptors are expressed in most neuroendocrine tumors, in neuroblastomas, in some medullary thyroid cancers (MTC), in small cell lung carcinoma (SCLC), and in many other cancers. Five subtypes of human somatostatin receptors (hSSTR) have been identified [46] and natural somatostatin has a high affinity for all these subtypes. However, somatostatin-14 has a very short biological half-life due to enzymatic degradation, which limits targeting of SST receptor expressing tissues in vivo. By rational design, the somatostatin analog octreotide with enhanced stability towards enzymatic degradation was developed. For radioiodination of this 8 amino acid peptide, phenylalanine in position 3 was replaced by a tyrosyl residue. The resulting ^{123}I-Tyr^3-octreotide was the first radiopeptide used for imaging of neuroendocrine tumors (NET) in a patient [47]. However, this compound cleared mainly via the hepatobiliary route and its complicated radioiodination method hampered its wide spread clinical application. By N-terminal conjugation of octreotide to the chelator DTPA, the so-called "pentreotide" was developed. DTPA conjugation enabled radiolabeling with ^{111}In, which allows a simpler labeling method compared to labeling with ^{123}I and results in a residualizing label. Furthermore, in contrast to ^{123}I-Tyr^3-octreotide, ^{111}In-DTPA-D-Phe^1-octreotide is mainly cleared via the kidneys, making interpretation of scintigraphic images of the upper abdomen easier [48]. ^{111}In-DTPA-D-Phe^1-octreotide became the first peptide-based radiopharmaceutical that has obtained regulatory approval in Europe and the United States [4, 49]. These days, ^{111}In-DTPA-D-Phe^1-octreotide or trade named OctreoScan® is commercially available as a kit.

Since the chelator DTPA is not suitable for labeling with radionuclides such as ^{90}Y and ^{177}Lu, because of in vivo instability, DOTA-conjugated somatostatin analogs were developed which ensure better stability of the radiometal-peptide complex over time. Labeled with ^{90}Y or ^{111}In, DOTA-D-Phe^1-Tyr^3-octreotide showed a more favorable biodistribution and tumor uptake in animal models compared to ^{111}In-DTPA-D-Phe^1-octreotide (Figure 4) [50, 51, 52]. Their clinical application has been tested in several studies [53, 54, 55].

Another promising somatostatin analog is ^{99m}Tc-HYNIC-D-Phe^1-Tyr^3-octreotide, which was first developed by the group in Basel [56]. This ^{99m}Tc-labeled somatostatin analog showed favorable detection capabilities of extrahepatic lesions as compared to ^{111}In-DTPA-D-Phe^1-octreotide. The patterns of accumulation of ^{99m}Tc-HYNIC-D-Phe^1-Tyr^3-octreotide in tumors and normal organs were comparable to those of ^{111}In-DTPA-D-Phe^1-octreotide. Further clinical studies are necessary to definitively determine whether this interesting compound may be able to replace ^{111}In-labeled somatostatin analogs in clinical routine [56, 57].

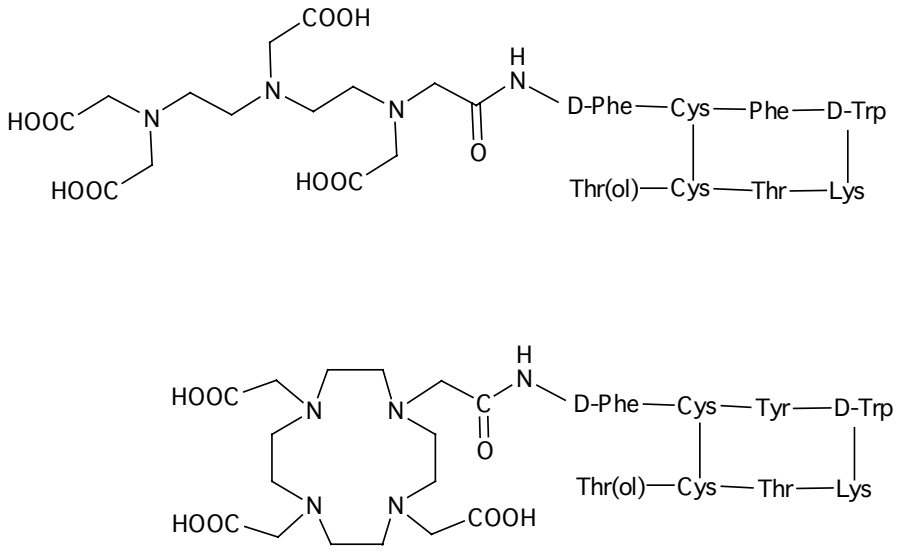

Figure 4. Structural formulas of DTPA-D-Phe^1-octreotide (top) and DOTA-D-Phe^1-Tyr^3-octreotide (DOTATOC) (bottom).

For the development of somatostatin analogs suitable for PET imaging, several studies have been performed. For example, several ^{64}Cu-labeled somatostatin analogs have been developed and these compounds demonstrated favorable results in animal models [58, 59]. ^{64}Cu-TETA-octreotide appeared to be a promising radiopharmaceutical for PET imaging of patients with neuroendrocrine tumors [60]. ^{18}F-labeled octreotide was successfully synthesized by Wester et al., however, this compound showed a fast tumor washout and high liver uptake. As a result, visualization of abdominal tumors was hampered and therefore its clinical application was limited [61]. Recently, a glycosylated ^{18}F-labeled somatostatin analog, N^{α}-(1-deoxy-D-fructosyl)-N^{ε}-(2-[^{18}F]fluoropropionyl)-Lys^0-Tyr^3-octreotate (Gluc-Lys([^{18}F]FP)-TOCA showed promising results in an animal model [62]. In patients with SSTR-positive tumors, PET with Gluc-Lys([^{18}F]FP)-TOCA allowed fast, high-contrast imaging of these tumors. The diagnostic performance of Gluc-Lys([^{18}F]FP)-TOCA was clearly superior to that of ^{111}In-DTPA-octreotide [63].

^{68}Ga is another interesting radionuclide for PET imaging, because it is available from an inhouse ^{68}Ge/^{68}Ga generator and therefore PET centers are not dependent on a cyclotron. Hofmann et al. evaluated ^{68}Ga-DOTA-D-Phe^1-Tyr^3-octreotide (^{68}Ga-DOTATOC) in patients [64]. This PET radiopharmaceutical appeared to be promising for imaging SSTR-positive tumors. Compared to ^{111}In-DTPA-octreotide, ^{68}Ga-DOTATOC seems to be favorable especially in detecting tumors with a low SSTR expression and small tumors [65]. Another somatostatin-based radiotracer with a high affinity for sstr2 and sstr5 is ^{68}GA-DOTA-1-Nal^3-octreotide (^{68}Ga-DOTANOC) [66]. It was shown that ^{68}Ga-DOTANOC is a good tracer for primary diagnostic and follow-up investigations in patients with suspected or proven somatostatin receptor-positive tumors.

Cholecystokinin/gastrin

The cholecystokinin (CCK) receptor is expressed on a variety of tumors [67]. CCK receptors can be distinguished pharmacologically by their affinity for gastrin, a 33 amino acid peptide hormone involved in gastric motility [68]. The CCK_1 (or formerly CCK-A) receptor has a low affinity for gastrin, whereas the CCK_2 (or formerly CCK-B) receptor has a high affinity for gastrin. Medullary thyroid carcinomas, small cell lung cancers, astrocytomas, and stromal ovarian cancers frequently express CCK_2 receptors. The expression of CCK_1 receptors in normal tissues in humans is quite restricted. CCK_1 receptors are found in gastroenteropancreatic tumors, meningiomas, and neuroblastoma [67].

Several radiolabeled gastrin analogs have been developed and their potential for targeted diagnostic imaging and radionuclide therapy of CCK_2 receptor expressing tumors have been investigated. For example, Behr et al. showed favorable results for the diagnostic and therapeutic application of ^{131}I-radioiodinated human gastrin-I [69]. In addition, Reubi et al. developed a series of non-sulfated CCK analogs, which were conjugated with DTPA or DOTA at the N-terminus [70]. Two of these analogs had a high affinity for the CCK_2 receptor and a low affinity for the CCK_1 receptor. In rats, one of these analogs conjugated with either DTPA or DOTA specifically localized in CCK_2 receptor expressing tumors [71]. However, in medullary thyroid cancer patients this CCK analog had a relatively low uptake in the strong CCK receptor-positive stomach and small lesions could not be detected [72]. First clinical studies using ^{111}In-DTPA-D-Glu^1-minigastrin, showed that this CCK analog can visualize metastatic MTC with high sensitivity [73, 74].

Bombesin

Bombesin, a 14 amino acid neuropeptide, has a high affinity for the human gastrin-releasing peptide receptor (GRP). These receptors are expressed in various types of cancer, such as colon cancer, glioblastoma, prostate cancer, and small cell lung cancer [2]. In analogy with the clinical usefulness of somatostatin receptor targeting [75, 76, 77], the use of radiolabeled bombesin analogs for GRP targeting has been explored. For example, in mice a ^{99m}Tc-labeled bombesin analog – demobesin - showed rapid background clearance and high and prolonged localization in PC-3 human prostate cancer xenografts [78]. In addition, an ^{111}In-labeled DTPA-bombesin analog appeared to be a promising radioligand for scintigraphy of GRP receptor expressing tumors. Phase I studies in patients with invasive prostate carcinoma are currently being undertaken [79]. However, the loss of bombesin receptors upon dedifferentiation of prostate cancer cells from androgen-controlled to androgen-independent growth may hamper clinical utility [80].

Substance P

Substance P is an 11 amino acid neuropeptide that plays an important role in a variety of processes, such as pain perception and cross-links in the neurocrine network through neurokinin 1 and 2 receptors. Receptors for substance P are mainly expressed in breast cancer, MTC, SCLC, and in brain tumors, such as astrocytoma and glioblastoma [81]. So far, no visualization of tumors

after intravenous application of radiolabeled substance P has been reported. Severe side-effects could occur after injection of substance P [82] and intravenous application is not tolerated well by patients. However, local application into tumor tissue does not cause these problems. ^{90}Y-labeled substance P has been used for intracavitary therapy of high grade gliomas [83].

GLP-1

The glucagon-like peptide 1 (GLP-1) receptor is overexpressed in nearly all insulinomas and gastrinomas. In addition, this receptor is expressed in a large number of intestinal and bronchial carcinoids. GLP-1 is an intestinal hormone that stimulates postprandial insulin secretion from pancreatic β-cells. However, GLP-1 is rapidly degraded in vivo. Therefore, a more stable GLP-1 receptor selective analog, exendin, was developed. This compound showed successful tumor targeting in a rat insulinoma model [84, 85]. Radioiodinated exendin showed a more pronounced pancreatic and tumor uptake as compared to GLP-1 and seems to have potential for scintigraphic purposes. Because of the very high expression of GLP-1 receptors in insulinomas and a few other tumors, radiolabeled GLP-1 analogs could also be used for therapy of these tumors. For tumor scintigraphy, radiometals have certain advantages over radioiodine. ^{111}In-labeled exendin is currently under development.

Vasoactive intestinal peptide

Vasoactive intestinal peptide (VIP) is a 28 amino acid neuroendocrine mediator isolated from the small intestine [86] and it is a member of the group of secretin-like peptides. VIP is a potent vasodilator and stimulates the secretion of several hormones. VIP receptors are expressed by most human epithelial cancers. Large numbers of high affinity receptors are expressed on adenocarcinomas of the gastroenteropancreatic system. Virgolini and coworkers claimed that radioiodinated VIP can be used to image and localize intestinal adenocarcinomas and endocrine tumors [87]. However, these findings were refined by the study of Hessenius et al., indicating that ^{123}I-VIP did not adequately accumulate in pancreatic adenocarcinomas [88]. These findings were confirmed by autoradiography studies of resected tumors, demonstrating lower VIP receptor expression in the tumor as compared to surrounding tissue. Recently, two studies with ^{99m}Tc-labeled VIP analogs in patients with high grade spindle cell sarcoma, ductal epithelial hyperplasia, and colorectal cancer suggested that labeling with this radionuclide may lead to better results [89, 90].

Neurotensin

In contrast to neuroendocrine pancreatic tumors, exocrine pancreatic tumors express only low numbers of somatostatin receptors. For the diagnosis of exocrine pancreatic tumors overexpression of other receptors in these tumors needed to be found. Reubi et al. reported that 75% of all ductal adenocarcinomas overexpress neurotensin (NT) receptors, and that normal pancreatic tissue, pancreatitis and endocrine pancreatic cancers do not express neurotensin receptors [91].

The neurotensin receptor has a high affinity for neurotensin, a 13 amino acid peptide found in brain and gut. However, the possible application of neurotensin in cancer diagnosis and therapy is limited due to its rapid degradation in vivo. Preclinical studies using ^{111}In-labeled DTPA- and DOTA-conjugated neurotensin analogs with modified lysine and arginine derivatives to enhance stability, suggest that these analogs may be applied in the management of patients with exocrine pancreatic cancer [92]. In vitro these NT analogs showed a high receptor affinity and enhanced stability. Indeed, the DTPA-conjugated NT analog showed receptor-mediated tumor uptake in mice with HT29 tumors.

RGD peptides

The $\alpha_v\beta_3$ integrin is a transmembrane protein consisting of two non-covalently bound subunits, α and β. Integrin $\alpha_v\beta_3$ is preferentially expressed on proliferating endothelial cells [93], whereas it is absent on quiescent endothelial cells. For growth beyond the size of 1-2 mm in diameter, tumors require the formation of new blood vessels. Consequently, $\alpha_v\beta_3$ expression on tumor vasculature is considered to be a marker of tumor-induced angiogenesis [94, 95, 96]. In addition, $\alpha_v\beta_3$ is expressed on the cell membrane of various tumor cell types, such as ovarian cancer, neuroblastoma, breast cancer, and melanoma. Due to this restricted expression of $\alpha_v\beta_3$ on the neovasculature of growing tumors and on certain tumor cell types, $\alpha_v\beta_3$ is considered a suitable target for tumor targeting [97]. Radiolabeled ligands for this integrin could be used as tracers to non-invasively visualize $\alpha_v\beta_3$ expression in tumors. Non-invasive visualization of $\alpha_v\beta_3$ expression might supply information about the angiogenic process and the responsiveness of a tumor for antiangiogenic drugs. Furthermore, non-invasive determination of $\alpha_v\beta_3$ expression potentially can be used to monitor the effect of antiangiogenic drugs in patients.

This integrin can bind to the arginine-glycine-aspartic acid (RGD) amino acid sequence present in extracellular matrix proteins, such as vitronectin, fibrinogen, and laminin [98]. Based on the RGD tripeptide sequence, a series of small peptides have been designed to antagonize the function of the $\alpha_v\beta_3$ integrin [99]. A series of RGD sequence containing peptides has been tested for their ability to bind the $\alpha_v\beta_3$ integrin. It was found that the cyclic derivative cyclic(Arg-Gly-Asp-D-Phe-Val) inhibited a 100-fold better the cell adhesion to vitronectin compared to the linear variant, having an IC_{50} value in the nanomolar range [100, 101]. Especially cyclic RGD peptides consisting of five amino acids have a high affinity for $\alpha_v\beta_3$. It was shown that besides the essential RGD sequence, a hydrophobic amino acid in position 4 increased the affinity, whereas the amino acid in position 5 had no influence on the affinity [102].

The first radiolabeled $\alpha_v\beta_3$ antagonist for the investigation of angiogenesis and metastasis in vivo, was [^{125}I]-3-iodo-D-Tyr^4-cyclo(-Arg-Gly-Asp-D-Tyr-Val-) [103]. This radioiodinated $\alpha_v\beta_3$ integrin antagonist had a high affinity for $\alpha_v\beta_3$, however, it was mainly excreted via the hepatobiliary route. To develop a clinically useful radiolabeled $\alpha_v\beta_3$ integrin antagonist, a variety of factors must be considered such as receptor affinity, $\alpha_v\beta_3$ specificity, hydrophilicity, and metabolic stability [104]. Subsequently, a glycosylated version, cyclo(Arg-Gly-Asp-D-Tyr-Lys[SAA]), was synthesized in

an attempt to produce a more hydrophilic compound that would clear predominantly via the kidneys [105]. This glycosylated peptide was radioiodinated and tested in vivo. In a mouse tumor model the glycosylated version showed a longer circulatory half-life and a significantly reduced uptake in the liver compared to the non-glycosylated peptide. In addition, the glycosylated RGD peptide had a clearly enhanced uptake in the tumor.

A non-glycosylated version of the peptide, cyclo(Arg-Gly-Asp-D-Tyr-Lys) was conjugated with DTPA. After radiolabeling this peptide with ^{111}In, this peptide was tested in vivo. This study showed that the introduction of the DTPA-moiety in the peptide via the ε-aminogroup of the lysine residue made the peptide hydrophilic and facilitated renal clearance, while the non-DTPA-conjugated peptide predominantly cleared via the liver [106].

A stable hydrophilic ^{18}F-labeled galactosylated cyclic pentapeptide has recently been developed, with a high affinity and selectivity for $\alpha_v\beta_3$ that accumulates specifically in $\alpha_v\beta_3$-positive tumors [107]. In a recent study it was shown that this PET-tracer can be used to visualize $\alpha_v\beta_3$ expression in tumors in patients [108]. In addition, comparison with immunohistochemical analysis of the tumor lesion indicated that PET using this tracer correctly identified the level of $\alpha_v\beta_3$ expression in tissue non-invasively [109].

Peptide-receptor radionuclide therapy

While a diagnostic radiopharmaceutical depends on a high tumor-to-background ratio for the best contrast, a therapeutic radiopharmaceutical also needs to have a high uptake in the tumor for a prolonged time. Since retention of the therapeutic radiopharmaceutical in the tumor is crucial, a high in vivo stability of radiolabeled peptide is indispensable. High affinity of the peptide for its receptor and rapid internalization of the peptide-receptor complex can enhance the retention of the radionuclide in receptor expressing tumors.

The selection of the appropiate isotope is an important issue in developing a therapeutic radiopharmaceutical. For receptor targeted radiotherapy, radionuclides with high cytotoxic potential have to be used. β-Particle emitters are good cytotoxic agents and have a relatively long penetration range. β-Particles are electrons that are emitted from the nucleus of a decaying radioactive atom. This results in a daughter nucleus in which one neutron is replaced by one proton. Depending on the energy of the commonly used β-particles, their penetration range varies from 2 to 12 mm in tissue. So far, PRRT has been performed mostly with β-particle emitters. The most frequently used radionuclides are ^{90}Y (β_{max} 2.3 MeV, $t_{1/2}$ 64 h), ^{186}Re (β_{max} 1.1 MeV, $t_{1/2}$ 91 h), ^{188}Re (β_{max} 2.1 MeV, $t_{1/2}$ 17 h), ^{131}I (β_{max} 0.6 MeV, $t_{1/2}$ 192 h), and ^{177}Lu (β_{max} 0.5 MeV, $t_{1/2}$ 161 h). High energy β-radiation with a corresponding long penetration range in tissue is less efficient when treating tumors with a relatively small diameter as most of the energy is deposited outside the lesion. Therefore, high energy particles such as ^{90}Y and ^{188}Re are considered more appropiate for the treatment of relatively larger tumors and tumors with a heterogeneous receptor distribution,

whereas low energy particles such as ^{177}Lu and ^{131}I could be better suited for the treatment of smaller tumor lesions [110].

Compared to β-particle emitters, α-particle emitters are mostly heavy elements with a relatively short penetration range of only a few cell diameters. These particles are positively charged with a mass and charge equal to the helium nucleus. Their emission results in a daughter nucleus with two fewer protons and two fewer neutrons. The emitted particles have energies ranging from 5-9 MeV with a relatively short penetration range of about 50 μm in tissue [111, 112]. Interesting candidates for peptide-receptor radionuclide therapy (PRRT) are α-emitters such as ^{211}At, ^{212}Bi, ^{213}Bi, and ^{225}Ac. So far, α-emitters have mainly been used to radiolabel antibodies for radioimmunotherapy (RIT) in animal studies. Recently, Vaidyanathan et al. labeled octreotate conjugates with ^{211}At. The application of this ^{211}At-labeled peptide conjugates for PRRT still has to prove its value [113]. In addition, Norenberg et al. demonstrated that ^{213}Bi-labeled DOTA^{0}-Tyr^{3}-octreotide (^{213}Bi-DOTATOC) had dose-related antitumor effects with minimal treatment-related organ toxicity [114].

Most experience with PRRT is based on the use of somatostatin analogs. Four of these analogs labeled with ^{177}Lu or ^{90}Y are in clinical use: DTPA^{0}-octreotide, DOTA^{0}-Tyr^{3}-octreotide (DOTATOC) [115], DOTA^{0}-Tyr^{3}-Thr^{8}-octreotide (DOTATATE) [116], and DOTA^{0}-2-Nal-Tyr^{3}-Thr-NH_2^{8}-octreotide (DOTA-lanreotide) [117]. In general, PRRT is well tolerated and only a limited number of patients shows relevant hematologic toxicity above greater than 3 (National Cancer Institute Common Toxicity Criteria). However, in PRRT with octreotide analogs the kidneys are the organs responsible for dose-limiting toxicity. Such toxicity is due to the retention of radiolabeled peptides in the renal cortex, leading to a relatively high radiation dose that may result in irreversible loss of kidney function. Several studies focussed on blocking the tubular reabsorption of radiolabeled peptides, thereby reducing the renal retention of these peptides [118, 119, 120, 121, 122, 123].

Peptides other than somatostatin analogs have gained clinical application in PRRT. ^{90}Y-labeled minigastrin has successfully been used for PRRT in patients with medullary thyroid carcinoma with response rates above 30% without severe side-effects [124, 125]. As mentioned above, the selection of the appropiate isotope is an important issue in PRRT; the response rate dropped when ^{111}In was used instead of ^{90}Y as radionuclide in gastrin receptor targeted therapy [126].

References

1. Reubi JC. Regulatory peptide receptors as molecular targets for cancer diagnosis and therapy. Q J Nucl Med 1997;41:63-70.

2. Behr TM, Gotthardt M, Barth A, Béhé M. Imaging tumors with peptide-based radioligands. Q J Nucl Med 2001;45(2):189-200.

3. Reubi JC. Neuropeptide receptors in health and disease: the molecular basis for in vivo imaging. J Nucl Med 1995;36:1825-35.

4. Weiner RE, Thakur ML. Radiolabeled peptides in diagnosis and therapy. Semin Nucl Med 2001;31:296-311.

5. Powell MF, Grey H, Gaeta F, Sette A, Colón S. Peptide stability in drug development: A comparison of peptide reactivity in different biological media. J Pharm Sci 1992;81:731-5.

6. Maecke HR, Heppeler A, Nock B. Somatostatin analogues labeled with different radionuclides. In: Nicolini M, Mazzi U, editors. Technetium, rhenium, and other metals in chemistry and nuclear medicine 4. Padova: SGEditoriali; 1995. pp 77-91.

7. Okarvi SM. Recent developments in ^{99m}Tc-labelled peptide-based radiopharmaceuticals: An overview. Nucl Med Commun 1999;20:1093-1112.

8. Okarvi SM. Peptide-Based Radiopharmaceuticals: Future Tools for Diagnostic Imaging of Cancer and Other Diseases. Medicinal Research Reviews 2004;24:357-97.

9. Veronese FM, Pasut G. PEGylation, successful approach to drug delivery. Drug Discovery Today 2005;10:1451-8.

10. Werle M, Bernkop-Schnürch A. Strategies to improve plasma half life time of peptide and protein drugs. Amino Acids 2006;30:351-67.

11. Wester HJ, Schottelius M, Poethko T, Bruus-Jensen K, Schwaiger M. Radiolabeled Carbohydrated Somatostatin Analogs: A review of the Current Status. Cancer Biother Radiopharm 2004;19:231-44.

12. Bolton AM, Hunter RM. The labeling of proteins to high specific radioactivities by conjugation to a ^{125}I-containing acylating agent. Biochem J 1973;133:529-38.

13. Khawli LA, Kassis AI. Synthesis of ^{125}I labeled *N*-succinimidyl *p*-iodobenzoate for use in radiolabelling antibodies. Nucl Med Biol 1989;16:727-33.

14. Zalutsky MR, Narula AS. A method for radiohalogenation of proteins resulting in decreased thyroid uptake of radioiodine. Appl Radiat Isot 1987;38:1051-5.

15. Garg PK, Zalutsky MR. *N*-succinimidyl 5-(trialkylstannyl)-3-pyridinecarboxylates: A new class of reagents for protein radioiodination. Bioconjugate Chem 1991;2:50-6.

16. Stein R, Govindan SV, Mattes MJ, Chen S, Reed L, Newsome G, McBride BJ, Griffiths GL, Hansen HJ, Goldenberg DM. Improved Iodine Radiolabels for Monoclonal Antibody Therapy. Cancer Res 2003;63:111-8.

17. Stein R, Goldenberg DM, Thorpe SR, Basu A, Mattes MJ. Effects of radiolabeling monoclonal antibodies with a residualizing iodine radiolabel on the accretion of radioisotope in tumors. Cancer Res 1995;55:3132-9.

18. Stein R, Goldenberg DM, Thorpe SR, Mattes MJ. Advantage of a Residualizing Iodine Radiolabel for Radioimmunotherapy of Xenografts of Human Non-Small-Cell Carcinoma of the Lung. J Nucl Med 1997;38:391-5.

19. Brechbiel MW, Gansow OA. Backbone-Substituted DTPA Ligands for ^{90}Y Radioimmunotherapy. Bioconjugate Chem 1991;2:187-94.

20. Meares CF, Moi MK, Diril H, Kukis DL, McCall MJ, Deshapnde SV, et al. Macrocyclic chelates of radiometals for diagnosis and therapy. Br J Cancer Suppl. 1990;10:21-6.

21. Heppeler A, Froidevaux S, Mäcke HR, Jermann E, Béhé M, Powell P, et al. Radiometal-Labelled Macrocyclic Chelator-Derivatised Somatostatin Analogue with Superb Tumour-Targeting Properties and Potential for Receptor-Mediated Internal Radiotherapy. Chem Europ J 1999;5:1974-81.

22. Prata MIM, Santos AC, Geraldes CFGC, de Lima JJP. Characterisation of $^{67}Ga^{3+}$ Complexes of Triaza Macrocyclic Ligands: Biodistribution and Clearance Studies. Nucl Med Biol 1999;26:707-10.

23. Bass LA, Wang M, Welch MJ, and Anderson CJ. In vivo Transchelation of Copper-64 from TETA-Octreotide to Superoxide Dismutase in Rat Liver. Bioconjugate Chem 2000;11:527-32.

24. Mirick GR, O'Donnell RT, DeNardo SJ, Shen S, Meares CF, DeNardo GL. Transfer of Copper from a Chelated ^{67}Cu-Antibody Conjugate to Ceruloplasmin in Lymphoma Patients. Nucl Med Biol 1999; 26:841-5.

25. Boswell CA, Sun X, Niu W, Weisman GR, Wong EH, Rheingold AL, Anderson CJ. Comparative in Vivo Stability of Copper-64-Labeled Cross-Bridged and Conventional Tetraazamacrocyclic Complexes. J Med Chem 2004;47:1465-74.

26. Hnatowich DJ. Recent developments in the radiolabeling of antibodies with iodine, indium, and technetium. Semin Nucl Med 1990;20:80-91.

27. Srivastava SC, Meares RC. Progress in research on ligands, nuclides and techniques for labeling monoclonal antibodies. Int J Rad Appl Instrum B 1991;18:589-603.

28. Guhlke S, Schaffland A, Zamora PO, Sartor J, Diekmann D, Bender H, Knapp FF, Biersack HJ. ^{188}Re- and ^{99m}Tc-MAG_3 as prosthetic groups for labeling amines and peptides: Approaches with pre- and post-conjugate labeling. Nucl Med Biol 1998;25:621-31.

29. Okarvi SM, Jammaz I. Synthesis, radiolabelling, and biological characteristics of a bombesin peptide analog as a tumor imaging agent. Anticancer Res 2003;23:2745-50.

30. Van Domselaar GH, Okarvi SM, Fanta M, Suresh MR, Wishart DS. Synthesis and ^{99m}Tc-labelling of bz-MAG3-triprolinyl-peptides, their radiochemical evaluation and *in vitro* receptor binding. J Label Compd Radiopharm 2000;43:1193-1204.

31. Chen JQ, Giblin MF, Wang N, Jurisson SS, Quinn TP. *In vivo* evaluation of ^{99m}Tc/^{188}Re-labeled linear alpha melanocyte stimulating hormone analogs for specific melanoma targeting. Nucl Med Biol 1999;26:687-93.

32. Decristoforo C, Mather SJ, Cholewinski W, Donnemiller E, Riccabona G, Moncayo R. ^{99m}Tc-EDDA/HYNIC-TOC: A new ^{99m}Tc-labelled radiopharmaceutical for imaging somatostatin receptor-positive tumours: First clinical results and intra-patient comparison with ^{111}In-labelled octreotide derivatives. Eur J Nucl Med 2000;27:1318-25.

33. Bangard M, Béhé M, Guhlke S, Otte R, Bender H, Maecke HR, Biersack HJ. Detection of somatostatin receptor-positive tumours using the new ^{99m}Tc-tricine-HYNIC-D-Phe^1-Tyr^3-octreotide: First results in patients and comparison with ^{111}In-DTPA-D-Phe^1-octreotide. Eur J Nucl Med 2000;27:628-37.

34. Lin KS, Luu AN, Baidoo KE, Pili R, Carducci MA, Wagner HN, Jr. *In vivo* evaluation of a promising 99mTc-labeled bombesin analog for breast cancer imaging. In; Nicolini M, Mazzi U, editors. Technetium, rhenium, and other metals in chemistry and nuclear medicine 6. Padova: SGEditoriali; 2002. pp 363-367.

35. Verbeke K, Verbeke A, Vanbilloen H, Verbruggen A. Preparation and preliminary evaluation of ^{99m}Tc-EC-For-MLFK. Nucl Med Biol 2002;29:585-92.

36. Maina T, Nock B, Nikolopoulou A, Sotiriou P, Loudos G, Maintas D, Cordopatis P, Chiotellis E. [^{99m}Tc]Demotate, a new ^{99m}Tc-based [Tyr^3]octreotate analogue for the detection of somatostatin receptor-positive tumours: synthesis and preclinical results. Eur J Nucl Med 2002;29:742-53.

37. Abrams MJ, Juweid M, tenKate CI, Schwartz DA, Hauser MM, Gaul FE, Fuccello AJ, Rubin RH, Strauss HW, Fischman AJ. Technetium-99m-human polyclonal IgG radiolabeled via the hydrazino nicotimamide derivative for imaging focal sites of infection in rats. J Nucl Med 1990;31:2022-8.

38. Wester H-J, Hamacher K, Stöcklin G. A comparative study of N.C.A. fluorine-18 labeling of proteins via acylation and photochemical conjugation. Nucl Med Biol 1996;23:365-72.

39. Vaidyanathan G, Binger DD, Zalutsky MR. Fluorine-18-labeled monoclonal antibody fragments: A potential approach for combining radioimmunoscintigraphy and positron emission tomography. J Nucl Med 1992;33:1535-41.

40. Hostetler ED, Edwards WB, Anderson CJ, Welch MJ. Synthesis of 4-[^{18}F]fluorobenzoyl octreotide and biodistribution in tumor-bearing Lewis rats. J Label Compounds Radiopharm 1999;42:S720-S721.

41. Vaidyanathan G, Zalutsky MR. Improved synthesis of *N*-succinimidyl 4-[^{18}F]fluorobenzoate and its application to the labeling of a monoclonal antibody fragment. Bioconjugate Chem 1994;5:352-6.

42. Fredriksson A, Johnström P, Stone-Elander S, Jonasson P, Nygren P-A, Ekberg Johansson B-L, Wahren J. Labeling of human C-peptide by conjugation with *N*-succinimidyl-4-[^{18}F]fluorobenzoate. J Label Compounds Radiopharm 2001;44:509-19.

43. Poethko T, Schottelius M, Thumshirn G, Hersel U, Herz M, Henriksen G, Kessler H, Schwaiger M, Wester HJ. Two-Step Methodology for High-Yield Routine Radiohalogenation of Peptides: ^{18}F-Labeled RGD and Octreotide Analogs. J Nucl Med 2004;45:892-902.

44. Schottelius M, Poethko T, Herz M, Reubi JC, Kessler H, Schwaiger M, Wester HJ. First ^{18}F-Labeled Tracer Suitable for Routine Clinical Imaging of sst Receptor expressing Tumors Using Positron Emission Tomography. Clin Cancer Res 2004;10:3593-606.

45. Brazeau P. Somatostatin: a peptide with unexpected physiologic activities. Am J Med 1986;81 Suppl 6B:8-13.

46. Patel YC. Somatostatin and Its Receptor Family. Front Neuroendocrinol 1999;20:157-98.

47. Lamberts SW, Bakker WH, Reubi JC, Krenning EP. Somatostatin-receptor imaging in the localization of endocrine tumors. N Engl J Med 1990;323:1246-9.

48. De Jong M, Breeman WAP, Bakker WH, Kooij PPM, Bernard BF, Hofland LJ, Visser TJ, Srinivasan A, Schmidt M, Erion JL, Bugaj JE, Mäcke HR, Krenning EP. Comparison of ^{111}In-labeled somatostatin analogues for tumor scintigraphy and radionuclide therapy. Cancer Res 1998;58:437-41.

49. Boerman OC, Oyen WJG, Corstens FHM. Radio-labeled receptor binding peptides: A new class of radiopharmaceuticals. Semin Nucl Med 2000;30:195-208.

50. Froidevaux S, Heppeler A, Eberle AN, et al. Preclinical comparison in AR4-2J tumor bearing mice of four radiolabeled DOTA-somatostatin analogs for tumor diagnosis and internal radiotherapy. Endocrinology 2000;141: 3304-12.

51. Stolz B, Weckbecker G, Smith-Jones PM, et al. The somatostatin receptor-targeted radiotherapeutic [^{90}Y-DOTA-DPhe^{1},Tyr^{3}]octreotide (^{90}Y-SMT 487) eradicates experimental rat pancreatic CA 20948 tumours. Eur J Nucl Med 1998;25:668-74.

52. De Jong M, Bakker WH, Breeman WA, et al. Pre-clinical comparison of [DTPA0] octreotide, [DTPA0,Tyr^{3}] octreotide and [DOTA0,Tyr^{3}] octreotide as carriers for somatostatin receptor-targeted scintigraphy and radionuclidetherapy. Int J Cancer 1998;75:406-11.

53. Otte A, Mueller-Brand J, Dellas S, et al. Yttrium-90-labelled somatostatin-analogue for cancer treatment. Lancet 1998;351:417-8.

54. Otte A, Herrmann R, Heppeler A, et al. Yttrium-90 DOTATOC: first clinical results. Eur J Nucl Med 1999:26:1439-47.

55. Kwekkeboom DJ, Kooij PP, Bakker WH, et al. Comparison of ^{111}In-DOTA-Tyr^{3}-octreotide and ^{111}In-DTPA-octreotide in the same patients: biodistribution, kinetics, organ and tumor uptake. J Nucl Med 1999;40:762-7.

56. Bangard M, Béhé M, Guhlke S, Otte R, Bender H, Maecke HR, et al. Detection of somatostatin receptor-positive tumors using the new 99mTc-tricine-HYNIC-D-Phe1-Tyr3-octreotide: first results in patients and comparison with 111In-DTPA-D-Phe1-octreotide. Eur J Nucl Med 2000;27:628-37.

57. Gabriel M, Decristoforo C, Donnemiller E, Ulmer H, Watfah Rychlinski C, Mather SJ, et al. An intrapatient comparison of ^{99m}Tc-EDDA/HYNIC-TOC with ^{111}In-DTPA-octreotide for diagnosis of somatostatin receptor expressing tumors. J Nucl Med 2003;44:708-16.

58. Anderson CJ, Pajeau TS, Edwards WB, et al. In vitro and in vivo evaluation of copper-64-octreotide conjugates J Nucl Med 1995;36:2315-25.

59. Lewis JS, Srinivasan A, Schmidt MA, et al. In vitro and in vivo evaluation of ^{64}Cu-TETA-Tyr^3-octreotate. A new somatostatin analog with improved target tissue uptake. Nucl Med Biol 1999;26:267-73.

60. Anderson CJ, Dehdashti F, Cutler PD, et al. ^{64}Cu-TETA-octreotide as a PET imaging agent for patients with neuroendocrine tumors. J Nucl Med 2001;42:213-21.

61. Wester HJ, Brockmann J, Rosch F, et al. PET-pharmacokinetics of ^{18}F-octreotide: a comparison with ^{67}Ga-DFO- and ^{86}Y-DTPA-octreotide. Nucl Med Biol 1997;24:275-86.

62. Wester HJ, Schottelius M, Scheidhauer K, et al. PET imaging of somatostin receptors: design, synthesis and preclinical evaluation of a novel ^{18}F-labelled, carbohydrated analogue of octreotide. Eur J Nucl Med Mol Imaging 2003;30:117-22.

63. Meisetschläger, Poethko T, Stahl A, Wolf I, Scheidhauer K, Schottelius M, Herz M, Wester HJ, Schwaiger M. Gluc-Lys($[^{18}$F]FP)-TOCA PET in Patients with SSTR-Positive Tumors: Biodistribution and Diagnostic Evaluation Compared with [^{111}In]DTPA-Octreotide. J Nucl Med 2006;47:566-73.

64. Hofmann M, Maecke H, Borner R, et al. Biokinetics and imaging with the somatostatin receptor radioligand ^{68}Ga-DOTATOC: preliminary data. Eur J Nucl Med 2001;28:1751-7.

65. Kowalski J, Henze M, Schuhmacher J, Mäcke HR, Hofmann M, Haberkorn U. Evaluation of Positron Emission Tomography Imaging Using [^{68}Ga]-DOTA-D Phe^1-Tyr^3-Octreotide in Comparison to [^{111}In]-DTPAOC SPECT. First Results in Patients with Neuroendocrine Tumors. Mol Imaging Biol 2003;5:42-8.

66. Wild D, Mäcke HR, Waser B, Reubi JC, Ginj M, Rasch H, Müller-Brand J, Hofmann M. ^{68}Ga-DOTANOC: a first compound for PET imaging with a high affinity for somatostatin receptor subtypes 2 and 5. Eur J Nucl Med Mol Imaging 2005;32:724.

67. Reubi JC, Schaer JC, Waser B. Cholecystokinin(CCK)-A and CCK-B/gastrin receptors in human tumors. Cancer Res 1997;57:1377-86.

68. Wank SA, Pisegna JR, de Weerth A. Cholecystokinin receptor family. Molecular cloning, structure, and functional expression in rat, guinea pig, and human. Ann N Y Acad Sci 1994;713: 49-66.

69. Behr TM, Jenner N, Radetzky S, et. al. Targeting of cholecystokinin-B/gastrin receptors in vivo: preclinical and initial clinical evaluation of the diagnostic and therapeutic potential of radiolabeled gastrin. Eur J Nucl Med 1998;25:424-30.

70. Reubi JC, Waser B, Schaer JC, et al. Unsulfated DTPA- and DOTA-CCK analogs as specific high-affinity ligands for CCK-B receptor expressing human and rat tissues in vitro and in vivo. Eur J Nucl Med 1998;25:481-90.

71. De Jong M, Bakker WH, Bernard BF, et al. Preclinical and initial clinical evaluation of ^{111}In-labeled nonsulfated CCK_8 analog: a peptide for CCK-B receptor-targeted scintigraphy and radionuclide therapy. J Nucl Med 1999;40:2081-7.

72. Kwekkeboom DJ, Bakker WH, Kooij PPM, et al. Cholecystokinin receptor imaging using an octapeptide DTPA-CCK analogue in patients with medullary thyroid carcinoma. Eur J Nucl Med 2000: 27:1312-7.

73. Béhé M, Behr TM. Cholecystokinin-B (CCK-B)/ Gastrin Receptor Targeting Peptides for Staging and Therapy of Medullary Thyroid Cancer and other CCK-B Receptor Expressing Malignancies. Biopolymers 2002;66:399-418.

74. Gotthardt M, Battmann A, Beuter D, Bauhofer A, Schipper ML, Béhé MP, et al. Comparison of In-111-D-Glu-1-Minigastrin, F-18-FDG PET, and CT scanning for the detection of metastatic medullary thyroid carcinoma. J Nucl Med 2003;44(5):169P.

75. Krenning EP, Kwekkeboom DJ, Bakker WH, Breeman WAP, Kooij PPM, Oei HY, van Hagen M, Postema PTE, de Jong M, Reubi JC, Visser TJ, Reijs AEM, Hofland LJ, Koper JW, Lamberts SWJ. Somatostatin receptor scintigraphy with [^{111}In-DTPA-D-Phe^{1}]- and [^{123}I-Tyr^{3}]-octreotide: the Rotterdam experience with more than 1000 patients. Eur J Nucl Med 1993;20:716-31.

76. Kwekkeboom D, Krenning EP, de Jong M. Peptide receptor imaging and therapy. J Nucl Med 2000;41:1704-13.

77. Otte A, Jermann E, Behe M, et al. DOTATOC: a powerful new tool for receptor-mediated radionuclide therapy. Eur J Nucl Med 1997;24:792-5.

78. Nock B, Nikolopoulou A, Chiotellis E, et al. ^{99m}Tc demobesin 1, a novel potent bombesin analogue for GRP receptor-targeted tumour imaging. Eur J Nucl Med Mol Imaging 2003;30:247-58.

79. Breeman WAP, de Jong M, Erion JL, Bugaj JE, Srinivasan A, Bernard BF, Kwekkeboom DJ, Visser TJ, Krenning EP. Preclinical Comparison of ^{111}In-labeled DTPA- or DOTA-Bombesin Analogs for Receptor-Targeted Scintigraphy and Radionuclide Therapy. J Nucl Med 2002;43:1650-6.

80. De Visser M, Van Weerden WM, De Ridder CM, Reneman S, Wildeman N, Melis M, Krenning EP, De Jong M. Androgen regulation of GRP receptor-expression in human prostate tumor xenografts. J Nucl Med 2005;46:396P.

81. Hennig IM, Laissue JA, Horisberger U, Reubi JC. Substance P receptors in human primary neoplasms. Int J Cancer 1995;61:786-92.

82. Van Hagen PM, Breeman WAP, Reubi JC, Postema, PTE, van den Anker-Lugtenburg PJ, Kwekkeboom DJ, et al. Visualization of the thymus by substance P receptor scintigraphy in man. Eur J Nucl Med 1996;23:1508-13.

83. Schumacher T, Hofer S, Good S, Reubi JC, Maecke H, Mueller-Brand J, et al. Diffusible Brachytherapie mit 90Y-Substanz P bei High Grade Gliomen: Erste Beobachtungen. In: Brink I, Högerle S, Moser E (Ed.): Nuklearmedizin als Paradigma molekularer Bildgebung, Blackwell, Berlin, Germany, 2002: 68.

84. Gotthardt M, Fischer M, Baltes N, Brandt D, Welcke U, Göke BM, Joseph K. Scintigraphic detection of insulinomas by [^{123}I]-Exendin4[Y39] in a rat tumor model. J Nucl Med 2000;41 Suppl 5:9p.

85. Gotthardt M, Fischer M, Holz JB, Jungclas H, Fritsch HW, Béhé M, et al. Use of the incretin hormone glucagon-like peptide-1 (GLP-1) for the detection of insulinomas: first experimental results. Eur J Nucl Med Mol Imaging 2002;29(5):597-60.

86. Said SI, Mutt V. Polypeptide with broad biological activity: isolation from small intestine. Science 1970;169:1217-8.

87. Virgolini I, Raderer M, Kurtaran A, Angelberger P, Banyai S, Yang Q, et al. Vasoactive intestinal peptide-receptor imaging for the localization of intestinal adenocarcinomas and endocrine tumors. N Engl J Med 1994;331:1116-21.

88. Hessenius C, Bäder M, Meinhold H, Böhmig M, Faiss S, Reubi JC, and Wiedenmann B. Vasoactive intestinal peptide receptor scintigraphy in patients with pancreatic adenocarcinomas or neuroendocrine tumours. Eur J Nucl Med 2000;27:1684-93.

89. Rao PS, Tahkur ML, Pallela V, Patti R, Reddy K, Li H, et al. ^{99m}Tc labeled VIP analog: evaluation for imaging colorectal cancer. Nucl Med Biol 2001;28:445-50.

90. Thakur ML, Marcus CS, Saeed S, Pallela V, Minami C, Diggles L, et al. Imaging tumors in humans with Tc-99m-VIP. Ann N Y Acad Sci 2000;921:37-44.

91. Reubi JC, Waser B, Friess H, Büchler M, Laissue J. Neurotensin receptors: a new marker for human ductal pancreatic adenocarcinoma. Gut 1998;42:546-50.

92. de Visser M, Janssen PJJM, Srinivasan A, Reubi JC, Waser B, Erion JL, Schmidt MA, Krenning EP, de Jong M. Stabilised ^{111}In-labelled DTPA- and DOTA-conjugated neurotensin analogues for imaging and therapy of exocrine pancreatic cancer. Eur J Nucl Med Mol Imaging 2003;30:1134-9.

93. Brooks PC. Role of integrins in angiogenesis. Eur J Cancer 1996;32A:2423-9.

94. Fiedler W, Graeven U, Ergun S, Verago S, Kilic N, Stockschlader M, et al. Vascular endothelial growth factor, a possible paracrine growth factor in human acute myeloid leukemia. Blood 1997;89:1870-5.

95. Foss HD, Araujo I, Demel G, Klotzbach H, Hummel M, Stein H. Expression of vascular endothelial growth factor in lymphomas and Castelman's disease. J Pathol 1997;183:44-50.

96. Perez-Atayde AR, Sallan SE, Tedrow U, Conners S, Allred E, Folkman J. Spectrum of tumor angiogenesis in the bone marrow of children with acute lymphoblastic leukemia. Am J Pathol 1997;150:815-21.

97. Folkman J. Angiogenesis in cancer, vascular, rheumatoid and other disease. Nat Med 1995;1:27-31.

98. Plow EF, Haas TA, Zhang L, Loftus J, Smith JW. Ligands binding to integrins. J Biol Chem 2000; 275: 21785-8.

99. Haubner R, Finsinger D, Kessler H. Stereoisomeric Peptide Libraries and Peptidomimetics for Designing Selective Inhibitors of the $\alpha_v\beta_3$ Integrin for a New Cancer Therapy. Angew Chem Int Ed Engl 1997;36:1374-89.

100. Aumailley M, Gurrath M, Muller G, Calvete J, Timpl R, Kessler H. Arg-Gly-Asp constrained within cyclic pentapeptides. Strong and selective inhibitors of cell adhesion to vitronectin and laminin fragment P1. FEBS Let 1991;291:50-4.

101. Gurrath M, Muller G, Kessler H, Aumailley M, Timpl R. Conformation/activity studies of rationally designed potent anti-adhesive RDG peptides. Eur J Biochem 1992;210:911-21.

102. Haubner R, Gratias R, Diefenbach B, Goodman SL, Jonczyk A, Kessler H. Structural and functional aspects of RGD-containing cyclic pentapeptides as highly potent and selective integrin $\alpha_v\beta_3$ antagonists. J Am Chem Soc 1996;118: 7461-72.

103. Haubner R, Wester HJ, Reuning U, Senekowitsch-Schmidtke R, Diefenbach B, Kessler H, et al. Radiolabeled $\alpha_v\beta_3$ Integrin Antagonists: A New Class of Tracers for Tumor Targeting. J Nucl Med 1999;40:1061-71.

104. Schottelius M, Wester HJ, Reubi JC, Senekowitsch-Schmidtke R, Schwaiger M. Improvement of pharmacokinetics of radioiodinated Tyr^3-octreotide by conjugation with carbohydrates. Bioconjugate Chem 2002;13:1021-30.

105. Haubner R, Wester HJ, Burkhart F, Senekowitsch-Schmidtke R, Weber W, Goodman SL, Kessler H, Schwaiger M. Glycosylated RGD-containing peptides: tracer for tumor targeting and angiogenesis imaging with improved biokinetics. J Nucl Med 2001;42:326-36.

106. Van Hagen PM, Breeman WA, Bernard HF, Schaar M, Mooij CM, Srinivasan A, Schmidt MA, Krenning EP, de Jong M. Evaluation of a radiolabelled cyclic DTPA-RGD analogue for tumour imaging and radionuclide therapy. Int J Cancer 2000;90:186-98.

107. Haubner R, Kuhnast B, Mang C, Weber WA, Kessler H, Wester HJ, Schwaiger M. [^{18}F]Galacto-RGD: synthesis, radiolabeling, metabolic stability, and radiation dose estimates. Bioconjugate Chem 2004;15:61-9.

108. Haubner R, Weber WA, Beer AJ, Vabuliene E, Reim D, Sarbia M, Becker KF, Goebel M, Hein R, Wester HJ, Kessler H, and Schwaiger M. Noninvasive visualization of the activated αvβ3 integrin in cancer patients by positron emission tomography and [^{18}F]Galacto-RGD. PloS Med 2005;2:e70.

109. Beer AJ, Haubner R, Sarbia M, Goebel M, Luderschmidt S, Grosu AL, Schnell O, Niemeyer M, Kessler H, Wester HJ, Weber WA, Schwaiger M. Positron Emission Tomography Using [^{18}F]Galacto-RGD Identifies the Level of $\alpha_v\beta_3$ Expression in Man. Clin Cancer Res 2006;12:3942-9.

110. O'Donoghue JA, Bardies M, Wheldon TE. Relationships between tumor size and curability for uniformly targeted therapy with β-emitting radionuclides. J Nucl Med. 1995;36:1902-9.

111. Kassis AI, Adelstein SJ. Radiobiologic Principles in Radionuclide Therapy. J Nucl Med 2005;46:4S-12S.

112. Schubiger PA, Alberto R, and Smith A. Vehicles, chelators, and radionuclides: crossing the "building blocks" of an effective therapeutic radioimmunoconjugate. Bioconjugate Chem 1996;7:165-79.

113. Vaidyanathan G, Affleck DJ, Schottelius M, Wester H, Friedman HS, Zalutsky MR. Synthesis and Evaluation of Glycosylated Octreotate Analogues Labeled with Radioiodine and ^{211}At via a Tin Precursor. Bioconjugate Chem 2006;17:195-203.

114. Norenberg JP, Krenning BJ, Konings IRHM, Kusewitt DF, Nayak TK, Anderson TL, de Jong M, Garmestani K, Brechbiel MW, Kvols LK. ^{213}Bi-[DOTA^0, Tyr^3]Octreotide Peptide Receptor Radionuclide Therapy of Pancreatic Tumors in a Preclinical Animal Model. Clin Cancer Res 2006;12(3):897-903.

115. Waldherr C, Pless M, Maecke HR, Haldemann A, Mueller-Brand J. The clinical value of [^{90}Y-DOTA-]-D-Phe^1-Tyr^3-octreotide (^{90}Y-DOTATOC) in the treatment of neuroendocrine tumours: a clinical phase II study. Ann Oncol 2001;12:941-5.

116. Kwekkeboom DJ, Bakker WH, Kam BL, et al. Treatment of patients with gastro-entero-pancreatic (GEP) tumours with the novel radiolabelled somatostatin analogue [^{177}Lu-DOTA^0,Tyr^3]octreotate. Eur J Nucl Med 2003;30:417-22.

117. Banerjee S, Das T, Chakraborty S, Samuel G, Korde A, Srivastava S, Venkatesh M, Pillai MRA. ^{177}Lu-DOTA-lanreotide: A novel tracer as a targeted agent for tumor therapy. Nucl Med Biol 2004;31:753-9.

118. De Jong M, Rolleman EJ, Bernard BF, et al. Inhibition of renal uptake of indium-111-DTPA-octreotide in vivo. J Nucl Med 1996;37:1388-92.

119. Behr TM, Sharkey RM, Juweid ME, et al. Reduction of the renal uptake of radiolabeled monoclonal antibody fragments by cationic amino acids and their derivatives. Cancer Res 1995;55: 3825-34.

120. Behr TM, Sharkey RM, Sgouros G, et al. Overcoming the nephrotoxicity of radiometal-labeled immunoconjugates: improved cancer therapy administered to a nude mouse model in relation to the internal radiation dosimetry. Cancer 1997;80:2591-2610.

121. Rolleman EJ, Valkema R, de Jong M, Kooij PPM, Krenning EP. Safe and effective inhibition of renal uptake of radiolabelled octreotide by a combination of lysine and arginine. Eur J Nucl Med 2003;30:9-15.

122. De Jong M, Barone R, Krenning E, et al. Megalin is essential for renal proximal tubule reabsorption of ^{111}In-DTPA-octreotide. J Nucl Med 2005;46:1696-1700.

123. Vegt E, Wetzels JFM, Russel FGM, Masereeuw R, Boerman OC, van Eerd JE, Corstens FHM, Oyen WJG. Renal Uptake of Radiolabeled Octreotide in Human Subjects Is Efficiently Inhibited by Succinylated Gelatin. J Nucl Med 2006;47: 432-6.

124. Behr TM, Jenner N, Radetzky S, Yücekent S, Raue F, Becker W. Targeting of cholecystokinin-B/gastrin receptors *in vivo*: preclinical and initial clinical evaluation of the diagnostic and therapeutic potential of radiolabeled gastrin. Eur J Nucl Med 1998;25:424-30.

125. Behr TM, Béhé M, Angerstein C, Gratz S, Mach R, Hagemann L, et al. Cholecystokinin-B/gastrin receptor binding peptides: preclinical development and evaluation of their diagnostic and therapeutic potential. Clin Cancer Res 1999;5 (suppl. 10):3124s-3138s.

126. Gotthardt M, Béhé MP, Schipper ML, Schlieck A, Höffken H, Behr TM. In-111-DTPA-D-Glu-1-Minigastrin used for therapy of metastatic medullary thyroid carcinoma and other neuroendocrine tumors: results of an ongoing dose-escalation study. J Nucl Med 2003;44(5):137P.

Chapter 2

Synthesis and biological evaluation of potent $\alpha_v\beta_3$ integrin receptor antagonists

Ingrid Dijkgraaf
John A. W. Kruijtzer
Cathelijne Frielink
Annemieke C. Soede
Hans W. Hilbers
Wim J. G. Oyen
Frans H. M. Corstens
Rob M. J. Liskamp
Otto C. Boerman

Nucl Med Biol 2006:33;953-961

Abstract

The $\alpha_v\beta_3$ integrin is expressed on sprouting endothelial cells as present in growing tumors, whereas it is absent on quiescent blood vessels. In addition, various tumor cell types express the $\alpha_v\beta_3$ integrin. The $\alpha_v\beta_3$ integrin, a transmembrane heterodimeric protein, binds to the arginine-glycine-aspartic acid (RGD) amino acid sequence of extracellular matrix proteins such as vitronectin and plays a pivotal role in invasion, proliferation, and metastasis. Due to the selective expression of $\alpha_v\beta_3$ integrin in tumors, radiolabeled RGD peptides and peptidomimetics are attractive candidates for tumor targeting.

Methods: A cyclic RGD peptide, a peptoid-peptide hybrid, an all-peptoid, and a peptidomimetic compound were synthesized, conjugated with DOTA, and radiolabeled with ^{111}In. Their in vitro and in vivo $\alpha_v\beta_3$ binding characteristics were determined.

Results: The IC_{50} values were 236 nM for DOTA-E-c(RGDfK), 219 nM for DOTA-peptidomimetic, > 10 mM for DOTA-all-peptoid, and 9.25 mM for the peptoid-peptide hybrid, DOTA-E-c(nRGDfK). The ^{111}In-labeled compounds, except the ^{111}In-DOTA-all-peptoid, showed specific uptake in human $\alpha_v\beta_3$ expressing tumors xenografted in athymic mice. Tumor uptake for ^{111}In-DOTA-E-c(RGDfK) was 1.73 ± 0.4 %ID/g (2 h p.i.), and that of ^{111}In-DOTA-peptidomimetic was 2.04 ± 0.3 %ID/g. Tumor uptake for the peptoid-peptide hybrid, ^{111}In-DOTA-E-c(nRGDfK), was markedly lower: 0.45 ± 0.07 %ID/g. The all-peptoid, ^{111}In-DOTA-E-c(nRGnDnFnK), did not show specific uptake in the tumor (0.11 ± 0.04 %ID/g).

Conclusions: The peptidomimetic compound and the cyclic RGD peptide have a high affinity for the $\alpha_v\beta_3$ integrin and these compounds have better tumor targeting characteristics than the peptoid-peptide hybrid and the all-peptoid.

Introduction

Integrins are an important class of receptors involved in cell-cell and cell-matrix interactions [1]. Integrins are heterodimeric, transmembrane glycoproteins consisting of an α- and a β-subunit. One of the most prominent members of this class of adhesion molecules is the $\alpha_v\beta_3$ integrin which plays a role in a series of pathological processes such as osteoporosis [2], restenosis after balloon angioplasty [3], inflammation [4], rheumatoid arthritis [5], metastasis [6], and tumor-induced angiogenesis [7]. The $\alpha_v\beta_3$ integrin is expressed on sprouting endothelial cells during angiogenesis, but not on quiescent endothelial cells. In addition, $\alpha_v\beta_3$ is expressed on various tumor cell types such as melanoma, ovarian carcinoma, gliomas, a.o.. This integrin interacts with the arginine-glycine-aspartic acid (RGD) amino acid sequence of extracellular matrix proteins such as vitronectin [8]. Based on this RGD tripeptide sequence a series of small peptides has been designed to antagonize the function of the $\alpha_v\beta_3$ integrin [9]. Some of these peptides, particularly the cyclic ones, have a relatively high and specific affinity for the $\alpha_v\beta_3$ integrin [10, 11].

Potentially, radiolabeled RGD peptides and analogs could be used to visualize angiogenesis in tumors. Therefore, several radiolabeled ligands for the $\alpha_v\beta_3$ integrin have been synthesized. The first radiolabeled $\alpha_v\beta_3$ antagonist for the investigation of angiogenesis and metastasis in vivo, was ^{125}I-3-iodo-D-Tyr^4-cyclo(-Arg-Gly-Asp-D-Tyr-Val-) [12]. To develop a clinically useful radiolabeled $\alpha_v\beta_3$ integrin antagonist, a variety of factors must be considered, such as receptor affinity, $\alpha_v\beta_3$ specificity, hydrophilicity, and metabolic stability [13]. After a systematic search, the group in Munich developed a stable ^{18}F-labeled galactosylated cyclic pentapeptide, with a high affinity and selectivity for $\alpha_v\beta_3$ that accumulated specifically in $\alpha_v\beta_3$-positive tumors and cleared rapidly via the kidneys [14]. In a recent study they showed that this PET tracer can be used to visualize $\alpha_v\beta_3$ expression in tumors in patients [15].

In peptidomimetic compounds, amino acids are replaced by non-peptidic building blocks [16]. These modifications can be divided into backbone modifications, like *N*-methylation and side chain modification, introducing unnatural amino acids. *N*-Methylation of peptide bonds could improve the binding characteristics of a peptide. For example, *N*-methylation of the valine residue of the $\alpha_v\beta_3$ antagonist cyclo(RGDfV) resulted in a more active compound, cyclo(RGDf-N(Me)V-). The antiangiogenic activity of this compound, Cilengitide, is currently in clinical phase II studies [17]. Peptoids are a class of peptidomimetics built from *N*-substituted glycine residues. In these so-called peptoid residues, the position of the amino acid side chain is shifted from the α-carbon atom to the nitrogen atom [18]. Evidently, these modifications have consequences for the biological activity of a peptoid or peptoid-peptide hybrid compared to the parent peptide.

The aim of this study was to develop RGD analogs with improved in vivo $\alpha_v\beta_3$ targeting characteristics. Here, we describe the synthesis and the radiolabeling of four 1,4,7,10-tetraazacyclododecane-N,N',N'',N'''-tetraacetic acid (DOTA)-conjugated compounds: a cyclic pentapeptide RGDfK (Figure 1A), a cyclic peptoid-peptide hybrid in which the arginine residue is replaced by the corresponding peptoid residue (Figure 1B), an all-peptoid in which all the amino acid residues are replaced by their corresponding peptoid residues (Figure 1C), and a peptidomimetic $\alpha_v\beta_3$ receptor antagonist recently described by Hood et al. [19] (Figure 1D). Stability, in vitro and in vivo $\alpha_v\beta_3$ binding characteristics are systematically studied.

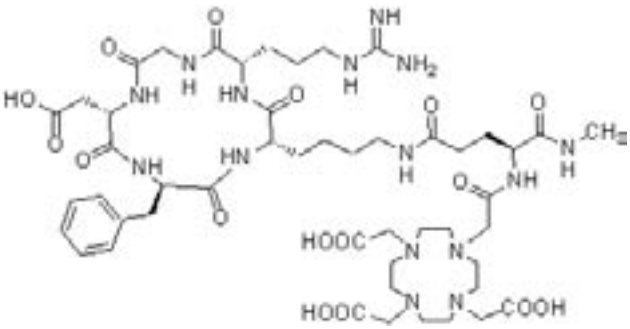

Figure 1A. Structural formula of the DOTA-conjugated monomeric RGD peptide, DOTA-E-c(RGDfK).

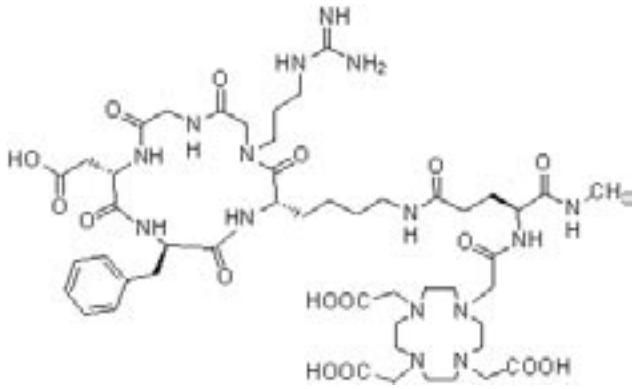

Figure 1B. Structural formula of the DOTA-conjugated peptoid-peptide hybrid, DOTA-E-c(nRGDfK).

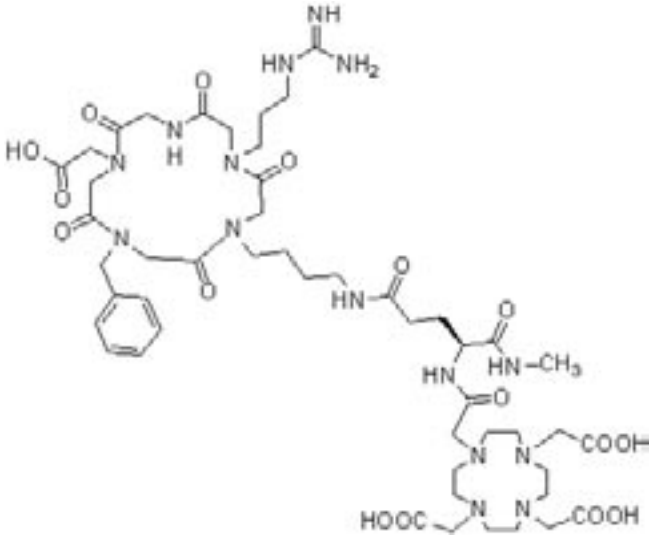

Figure 1C. Structural formula of the DOTA-conjugated all-peptoid, DOTA-E-c(nRGnDnFnK).

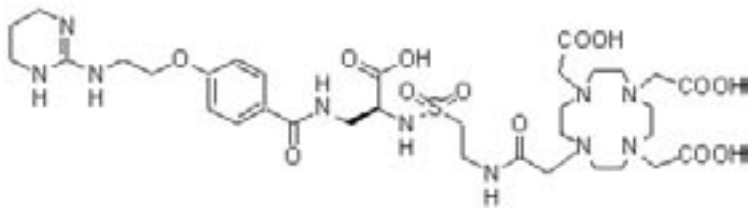

Figure 1D. Structural formula of the DOTA-conjugated peptidomimetic.

Materials and methods

General

Chemicals and resins were obtained from commercial sources and used without further purification unless stated otherwise. N,N-diisopropylethylamine (DiPEA) was distilled over ninhydrin and KOH. 9-Fluorenylmethoxycarbonyl (Fmoc) amino acids were purchased from MultiSynTech (Witten, Germany). Fmoc-D-Phe-OH was purchased from Alexis (Lausen, Switzerland). Arginine and lysine were protected by the 2,2,4,6,7-pentamethyldihydro-benzofuran-5-sulfonyl (Pbf) and *tert*-butoxycarbonyl (Boc) groups, respectively. Aspartic acid was protected as a *tert*-butyl ester (OtBu). Synthesis of the peptoid monomers Fmoc-NArg(Boc)$_2$-OH, Fmoc-NPhe-OH, Fmoc-NLys(Boc)-OH, and Fmoc-NAsp(OtBu)-OH was carried out as described previously [20]. Glycine was chosen as the C-terminal amino acid in order to avoid racemization during the cyclization step. The other amino acids were coupled using standard Fmoc chemistry. ArgoGel™-MB-OH resin was purchased from Argonaut (Hengoed, United Kingdom). Solvents were purchased from Biosolve (Valkenswaard, The Netherlands). Solvents were stored on molecular sieves (Merck, 0.4 nm), when dry solvents were required. Electrospray ionization (ESI) mass spectrometry was carried out using a Shimadzu LCMS QP-8000 single quadrupole bench top mass spectrometer, coupled with a QP-8000 data system. Analytical HPLC was performed on a Shimadzu LC-10AT Class-VP automated HPLC using an analytical reversed-phase column (Alltech Adsorbosphere C18, 300 Å, 5 µm, 4.6 mm × 250 mm or Alltech Adsorbosphere C8, 90 Å, 5 µm, 4.6 mm × 250 mm) and a UV detector operating at 214 nm and 220 nm. Elution was effected using an appropriate gradient from 0.1% trifluoroacetic acid (TFA) in H_2O/CH_3CN (95/5, v/v) to 0.1% TFA in CH_3CN/H_2O (95/5, v/v). Preparative HPLC was performed using an Alltech Adsorbosphere C8 (10 µm, 22 mm × 250 mm) column with an appropriate gradient from 0.1% TFA in H_2O/CH_3CN (95/5, v/v) to 0.1% TFA in CH_3CN/H_2O (70/30, v/v).

Loading of the ArgoGel™-MB-OH resin

The coupling of Fmoc-Gly-OH to ArgoGel™-MB-OH was performed as described by Sieber [21]. Briefly, 2.94 g ArgoGel™-MB-OH and 3.42 g (11.5 mmol) Fmoc-Gly-OH were placed in a roundbottom flask and dried in a desiccator overnight. Then, 20 mL dry N,N-dimethylformamide (DMF) and 0.93 mL (11.5 mmol) pyridine were added. Subsequently, 1.7 mL (11.9 mmol) 2,6-Dichloro-benzoyl chloride (DCB) was added. After swirling for 72 h at room temperature, the reaction mixture was filtered and the resin was washed three times with DMF, MeOH, dichloromethane (DCM), and Et_2O. The loading of the resin was 0.30 mmol/g.

Synthesis of peptide (1), peptoid-peptide hybrid (2), and all-peptoid (3)

The peptide, the peptoid-peptide hybrid, and the all-peptoid were synthesized using Fmoc-based solid-phase peptide chemistry on Fmoc-Gly-MB-ArgoGel™ resin in an automatic ABI 433A peptide synthesizer instrument in which the couplings of amino acid residues 2-5 were carried out using

the ABI FastMoc 0.25 mmol protocol with a coupling time of 45 min instead of 20 min [22, 23]. The deprotection and coupling reactions were followed by monitoring the dibenzofulvene-piperidine adduct at 301 nm [23]. The α-amino Fmoc protecting group was removed using 20% piperidine in N-methyl-2-pyrrolidone (NMP). 0.36 M 2-(1H-benzotriazole-1-yl)-1,1,3,3-tetramethyluronium hexafluorophosphate (HBTU)/1-hydroxybenzotriazole (HOBt) in NMP was used as coupling solution. The peptoid-peptide hybrid and the all-peptoid were synthesized analogously, with minor modifications: coupling of the amino acids and the peptoid monomers was carried out with 1 equivalent O-(7-azabenzotriazol-1-yl)-1,1,3,3-tetramethyluronium hexafluorophosphate (HATU) and 1 equivalent 1-hydroxy-7-azabenzotriazole (HOAt). After cleavage of the protected peptide from the resin with 1% TFA/DCM the protected peptide, peptoid-peptide hybrid and all-peptoid were cyclized in DMF (1 mg/mL) using 1 equivalent benzotriazole-1-yl-oxy-tris-(dimethylamino)-phosphonium hexafluorophosphate (BOP), 1 equivalent HOBt, and 2 equivalents DiPEA. Subsequent final deprotection of the protecting groups was performed by treatment with TFA/triisopropylsilane (TIS)/H_2O (95/2.5/2.5; 10 mL).

Boc-Glu(OBzl)-NHMe (5)

Boc-Glu(OBzl)-OH (**4**) (1.69 g, 5.0 mmol) and BOP (2.19 g, 5.0 mmol) were dissolved in 22 mL DCM. Subsequently, 1.8 mL (10 mmol) DiPEA was added. After stirring for 1 minute at ambient temperature, 10 mL (20 mmol) 2 M methylamine in tetrahydrofuran (THF) was added. After stirring for 1.5 h at room temperature, the reaction mixture was concentrated in vacuo to remove DCM and excess methylamine and resuspended in EtOAc. The organic layer was washed with saturated $NaHCO_3$ (2 × 50 mL), 1 N $KHSO_4$ (2 × 50 mL), water (1 × 80 mL), and brine (1 × 80 mL). The organic layer was dried over $MgSO_4$ and concentrated in vacuo to give a white solid which was crystallized from EtOAc/hexane to afford Boc-Glu(OBzl)-NHMe (**5**) (1.06 g, 3.0 mmol) in 60% yield. The resulting crude product can be used without further purification. R_f (chloroform/methanol/acetic acid 95:20:3) = 0.79.

Boc-Glu-NHMe (6)

Boc-Glu(OBzl)-NHMe (**5**) (0.98 g, 2.8 mmol) was dissolved in MeOH and hydrogenated (1 atm) in the presence of 10% Pd/C (ca. 100 mg). After stirring for 2 h, the reaction mixture was filtered through Hyflo and evaporation of the solvent in vacuo yielded Boc-Glu-NHMe (**6**) as a white solid. Crystallization from EtOAc/hexane afforded 0.7 g (2.7 mmol) Boc-Glu-NHMe in 96% yield. R_f (chloroform/methanol/acetic acid 95:20:3) = 0.55; ESI-MS: m/z = 283.3 (M + Na^+); ^{1}H NMR (DMSO-d_6, 300 MHz): 7.76 (d, 1H, N*H*CH); 6.90 (s, br, 1H, N*H*CH_3); 3.85 (m, 1H, C*H*CH_2); 2.54 (d, 3H, NHC*H*$_3$); 2.18 (t, 2H, C*H*$_2$COOH); 1.73 (m, 2H, CHC*H*$_2$); 1.37 (s, 9H, 3 C*H*$_3$).

Boc-Glu-NHMe coupling to c(RGDfK), c(nRGDfK), and c(nRGnDnFnK)

132 mg (0.51 mmol) Boc-Glu-NHMe and 57.4 mg (0.50 mmol) N-hydroxysuccinimide were placed in a rondbottom flask. Then, 109 mg (0.53 mmol) 1,3-Dicyclohexylcarbodiimide (DCC)

was dissolved in 5 mL DCM and added to Boc-Glu-NHMe and N-hydroxysuccinimide (HOSu). After stirring for 2 h at room temperature, the reaction mixture was concentrated in vacuo and the residue was titurated in EtOAc. This was filtrated and the filtrate was concentrated in vacuo. The residue was redissolved in 5 mL DCM. The unprotected cyclic pentapeptide, cyclic peptoid-peptide hybrid or cyclic all-peptoid and 131 µL DiPEA (0.75 mmol) were dissolved in 5 mL DMF. Subsequently, this mixture was added to the Boc-Glu(OSu)-NHMe ester dissolved in 5 mL DCM.

Synthesis of peptidomimetic

The peptidomimetic, 2-(2-Amino-ethanesulfonylamino)-3-{4-[2-(1,4,5,6-tetrahydro-pyrimidin-2-ylamino)-ethoxy]-benzoylamino}-propionic acid, was synthesized essentially as described by Hood et al. [19], with minor modifications. The required Cbz-taurylsulfonyl chloride was synthesized according to Brouwer et al. [24]. For the hydrogenation of 4-[2-(pyrimidin-2-ylamino)ethyloxy]benzoyl-2-(S)-benzyloxycarbonylaminoethylsulfonylamino-β-alanine (0.27 g) was dissolved in 65 mL water. This solution was treated with 10% palladium over carbon (0.13 g) and hydrogenated at 45 psi of hydrogen gas for 22 h.

DOTA-conjugation

c(RGDfK)-E(Boc) (**7**) was deprotected by dissolving the compound in DCM/TFA (1:1). After stirring for 2.5 h at room temperature, the reaction mixture was concentrated in vacuo and coevaporated with $CHCl_3$.

84.8 mg (0.22 mmol) HBTU and 70 µL (0.40 mmol) DiPEA were dissolved in 10 mL dry DMF. 1 mL of this solution was added to 14 mg (24 µmol) DOTA-tris(tertBu) (**9**) (Macrocyclics, Dallas, TX, USA) and stirred for 5 minutes at room temperature. The c(RGDfK)-E (13.6 mg) was added and the mixture was stirred for 4.5 h under nitrogen at room temperature. Then the reaction mixture was concentrated in vacuo and the residue was dissolved in 4.75 mL TFA and 250 µL H_2O for deprotection of the Boc-group. This reaction mixture was stirred under nitrogen for 5 h. Subsequently, the reaction mixture was concentrated in vacuo and the residue was dissolved in MeCN/H_2O (1/1) and lyophilized to afford a fluffy solid. The conjugation of DOTA-tris(tertBu) to c(nRGDfK)-E, c(nRGnDnFnK)-E, and to the peptidomimetic and the subsequent deprotection was performed analogously. The crude DOTA-conjugated c(RGDfK)-E, c(nRGDfK)-E, c(nRGnDnFnK)-E, and peptidomimetic were purified by preparative RP-HPLC. Analytical data, including mass spectrometry data, are given in Table 1.

Table 1. Analytical data of DOTA-E-c(RGDfK), DOTA-E-c(nRGDfK), DOTA-E-c(nRGnDnFnK), and DOTA-peptidomimetic.

compound	formula	MW (g/mol)	ESI-MS $(M+H)^+$ calculated	ESI-MS $(M+H)^+$ measured	t_r (min)
DOTA-E-c(RGDfK)	$C_{49}H_{77}N_{15}O_{16}$	1132.23	1132.58	1132.65	18.98
DOTA-E-c(nRGDfK)	$C_{49}H_{77}N_{15}O_{16}$	1132.23	1132.58	1132.65	20.00
DOTA-E-c(nRGnDnFnK)	$C_{49}H_{77}N_{15}O_{16}$	1132.23	1132.58	1132.75	20.00
DOTA-peptidomimetic	$C_{34}H_{54}N_{10}O_{13}S$	842.92	843.47	843.90	19.61

Radiolabeling of the RGD peptides and RGD peptidomimetics

^{111}In-DOTA-E-c(RGDfK), ^{111}In-DOTA-E-c(nRGDfK), and ^{111}In-DOTA-E-c(nRGnDnFnK) were prepared by adding 18.5 MBq $^{111}InCl_3$ (Mallinckrodt, Petten, The Netherlands) to 18.6 µg (16.4 nmol) DOTA-E-c(RGDfK), DOTA-E-c(nRGDfK) or DOTA-E-c(nRGnDnFnK) dissolved in 300 µL 0.5 M ammonium acetate buffer, pH 6.0, containing 0.6 mg/mL gentisic acid. The DOTA-peptidomimetic was radiolabeled with $^{111}InCl_3$ analogously, except that the DOTA-peptidomimetic (14 µg, 16.6 nmol) was dissolved in 500 µL instead of 300 µL 0.5 M ammonium acetate buffer pH 6.0, containing 0.6 mg/mL gentisic acid. The reaction mixtures were degassed under vacuum and the mixtures were heated at 100 °C for 15 minutes. The radiochemical purity was determined by reversed-phase high-performance liquid chromatography (RP-HPLC) (HP 1100 series, Hewlett Packard, Palo Alto, CA, USA) using a C18 column (RX-C18, 4.6 × 250 mm, Zorbax) eluted with a gradient mobile phase (8-20% B over 25 min, solvent A = 25 mM ammonium acetate buffer, solvent B = acetonitrile) at 1 mL/min. The radioactivity of the eluate was monitored using an in-line radiodetector (Flo-One Beta series, Radiomatic, Meriden, CT, USA).

In vitro stability

The stability of the ^{111}In-labeled compounds was determined by incubating the compounds in 90-110 µL human serum for 2 h, 6 h, and 24 h at 37 °C. The stability of the compounds was also determined after 4 h of incubation in phosphate-buffered saline (PBS) at 37 °C. Before analysis of the serum samples the serum proteins were precipitated by adding an equal volume of MeCN to the samples. Samples were centrifuged for 5 minutes at 14000 rpm and 20 µL of supernatant was analyzed on RP-HPLC. The PBS samples were analyzed without any sample preparation.

Solid-phase receptor binding assay

The IC_{50} of DOTA-E-c(RGDfK), DOTA-E-c(nRGDfK), DOTA-E-c(nRGnDnFnK), and the DOTA-peptidomimetic for $\alpha_v\beta_3$ integrin was determined using a solid-phase competitive binding assay. ^{111}In-labeled DOTA-E-[c(RGDfK)]$_2$ (3 MBq/µg) was prepared as described previously [25] and was used as the tracer in this assay.

Microtiter 96-well vinyl assay plates (Corning B.V., Schiphol-Rijk, The Netherlands) were coated with 100 µL/well of a solution of purified human integrin $\alpha_v\beta_3$ (150 ng/mL) in Triton X-100 Formulation (Chemicon International, Temecula, CA, USA) in coating buffer (25 mM Tris-HCl, pH 7.4, 150 mM NaCl, 1 mM $CaCl_2$, 0.5 mM $MgCl_2$ and 1 mM $MnCl_2$) for 17 h at 4 °C. The plate was washed twice with binding buffer (0.1% bovine serum albumin (BSA) in coating buffer). The wells were blocked for 2 h with 200 µL blocking buffer (1% BSA in coating buffer). The wells were washed twice with binding buffer. Then 100 µL binding buffer containing 11.1 kBq of ^{111}In-DOTA-E-[c(RGDfK)]$_2$ and appropiate dilutions of non-labeled DOTA-E-c(RGDfK), DOTA-E-c(nRGDfK), DOTA-E-c(nRGnDnFnK), DOTA-peptidomimetic, and DOTA-E-[c(RGDfK)]$_2$ in binding buffer were incubated in the wells at 37 °C for 1 h. After incubation, the plate was washed three times with binding buffer. The wells were cut and radioactivity in each well was counted in a γ-counter

(1480 Wizard, Wallac, Turku, Finland). IC_{50} values of the RGD peptides and peptidomimetics were calculated by non-linear regression using GraphPad Prism (GraphPad Prism 4.0 Software Package, San Diego, CA, USA). Each data point is the average of triplicate wells. K_i values were calculated from IC_{50} values using the Cheng-Prusoff equation as described by Cheng [26, 27]. The Hill slope (K) of DOTA-E-$[c(RGDfK)]_2$ concentration-response curve was 0.6.

Biodistribution studies

6-8 Weeks old female nude BALB/c mice were injected subcutaneously (s.c.) in the left flank with 0.2 mL of a cell suspension of IGROV1 human ovarian carcinoma cells (1×10^7 cells/mL). Two weeks after inoculation of the tumor cells, when the diameter of the tumor was 6-8 mm, mice were randomly divided in three groups (4 mice/group).

For biodistribution studies, mice received 370 kBq of each of the ^{111}In-labeled compounds via a tail vein. Mice were killed at 2 h postinjection (p.i.). Blood, tumor, and the major organs and tissues were collected, weighed, and counted in a γ-counter. The percentage injected dose per gram (%ID/g) was determined for each sample.

The receptor-mediated localization of the ^{111}In-labeled compounds was investigated by determining the biodistribution of the ^{111}In-labeled compounds in the presence of an excess unlabeled compound (n=2).

Results

Radiolabeling

RP-HPLC analysis indicated that the radiochemical purity of ^{111}In-DOTA-E-c(RGDfK), ^{111}In-DOTA-E-c(nRGDfK), ^{111}In-DOTA-E-c(nRGnDnFnK), and ^{111}In-DOTA-peptidomimetic used in the experiments always exceeded 95%, when radiolabeled at a specific activity of 1 MBq/nmol. The elution profile of ^{111}In-DOTA-E-c(RGDfK), ^{111}In-DOTA-E-c(nRGDfK), ^{111}In-DOTA-E-c(nRGnDnFnK), and ^{111}In-DOTA-peptidomimetic showed a single peak for each of the four compounds with a retention time of 14 min for ^{111}In-DOTA-E-c(RGDfK), ^{111}In-DOTA-E-c(nRGDfK), and ^{111}In-DOTA-E-c(nRGnDnFnK). The retention time of the ^{111}In-DOTA-peptidomimetic was 9 min.

In vitro stability

^{111}In-DOTA-E-c(RGDfK), ^{111}In-DOTA-E-c(nRGDfK), and ^{111}In-DOTA-peptidomimetic were stable for at least 4 h in PBS. There was no evidence of degradation of ^{111}In-DOTA-E-c(RGDfK) and ^{111}In-DOTA-E-c(nRGDfK) after incubation for 6 h in human serum. The ^{111}In-DOTA-peptidomimetic was less stable. After incubation in human serum for 6 h, only 50% of the activity was still associated with the labeled compound.

Solid-phase receptor binding assay

The results of a competitive displacement study to compare the affinity of DOTA-E-c(RGDfK), DOTA-E-c(nRGDfK), DOTA-E-c(nRGnDnFnK), and the DOTA-peptidomimetic for the $\alpha_v\beta_3$ integrin are summarized in Figure 2. The IC_{50} values were 236 nM for DOTA-E-c(RGDfK), 9.25 mM for DOTA-E-c(nRGDfK), and 219 nM for the DOTA-peptidomimetic (Figure 2). The IC_{50} value of DOTA-E-c(nRGnDnFnK) was > 10 mM. Calculated K_i values using Cheng-Prusoff equation were 8.92 nM for DOTA-E-c(RGDfK), 403 nM for DOTA-E-c(nRGDfK), and 8.62 nM for DOTA-peptidomimetic.

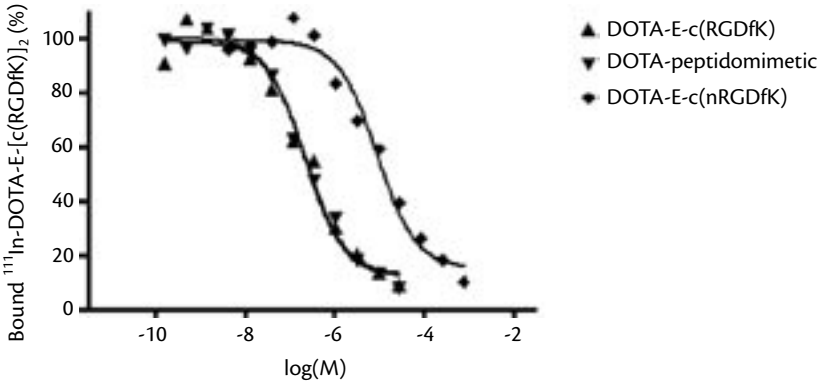

Figure 2. Competition of specific binding of ^{111}In-DOTA-E-[c(RGDfK)]$_2$ with DOTA-peptidomimetic, DOTA-E-c(nRGDfK), and DOTA-E-c(RGDfK).

Biodistribution studies

The results of the study of ^{111}In-DOTA-E-c(RGDfK), ^{111}In-DOTA-E-c(nRGDfK), and ^{111}In-DOTA-peptidomimetic in athymic mice with s.c. IGROV1 tumors are summarized in Figure 3. The ^{111}In-labeled peptide, the peptoid-peptide hybrid, the all-peptoid, and the peptidomimetic all cleared rapidly from the blood (0.02 ± 0.003 %ID/g, 0.02 ± 0.0003 %ID/g, 0.01 ± 0.002 %ID/g, and 0.07 ± 0.008 %ID/g, 2 h p.i.). The uptake in the tumor of the peptide (1.73 ± 0.37 %ID/g) and the peptidomimetic (2.04 ± 0.30 %ID/g) were higher than that of the peptoid-peptide hybrid (0.45 ± 0.07 %ID/g). The all-peptoid had the lowest uptake in the tumor (0.11 ± 0.04 %ID/g). As the blood level of the peptide was lower than the blood level of the peptidomimetic 2 h p.i., the tumor-to-blood ratio of the peptide was higher (74.0 ± 16.5) than that of the peptidomimetic (29.7 ± 3.23). The tumor-to-blood ratio of the peptoid-peptide hybrid was 24.5 ± 3.7. Coinjection of an excess of unlabeled compound resulted in a significant decrease of radioactivity in the tumor, indicating that the uptake of ^{111}In-DOTA-E-c(RGDfK), ^{111}In-DOTA-E-c(nRGDfK), and ^{111}In-DOTA-peptidomimetic in the tumor was $\alpha_v\beta_3$-mediated. Uptake in normal organs such as spleen, liver, intestine, and colon was also reduced in the presence of an excess cold DOTA-E-c(RGDfK), DOTA-E-c(nRGDfK), and DOTA-peptidomimetic, indicating that part of the uptake in these tissues was also $\alpha_v\beta_3$-mediated.

Uptake of ^{111}In-DOTA-E-c(nRGnDnFnK) in the tumor was not $\alpha_v\beta_3$-mediated, since coinjection of an excess of unlabeled DOTA-E-c(nRGnDnFnK) showed no significant decrease of the activity concentration in the tumor (0.12 ±0.04 %ID/g).

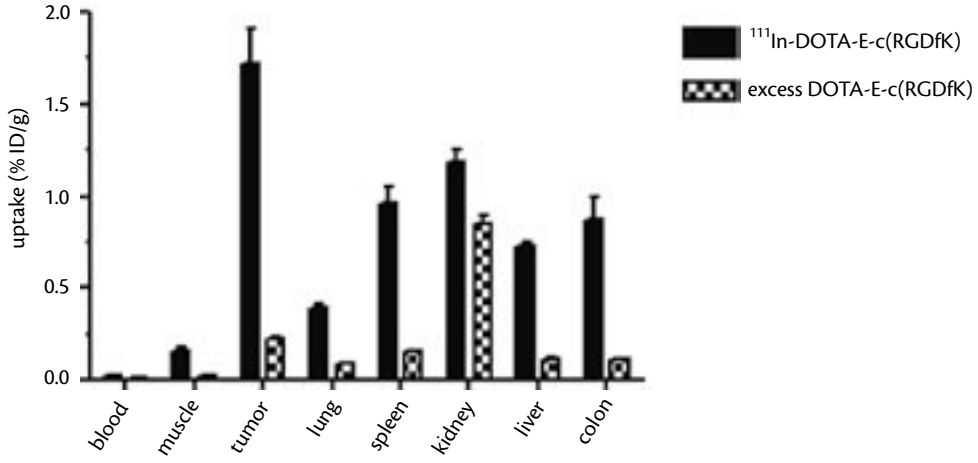

Figure 3A. Biodistribution of ^{111}In-DOTA-E-c(RGDfK) in the absence and presence of an excess of unlabeled DOTA-E-c(RGDfK) at 2 h p.i. in athymic mice with s.c. IGROV1 tumors.

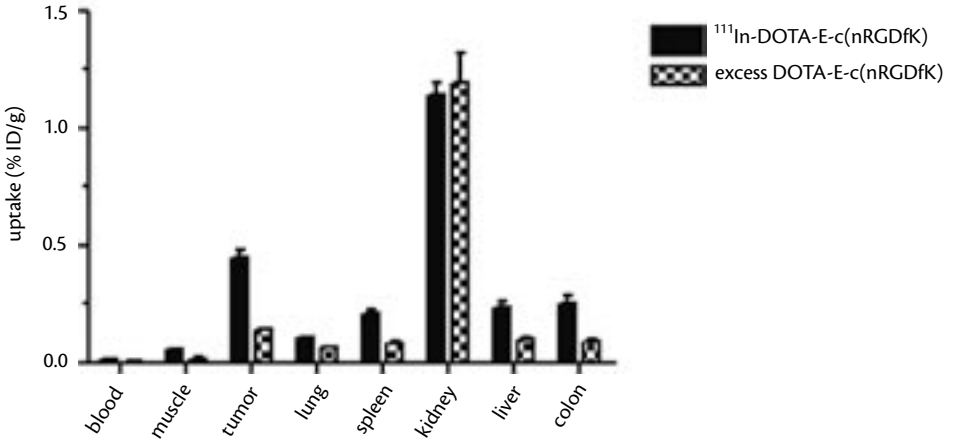

Figure 3B. Biodistribution of ^{111}In-DOTA-E-c(nRGDfK) in the absence and presence of an excess unlabeled DOTA-E-c(nRGDfK) at 2 h p.i. in athymic mice with s.c. IGROV1 tumors.

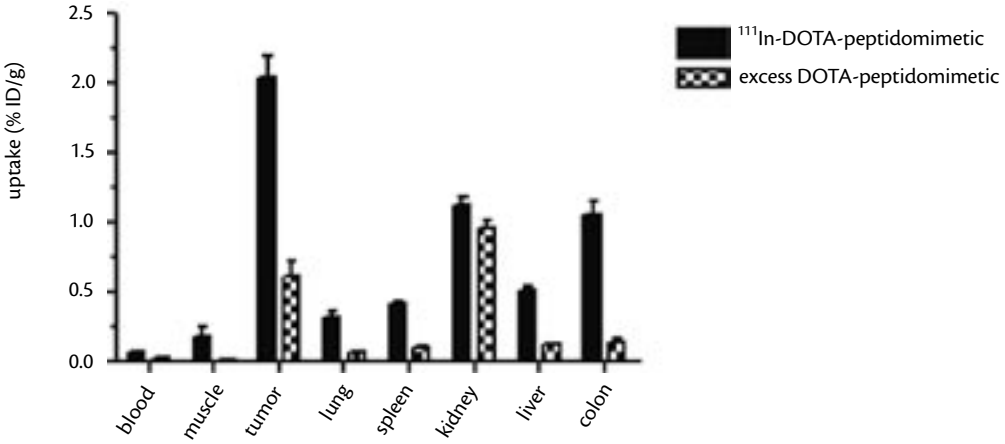

Figure 3C. Biodistribution of ^{111}In-DOTA-peptidomimetic in the absence and presence of an excess unlabeled DOTA-peptidomimetic at 2 h p.i. in athymic mice with s.c. IGROV1 tumors.

Discussion

Here, we describe the synthesis of four $\alpha_v\beta_3$ integrin binding compounds (Scheme 1 and 2). The radiolabeling, the stability and the in vitro and in vivo tumor targeting characteristics of these compounds were determined.

The binding affinity for $\alpha_v\beta_3$ of the four compounds was determined in a solid-phase competitive binding assay. The DOTA-peptidomimetic and DOTA-E-c(RGDfK) had the highest affinity. The IC_{50} of c(nRGDfK)-E was more than 20 times higher, indicating that the substitution of the arginine residue by its peptoid residue analog markedly affected the affinity for the $\alpha_v\beta_3$ integrin. Apparently, the altered position of the amino acid side chain greatly affected $\alpha_v\beta_3$ binding. This could be due to the unfavorable location of the side chain of the peptoid, the increased flexibility of the peptoid-peptide hybrid compared to the peptide, or to the fact that a potential hydrogen bond cannot be formed since there is no hydrogen atom present on the backbone nitrogen atom [16]. The last two factors could also explain the fact that the all-peptoid has no affinity for $\alpha_v\beta_3$ as determined in vitro. Recently, Xiong et al. described that each residue of the Arg-Gly-Asp sequence participates extensively in the interaction with the $\alpha_v\beta_3$ integrin [28]. This could explain that minor modifications in the RGD sequence, such as in the peptoid-peptide hybrid, reduce the affinity for the $\alpha_v\beta_3$ integrin. The IC_{50} values of the compounds were relatively high compared to other $\alpha_v\beta_3$ binding ligands. However, K_i values calculated from these IC_{50} values are in the single digit nanomolar range for DOTA-E-c(RGDfK) and DOTA-peptidomimetic, indicating that these compounds have a relatively high affinity for the $\alpha_v\beta_3$ integrin.

Stability tests revealed good stability of ^{111}In-DOTA-E-c(RGDfK) and ^{111}In-DOTA-E-(nRGDfK) after incubation for 6 h in human serum. In serum, ^{111}In-DOTA-peptidomimetic showed some degradation after 6 h.

The tumor targeting potential of the radiolabeled cyclic RGD peptide, the peptoid-peptide hybrid analog, and the peptidomimetic integrin $\alpha_v\beta_3$ receptor antagonist were evaluated in athymic mice with s.c. IGROV1 tumors. The IGROV1 tumor consistently expresses $\alpha_v\beta_3$ at a relatively high level. In this model, the cyclic RGD peptide and the peptidomimetic showed the highest uptake in the tumor, 1.73 ± 0.4 %ID/g and 2.04 ± 0.3 %ID/g, respectively. Apparently, the in vitro minor instability of DOTA-peptidomimetic does not hamper in vivo tumor targeting. The uptake of the peptoid-peptide hybrid was significantly lower: 0.45 ± 0.07 %ID/g. This is in line with its lower affinity. The all-peptoid had no detectable affinity for $\alpha_v\beta_3$ (IC_{50} > 10 mM) and this compound did not show specific tumor uptake in this model.

In the presence of an excess of unlabeled compound, the specificity of the tumor targeting of the peptide and the peptidomimetic could be demonstrated. Even for the peptoid-peptide hybrid the uptake in the presence of an excess cold agent was significantly reduced, indicating that this compound also showed some specific localization in the tumor. Remarkably, non-tumor tissues such as liver, spleen, and colon also showed specific uptake of the three compounds, suggesting $\alpha_v\beta_3$ expression in these tissues. Indeed, $\alpha_v\beta_3$ expression on the vasculature of these tissues in humans was described by Max et al. [29]. Presumably, the murine tissues such as lung, liver, spleen, and colon also express $\alpha_v\beta_3$ on their vasculature, causing specific uptake in these tissues of the radiolabeled compounds.

The four compounds cleared rapidly from the blood via the kidneys. ^{111}In-DOTA-peptidomimetic cleared slower from the blood than ^{111}In-DOTA-E-c(RGDfK) and ^{111}In-DOTA-c(nRGDfK)-E, resulting in lower tumor-to-blood ratios for ^{111}In-DOTA-peptidomimetic. Recently, Chen et al. studied the ^{64}Cu-labeled RGD peptide ^{64}Cu-DOTA-c(RGDyK) in a MDA-MB-435 breast cancer xenograft model. Although tested in another model, our RGD peptide showed a similar biodistribution compared to their compound [30]. In contrast to ^{111}In-DOTA-E-c(RGDfK), ^{64}Cu-DOTA-c(RGDyK) showed persistent activity in liver and kidney. The uptake in these organs could be reduced by PEGylating the compound [31, 32].

In conclusion, in vivo $\alpha_v\beta_3$ targeting of the non-amino acid containing peptidomimetic was as high as that of the native DOTA-conjugated cyclic RGD peptide. Modification of the cyclic RGD peptide to a peptoid-peptide hybrid resulted in loss of affinity for $\alpha_v\beta_3$ and thus lower tumor uptake. The all-peptoid analog has no affinity for $\alpha_v\beta_3$ and no tumor targeting.

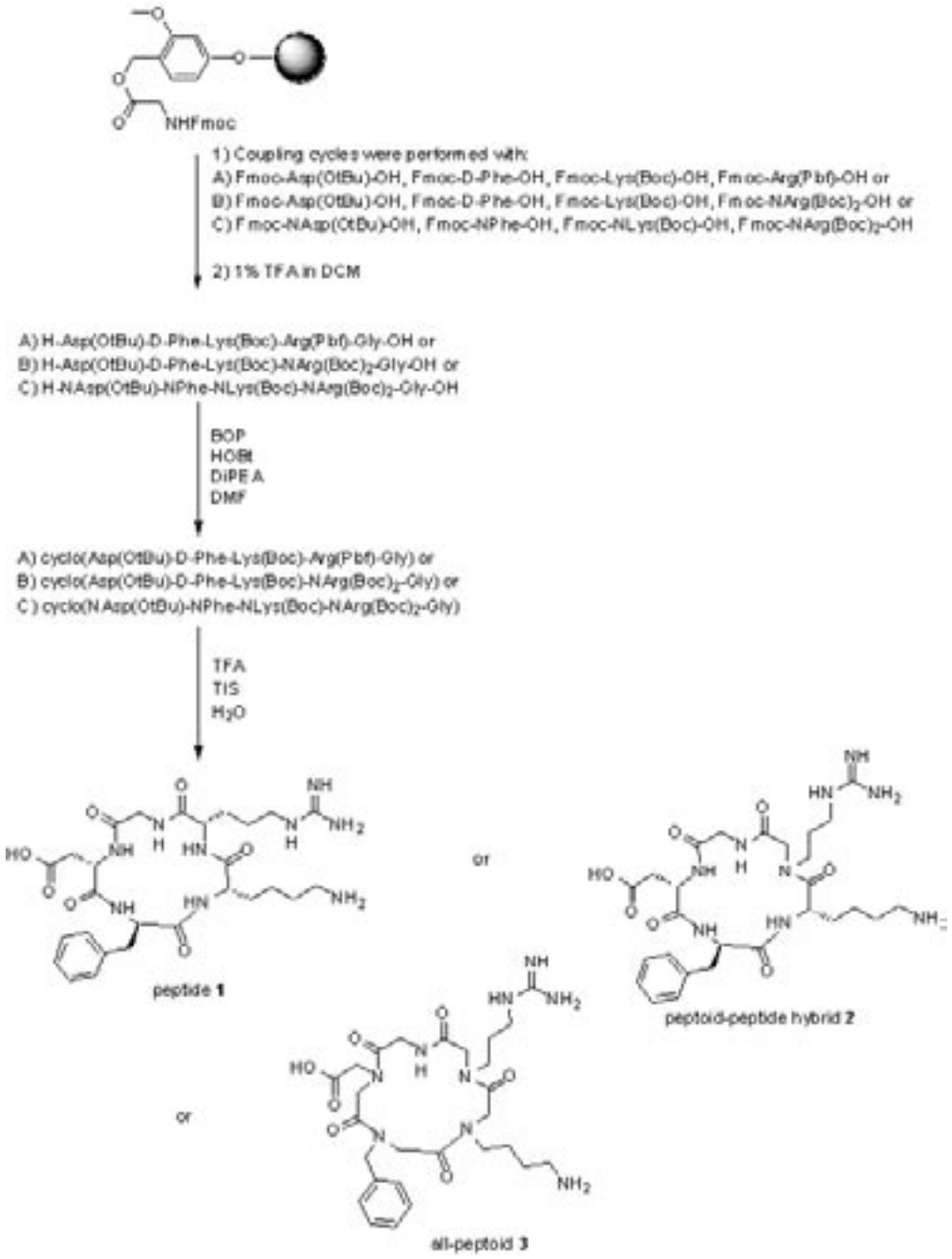

Scheme 1. Synthesis of the peptide, peptoid-peptide hybrid, and the all-peptoid.

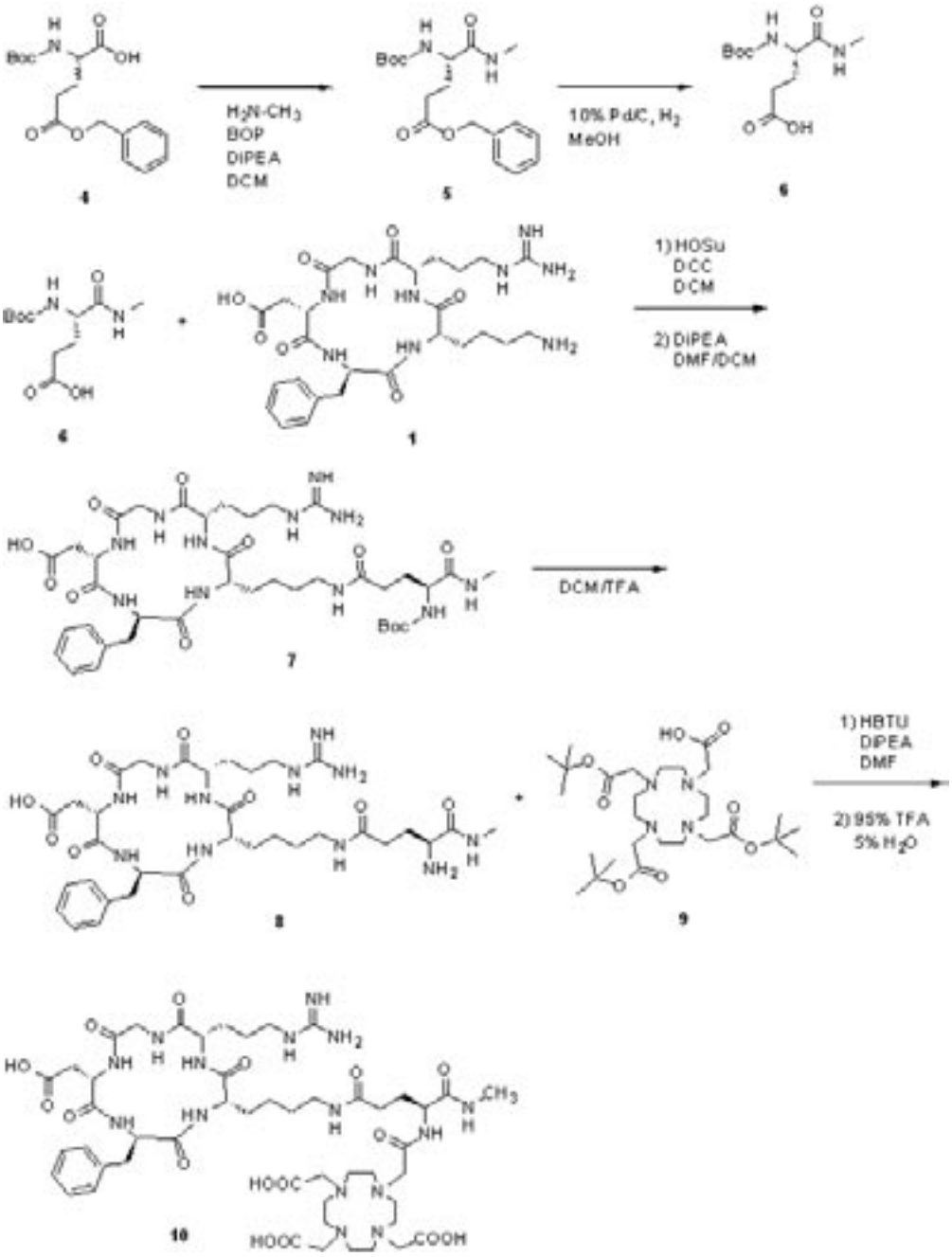

Scheme 2. Synthesis and coupling of Boc-Glu-NHMe to the peptide, peptoid-peptide hybrid, and the all-peptoid and subsequent DOTA-conjugation.

References

1. Ruoslathi E, Pierschbacher MD. New perspectives in cell adhesion: RGD and integrins. Science 1987;238:491-7.
2. Teitelbaum SL. Bone resorption by osteoclasts. Science 2000;289:1504-8.
3. Bishop GG, McPherson JA, Sanders JM, Hesselbacher SE, Feldman MJ, McNamara CA, et al. Selective alpha(v)beta(3)-receptor blockade reduces macrophage infiltration and restenosis after balloon angioplasty in the atherosclerotic rabbit. Circulation 2001;103:1906-11.
4. Albelda SM, Smith CW, Ward PA. Adhesion molecules and inflammatory injury. FASEB J 1994;8:504-12.
5. Storgard CM, Stupack DG, Jonczyk A, Goodman SL, Fox RI, Cheresh DA. Decreased angiogenesis and arthritic disease in rabbits treated with an alpha(v)beta(3) antagonist. J Clin Invest 1999;103:47-54.
6. Clezardin P. Recent insights into the role of integrins in cancer metastasis. Cell Mol Life Sci 1998; 54:541-8.
7. Eliceiri BP, Cheresh DA. The role of alpha(v) integrins during angiogenesis: insights into potential mechanisms of action and clinical development. J Clin Invest 1999;103:1227-30.
8. Smith JW, Cheresh DA. The Arg-Gly-Asp Binding Domain of the Vitronectin Receptor. Photoaffinity cross-linking implicates amino acid residues 61-203 of the β subunit. J Biol Chem 1988;263:18726-31.
9. Haubner R, Finsinger D, Kessler H. Stereoisomeric Peptide Libraries and Peptidomimetics for Designing Selective Inhibitors of the $\alpha_v\beta_3$ Integrin for a New Cancer Therapy. Angew Chem Int Ed Engl 1997;36:1374-89.
10. Aumailley M, Gurrath M, Muller G, Calvete J, Timpl R, Kessler H. Arg-Gly-Asp constrained within cyclic pentapeptides. Strong and selective inhibitors of cell adhesion to vitronectin and laminin fragment P1. FEBS Lett 1991;291:50-4.
11. Gurrath M, Muller G, Kessler H, Aumailley M, Timpl R. Conformation/activity studies of rationally designed potent anti-adhesive RDG peptides. Eur J Biochem 1992;210:911-21.
12. Haubner R, Wester HJ, Reuning U, Senekowitsch-Schmidtke R, Diefenbach B, Kessler H, et al. Radiolabeled $\alpha_v\beta_3$ Integrin Antagonists: A New Class of Tracers for Tumor Targeting. J Nucl Med 1999;40:1061-71.
13. Schottelius M, Wester HJ, Reubi JC, Senekowitsch-Schmidtke R, Schwaiger M. Improvement of pharmacokinetics of radioiodinated Tyr^3-octreotide by conjugation with carbohydrates. Bioconjug Chem 2002;13:1021-30.
14. Haubner R, Kuhnast B, Mang C, Weber WA, Kessler H, Wester HJ, et al. [^{18}F]Galacto-RGD: synthesis, radiolabeling, metabolic stability, and radiation dose estimates. Bioconjug Chem 2004;15:61-9.
15. Haubner R, Weber WA, Beer AJ, Vabuliene E, Reim D, Sarbia M, et al. Noninvasive visualization of the activated $\alpha v\beta 3$ integrin in cancer patients by positron emission tomography and [^{18}F]Galacto-RGD. PloS Med 2005;2:e70.
16. de Haan EC, Wauben MHM, Grosfeld-Stulemeyer MC, Kruijtzer JAW, Liskamp RMJ, Moret EE. Major histocompatibility complex class II binding characteristics of peptoid-peptide hybrids. Bioorg Med Chem 2002;10: 1939-45.
17. Dechantsreiter MA, Planker E, Mathä B, Lohof E, Hölzemann G, Jonczyk A, et al. N-Methylated Cyclic RGD Peptides as Highly Active and Selective $\alpha_v\beta_3$ Integrin Antagonists. J Med Chem 1999;42:3033-40.
18. Simon RJ, Kania RS, Zuckermann RN, Huebner VD, Jewell DA, Banville S, et al. Peptoids: A modular approach to drug discovery. Proc Natl Acad Sci U.S.A. 1992;89;9367-71.
19. Hood JD, Bednarski M, Frausto R, Guccione S, Reisfeld RA, Xiang R, et al. Tumor regression by targeted gene delivery to the neovasculature. Science 2002;296:2404-7.

20. Kruijtzer JAW, Hofmeyer LJF, Heerma W, Versluis C, Liskamp RMJ. Solid-phase synthesis of peptoids using Fmoc-protected N-substituted glycines: the synthesis of (retro)peptoids of Leu-enkephalin and substance P. Chem Eur J 1998;4:1570-80.

21. Sieber P. An improved method for anchoring of 9-fluorenylmethoxycarbonyl-amino acids to 4-alkoxybenzyl alcohol resins. Tetrahedron Lett 1987;28:6147-50.

22. Applied Biosystems Model 433A Peptide Synthesizers User's Manual june 1993, Version 1.0.

23. Applied Biosystems Research News june 1993, Model 433A Peptide Synthesizer, 1-12.

24. Brouwer AJ, Monnee MCF, Liskamp RMJ. An efficient synthesis of N-protected beta-aminoethanesulfonyl chlorides: Versatile building blocks for the synthesis of oligopeptidosulfonamides. Synthesis 2002;11:1579-84.

25. Janssen M, Frielink C, Dijkgraaf I, Oyen W, Edwards DS, Rajopadhye M, et al. Improved tumor targeting of radiolabeled RGD peptides using rapid dose fractionation. Cancer Biother Radiopharm 2004;19:399-404.

26. Cheng HC. The power issue: determination of K_B or K_i from IC_{50}. A closer look at the Cheng-Prusoff equation, the Schild plot and related power equations. J Pharmacol Toxicol Methods 2002;46:61-71.

27. Cheng HC. The influence of cooperativity on the determination of dissociation constants: examination of the Cheng-Prusoff equation, the Scatchard analysis, the Schild analysis and related power equations. Pharmacol Res 2004;50:21-40.

28. Xiong JP, Stehle T, Zhang R, Joachimiak A, Frech M, Goodman SL, et al. Crystal Structure of the Extracellular Segment of Integrin αvβ3 in Complex with an Arg-Gly-Asp Ligand. Sience 2002;296:151-5.

29. Max R, Gerritsen RRCM, Nooijen PTGA, Goodman SL, Sutter A, Keilholz U, et al. Immunohistochemical analysis of integrin αvβ3 expression on tumor-associated vessels of human carcinomas. Int J Cancer 1997;71:320-4.

30. Chen X, Park R, Tohme M, Shahinian AH, Bading JR, Conti PS. MicroPET and Autoradiographic Imaging of Breast Cancer α_v-Integrin Expression Using ^{18}F- and ^{64}Cu-Labeled RGD Peptide. Bioconjugate Chem 2004;15:41-9.

31. Chen X, Park R, Shahinian AH, Bading JR, Conti PS. Pharmacokinetics and tumor retention of ^{125}I-labeled RGD peptide are improved by PEGylation. Nucl Med Biol 2004;31:11-9.

32. Chen X, Hou Y, Tohme M, Park R, Khankaldyyan V, Gonzales-Gomez I, et al. Pegylated Arg-Gly-Asp Peptide: ^{64}Cu Labeling and PET Imaging of Brain Tumor $\alpha_v\beta_3$-Integrin Expression. J Nucl Med 2004;45:1776-83.

Chapter 3

Improved targeting of the $\alpha_v\beta_3$ integrin by multimerization of RGD peptides

Ingrid Dijkgraaf
John A. W. Kruijtzer
Shuang Liu
Annemieke C. Soede
Wim J. G. Oyen
Frans H. M. Corstens
Rob M. J. Liskamp
Otto C. Boerman

Eur J Nucl Med Mol Imaging 2007:34;267-273

Abstract

The integrin $\alpha_v\beta_3$ is expressed on sprouting endothelial cells and on various tumor cell types. Due to the restricted expression of $\alpha_v\beta_3$ in tumors, $\alpha_v\beta_3$ is considered a suitable receptor for tumor targeting. In this study, the $\alpha_v\beta_3$ binding characteristics of an ^{111}In-labeled monomeric, dimeric, and tetrameric RGD analog were compared.

Methods: A monomeric (E-c(RGDfK)), dimeric (E-[c(RGDfK)]$_2$), and tetrameric (E{E[c(RGDfK)]$_2$}$_2$) RGD peptide were synthesized, conjugated with DOTA, and radiolabeled with ^{111}In. In vitro $\alpha_v\beta_3$ binding characteristics were determined in a competitive binding assay. In vivo $\alpha_v\beta_3$ targeting characteristics of the compounds were assessed in mice with SK-RC-52 xenografts.

Results: The IC_{50} values for DOTA-E-c(RGDfK), DOTA-E-[c(RGDfK)]$_2$, and DOTA-E{E[c(RGDfK)]$_2$}$_2$ were 120 nM, 69.9 nM, and 19.6 nM, respectively. At all time points, the tumor uptake of the dimer was significantly higher as compared to that of the monomer. Tumor uptake of the tetramer (7.40 ± 1.12 %ID/g) was significantly higher than that of the monomer (2.30 ± 0.34 %ID/g), $P<0.001$ and the dimer (5.17 ± 1.22 %ID/g), $P<0.05$ at 8 h p.i.. At 24 h p.i. the tumor uptake was significantly higher for the tetramer (6.82 ± 1.41 %ID/g), compared to that of the dimer (4.22 ± 0.96 %ID/g), $P<0.01$ and the monomer (1.90 ± 0.29 %ID/g).

Conclusions: Multimerization of c(RGDfK) resulted in enhanced affinity for $\alpha_v\beta_3$ as determined in vitro. Tumor uptake of a tetrameric RGD peptide was significantly higher compared to that of the monomeric and dimeric analogs, presumably due to the enhanced statistical likelihood for rebinding to $\alpha_v\beta_3$.

Introduction

The $\alpha_v\beta_3$ integrin is a transmembrane protein consisting of two non-covalently bound subunits, α and β. Integrin $\alpha_v\beta_3$ is preferentially expressed on proliferating endothelial cells [1], whereas it is absent on quiescent endothelial cells. For growth beyond the size of 1-2 mm in diameter, tumors require the formation of new blood vessels. Consequently, $\alpha_v\beta_3$ expression on tumor vasculature is considered as a marker of tumor-induced angiogenesis [2-4]. In addition, $\alpha_v\beta_3$ is expressed on the cell membrane of various tumor cell types, such as ovarian cancer, neuroblastoma, breast cancer, melanoma, a.o.. Due to this restricted expression of $\alpha_v\beta_3$ in tumors, $\alpha_v\beta_3$ is considered a suitable target for tumor targeting [5]. This integrin can bind to the arginine-glycine-aspartic acid (RGD) amino acid sequence present in extracellular matrix proteins such as vitronectin, fibrinogen, and laminin [6]. Based on the RGD tripeptide sequence a series of small peptides have been designed to antagonize the function of the $\alpha_v\beta_3$ integrin [7]. Especially the cyclic peptide derivatives have a relatively high affinity for the $\alpha_v\beta_3$ integrin. A series of RGD sequence containing peptides has been tested for their ability to bind the $\alpha_v\beta_3$ integrin. It was found that the cyclic derivative cyclic(Arg-Gly-Asp-D-Phe-Val) was a 100-fold better inhibitor of cell adhesion to vitronectin than the linear variant, having an IC_{50} value in the nanomolar range [8, 9].

In previous studies we have shown that radiolabeled c(RGDfK)-peptides specifically accumulated in $\alpha_v\beta_3$-positive ovarian cancer xenografts in athymic mice [10]. The aim of this study was to develop modified ligands for improved $\alpha_v\beta_3$ integrin targeting by preparing multimers of cyclic RGD peptides. A multimeric RGD peptide could theoretically bind multivalently and thus more avidly to the target cell. However, the distance between the RGD units of the multivalent RGD peptides is too short to allow simultaneous binding to multiple $\alpha_v\beta_3$ integrins on the cell surface. Therefore, in this chapter we avoid to use the term avidity and only use affinity.

Multivalent interactions are frequently used in nature to increase the affinity of weak ligand-receptor interactions [11, 12]. For example, the attachment of an influenza virus to its target cell occurs through multiple simultaneous interactions between hemagglutinin (HA) and sialic acid (SA) [12]. Multivalent structures for the design of drugs and research agents have become a new focus of investigation. Several research groups, including ours, have applied multivalent compounds to enhance the interaction between the ligand and the target cell [13]. Goel et al. radiolabeled divalent and tetravalent scFv's of monoclonal antibody (MAb CC49 with ^{99m}Tc and analyzed the imaging potential of these novel radioimmunoconjugates. Biodistribution studies demonstrated that ^{99m}Tc-[sc(Fv)$_2$]$_2$ had approximately 3-fold higher tumor localization than ^{99m}Tc-sv(Fv)$_2$ [14]. Recently, a new multivalent synthetic inhibitor of epidemic keratoconjunctivitis-causing adenovirus was evaluated by Johansson et al. [11]. Their results clearly indicated that the inhibition is significantly increased with higher orders of valency. Similarly, Kok et al. and Maheshwari et al. showed increased affinity of RGD ligands with the target cell due to multivalent interactions [15, 16].

Here we describe the synthesis of a monomeric, E-c(RGDfK), dimeric, E-[c(RGDfK)]$_2$, and tetrameric RGD peptide, E{E[c(RGDfK)]$_2$}$_2$. The RGD peptides were conjugated with 1,4,7,10-tetraazacyclododecane-N,N',N'',N'''-tetraacetic acid (DOTA) and radiolabeled with ^{111}In. Subsequently, the in vitro affinity and the in vivo tumor targeting characteristics of the peptides to $\alpha_v\beta_3$ expressing tumors were determined.

Materials and methods

Synthesis of DOTA-conjugated RGD peptides

The monomeric RGD peptide was synthesized using Fmoc-based solid-phase peptide synthesis as described previously [17]. The structural formula of DOTA-E-c(RGDfK) is shown in Figure 1a.

The synthesis of the dimeric cyclic RGD peptide E-[c(RGDfK)]$_2$ conjugated with DOTA was described previously [18]. The structural formula of DOTA-E-[c(RGDfK)]$_2$ is shown in Figure 1b.

The synthesis of the tetrameric cyclic RGD peptide E{E[c(RGDfK)]$_2$}$_2$ conjugated with DOTA was described previously [19]. The structural formula of DOTA-E{E[c(RGDfK)]$_2$}$_2$ is shown in Figure 1c.

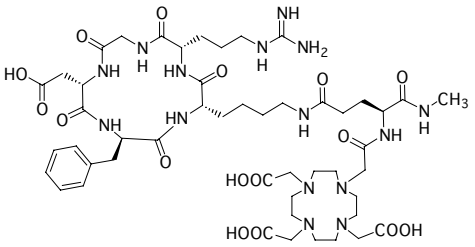

Figure 1a. Structural formula of the DOTA-conjugated monomeric RGD peptide, DOTA-E-c(RGDfK).

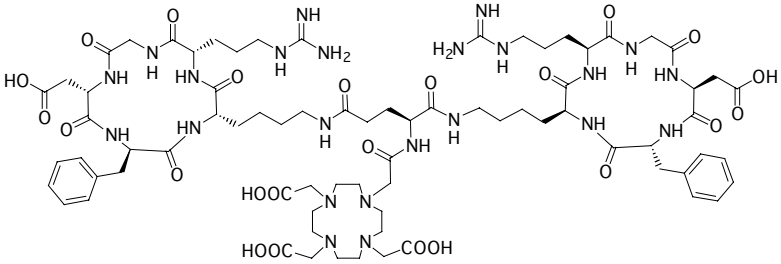

Figure 1b. Structural formula of the DOTA-conjugated dimeric RGD peptide, DOTA-E-$[c(RGDfK)]_2$.

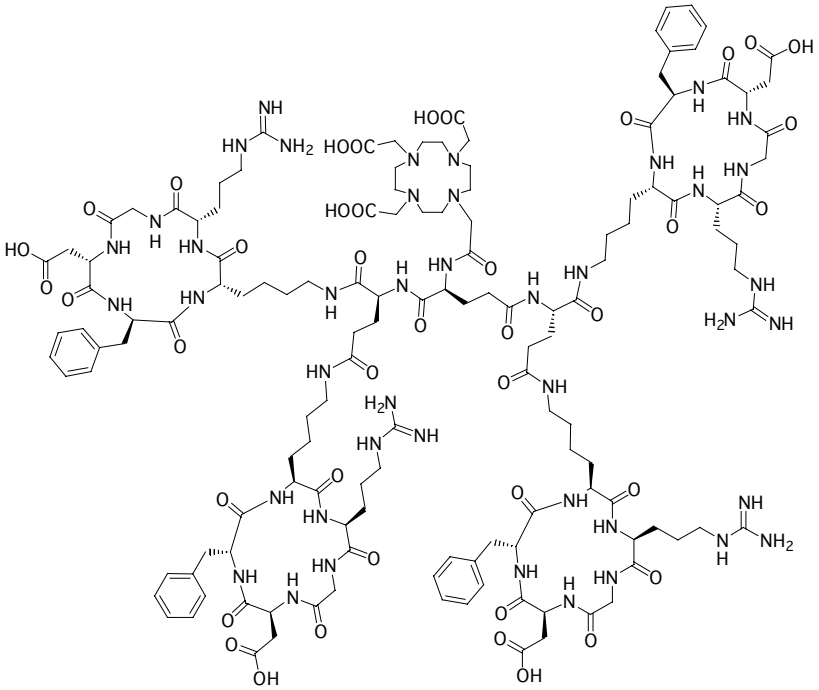

Figure 1c. Structural formula of the DOTA-conjugated tetrameric RGD peptide, DOTA-E$\{E[c(RGDfK)]_2\}_2$.

Radiolabeling of the RGD peptides

^{111}In-DOTA-E-c(RGDfK) was prepared by adding 14 MBq $^{111}InCl_3$ (Mallinckrodt, Petten, The Netherlands) to 15 µg (13.3 nmol) DOTA-E-c(RGDfK) dissolved in 300 µL 0.5 M ammonium acetate buffer, pH 6.0, containing 0.6 mg/mL gentisic acid. DOTA-E-$[c(RGDfK)]_2$ and DOTA-E$\{E[c(RGDfK)]_2\}_2$ were radiolabeled with $^{111}InCl_3$ analogously with minor modifications. DOTA-E-$[c(RGDfK)]_2$ (28 µg, 16.4 nmol) and DOTA-E$\{E[c(RGDfK)]_2\}_2$ (15 µg, 4.79 nmol) were dissolved in 500 µL 0.5 M ammonium acetate buffer pH 6.0, containing 0.6 mg/mL gentisic acid. DOTA-E-$[c(RGDfK)]_2$ was radiolabeled with 17 MBq $^{111}InCl_3$ and DOTA-E$\{E[c(RGDfK)]_2\}_2$ was radiolabeled with 13 MBq $^{111}InCl_3$. The reaction mixtures were degassed and subsequently the mixtures were heated at 100 °C for 15 minutes. ^{111}In-DOTA-E$\{E[c(RGDfK)]_2\}_2$ was further purified on a C-18 SepPak cartridge (Waters, Milford, MA). After applying the sample on the methanol-activated cartridge, the cartridge was washed with 5 mL 25 mM ammonium acetate and eluted with 25% acetonitrile in 25 mM ammonium acetate. The radiochemical purity was determined by reversed-phase high-performance liquid chromatography (RP-HPLC) (HP 1100 series, Hewlett Packard, Palo Alto, CA, USA) using a C18 column (RX-C18, 4.6 mm × 250 mm, Zorbax) eluted with a gradient mobile phase (8-20% B over 25 min or 8-100% B over 30 min, solvent A = 25 mM ammonium acetate buffer, solvent B = acetonitrile) at 1 mL/min. The radioactivity of the eluate was monitored using an in-line radiodetector (Flo-One Beta series, Radiomatic, Meriden, CT, USA).

Solid-phase $\alpha_v\beta_3$ binding assay

The affinity of DOTA-E-c(RGDfK), DOTA-E-$[c(RGDfK)]_2$, and DOTA-E$\{E[c(RGDfK)]_2\}_2$ for $\alpha_v\beta_3$ was determined using a solid-phase competitive binding assay. ^{111}In-labeled DOTA-E-$[c(RGDfK)]_2$ (3 MBq/µg) was prepared as described above and was used as the tracer in this assay. Microtiter 96-well vinyl assay plates (Corning B.V., Schiphol-Rijk, The Netherlands) were coated with 100 µL/well of a solution of purified human integrin $\alpha_v\beta_3$ (150 ng/mL) in Triton X-100 Formulation (Chemicon International, Temecula, CA, USA) in coating buffer (25 mM Tris-HCl, pH 7.4, 150 mM NaCl, 1 mM $CaCl_2$, 0.5 mM $MgCl_2$ and 1 mM $MnCl_2$) for 17 h at 4 °C. The plates were washed twice with binding buffer (0.1% bovine serum albumin (BSA) in coating buffer). The wells were blocked for 2 h with 200 µL blocking buffer (1% BSA in coating buffer). The plates were washed twice with binding buffer. Then 100 µL binding buffer containing 11.1 kBq of ^{111}In-DOTA-E-$[c(RGDfK)]_2$ and appropiate dilutions of non-labeled DOTA-E-c(RGDfK), DOTA-E-$[c(RGDfK)]_2$, and DOTA-E$\{E[c(RGDfK)]_2\}_2$ in binding buffer were incubated in the wells at 37 °C for 1 h. After incubation, the plates were washed three times with binding buffer. The wells were cut out and radioactivity in each well was determined in a γ-counter (1480 Wizard, Wallac, Turku, Finland). IC_{50} values of the RGD peptides were calculated by non-linear regression using GraphPad Prism (GraphPad Prism 4.0 Software, San Diego, CA, USA). Each data point is the average of three determinations.

Biodistribution studies

In the right flank of 6-8 weeks old female nude BALB/c mice, 0.2 mL of a cell suspension of 15 × 10^6 cells/mL SK-RC-52 cells was injected subcutaneously (s.c.). Two weeks after inoculation of the tumor cells, mice were randomly divided into three groups (15 mice/group).

Mice received equivalent amounts of RGD binding units, resulting in similar amounts of mass (0.5 µg/mouse) ^{111}In-DOTA-E-c(RGDfK) (0.52 MBq), ^{111}In-DOTA-E-$[c(RGDfK)]_2$ (0.43 MBq), or ^{111}In-DOTA-E$\{E[c(RGDfK)]_2\}_2$ (0.34 MBq) via a tail vein. Mice were killed by CO_2 asphyxiation 2, 8, and 24 h postinjection (p.i.) (5 mice/group). Blood, tumor, and the major organs and tissues were collected, weighed, and counted in a γ-counter. The percentage injected dose per gram (%ID/g) was determined for each sample.

Statistical analysis

All mean values are given ± standard deviation (S.D.). Statistical analysis was performed using the One-way Analysis of Variance. Bonferroni corrections for multiple comparisons were applied. The level of significance was set at $P<0.05$.

Results

Radiolabeling

RP-HPLC analysis indicated that the radiochemical purity of ^{111}In-DOTA-E-c(RGDfK), ^{111}In-DOTA-E-$[c(RGDfK)]_2$, and ^{111}In-DOTA-E$\{E[c(RGDfK)]_2\}_2$ preparations used in these experiments was at least 93%. The elution profile of ^{111}In-DOTA-E-c(RGDfK), ^{111}In-DOTA-E-$[c(RGDfK)]_2$, and ^{111}In-DOTA-E$\{E[c(RGDfK)]_2\}_2$ showed a single peak for each of the three compounds with an elution time of 14 min and 26 min for ^{111}In-DOTA-E-c(RGDfK) and ^{111}In-DOTA-E-$[c(RGDfK)]_2$, respectively. The retention time of ^{111}In-DOTA-E$\{E[c(RGDfK)]_2\}_2$ was 15 min. Note that different gradients were used for elutions.

Solid-phase $\alpha_v\beta_3$ binding assay

The affinity of DOTA-E-c(RGDfK), DOTA-E-$[c(RGDfK)]_2$, and DOTA-E$\{E[c(RGDfK)]_2\}_2$ for the $\alpha_v\beta_3$ integrin was determined in a competitive binding assay. The results of these assays are summarized in Figure 2. Binding of ^{111}In-labeled dimeric peptide, ^{111}In-DOTA-E-$[c(RGDfK)]_2$, to $\alpha_v\beta_3$ was competed by DOTA-E-c(RGDfK), DOTA-E-$[c(RGDfK)]_2$, and DOTA-E$\{E[c(RGDfK)]_2\}_2$ in a concentration dependent manner. The IC_{50} values were 120 nM for DOTA-E-c(RGDfK), 69.9 nM for DOTA-E-$[c(RGDfK)]_2$, and 19.6 nM for DOTA-E$\{E[c(RGDfK)]_2\}_2$.

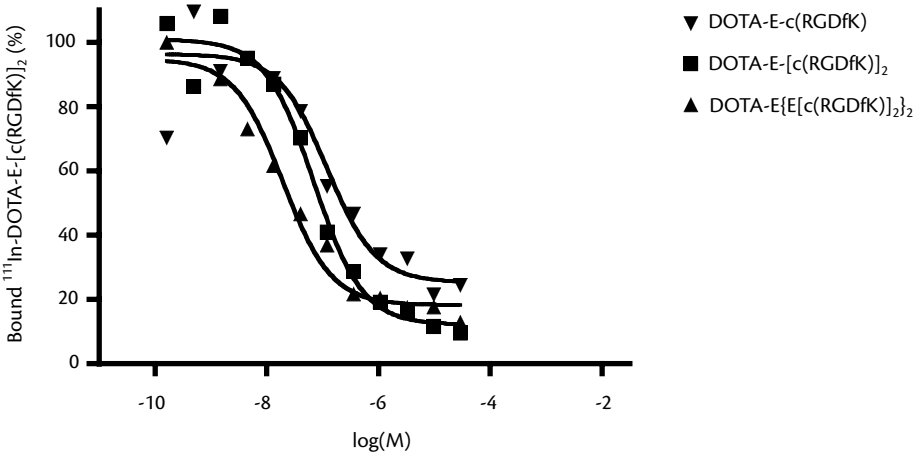

Figure 2. Competition of specific binding of ^{111}In-DOTA-E-[c(RGDfK)]$_2$ with DOTA-E-c(RGDfK), DOTA-E-[c(RGDfK)]$_2$, and DOTA-E{E[c(RGDfK)]$_2$}$_2$.

Biodistribution studies

The results of the biodistribution studies of ^{111}In-DOTA-E-c(RGDfK), ^{111}In-DOTA-E-[c(RGDfK)]$_2$, and ^{111}In-DOTA-E{E[c(RGDfK)]$_2$}$_2$ in athymic mice with s.c. SK-RC-52 tumors are summarized in Table 1, Figure 3a, and 3b.

Table 1. Biodistribution data of ^{111}In-DOTA-E-c(RGDfK), ^{111}In-DOTA-E-[c(RGDfK)]$_2$, and ^{111}In-DOTA-E{E[c(RGDfK)]$_2$}$_2$ in the presence and absence of an excess of unlabeled DOTA-E-[c(RGDfK)]$_2$ in athymic mice with s.c. SK-RC-52 tumors 2 h after injection. The organ uptake is expressed as %ID/g.

	Monomer	Monomer + excess cold	Dimer	Dimer + excess cold	Tetramer	Tetramer + excess cold
Blood	0.04 ± 0.01	0.01 ± 0.01	0.10 ± 0.02	0.02 ± 0.01	0.09 ± 0.01	0.03 ± 0.01
Muscle	0.19 ± 0.02	0.17 ± 0.17	0.37 ± 0.06	0.03 ± 0.00	0.49 ± 0.06	0.07 ± 0.02
Tumor	2.70 ± 0.29	0.39 ± 0.05	5.61 ± 0.85	0.47 ± 0.08	7.32 ± 2.45	0.84 ± 0.12
Lung	0.38 ± 0.05	0.08 ± 0.01	1.12 ± 0.18	0.13 ± 0.01	1.37 ± 0.36	0.20 ± 0.05
Spleen	1.43 ± 0.10	0.16 ± 0.01	2.40 ± 0.38	0.22 ± 0.02	2.53 ± 0.31	0.28 ± 0.03
Kidney	1.85 ± 0.15	1.38 ± 0.07	3.56 ± 0.28	1.90 ± 0.33	6.15 ± 0.41	5.30 ± 0.53
Liver	1.32 ± 0.05	0.18 ± 0.01	2.71 ± 0.21	0.24 ± 0.03	2.41 ± 0.49	0.28 ± 0.03
Intestine	3.18 ± 0.68	0.21 ± 0.01	6.65 ± 1.11	0.20 ± 0.04	7.30 ± 0.73	0.49 ± 0.10
Colon	1.71 ± 0.11	0.18 ± 0.02	3.77 ± 0.79	0.16 ± 0.01	3.94 ± 0.54	0.67 ± 0.11

^{111}In-DOTA-E-c(RGDfK), ^{111}In-DOTA-E-[c(RGDfK)]$_2$, and ^{111}In-DOTA-E{E[c(RGDfK)]$_2$}$_2$ all cleared rapidly from the blood. At 8 h p.i. tumor uptake of the tetramer (7.40 ± 1.12 %ID/g) was significantly higher compared to the monomer (2.30 ± 0.34 %ID/g), $P<0.001$ and the dimer (5.17 ± 1.22 %ID/g), $P<0.05$. Furthermore, uptake of the dimer in the tumor was significantly higher compared to the

monomer, P<0.01 (Figure 3a). At 24 h p.i. uptake in the tumor was significantly higher for the tetramer (6.82 ± 1.41 %ID/g), compared to the dimer (4.22 ± 0.96 %ID/g), P<0.01 and the monomer (1.90 ± 0.29 %ID/g), P<0.001 (Figure 3b). Coinjection of an excess unlabeled DOTA-E-$[c(RGDfK)]_2$ (50 μg) along with 0.5 μg of ^{111}In-DOTA-E-c(RGDfK), ^{111}In-DOTA-E-$[c(RGDfK)]_2$ or ^{111}In-DOTA-E$\{E[c(RGDfK)]_2\}_2$ resulted in a significant decrease of radioactivity concentration in the tumor, indicating that uptake of the major fraction of ^{111}In-DOTA-E-c(RGDfK), ^{111}In-DOTA-E-$[c(RGDfK)]_2$, and ^{111}In-DOTA-E$\{E[c(RGDfK)]_2\}_2$ in the tumor was $\alpha_v\beta_3$-mediated. Uptake in non-target organs like lung, spleen, and intestine was also reduced in the presence of an excess of unlabeled RGD peptide, indicating that the uptake in these tissues was also at least partly $\alpha_v\beta_3$-mediated.

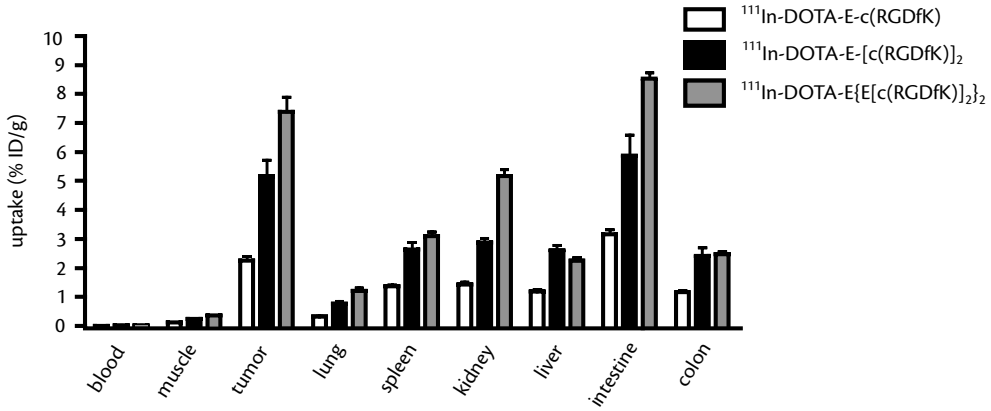

Figure 3a. Biodistribution of ^{111}In-DOTA-E-c(RGDfK), ^{111}In-DOTA-E-$[c(RGDfK)]_2$, and ^{111}In-DOTA-E$\{E[c(RGDfK)]_2\}_2$ at 8 h p.i. in athymic mice with s.c. SK-RC-52 tumors (5 mice/group).

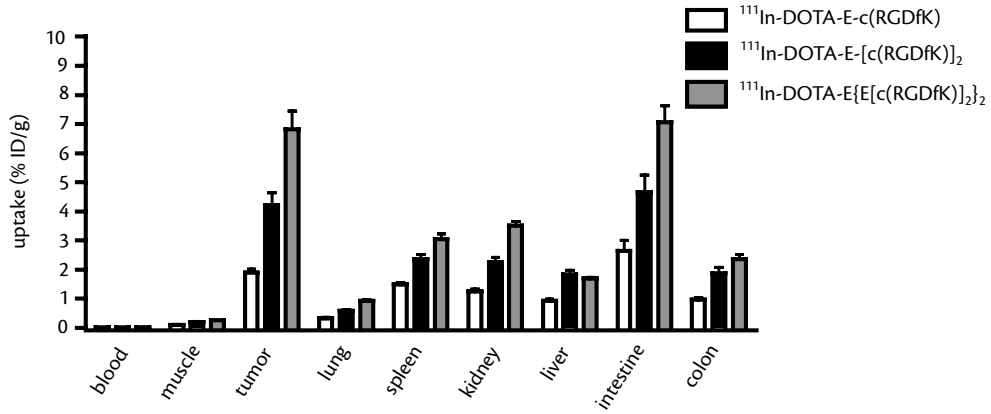

Figure 3b. Biodistribution of ^{111}In-DOTA-E-c(RGDfK), ^{111}In-DOTA-E-$[c(RGDfK)]_2$, and ^{111}In-DOTA-E$\{E[c(RGDfK)]_2\}_2$ at 24 h p.i. in athymic mice with s.c. SK-RC-52 tumors (5 mice/group).

Discussion

In this study, the potential advantage of using multimeric RGD peptides for targeting of the $\alpha_v\beta_3$ integrin receptor was investigated. The binding affinity of DOTA-E{E[c(RGDfK)]$_2$}$_2$ (IC_{50} = 19.6 nM), as determined in a solid-phase competitive binding assay, was about 4 times higher compared to DOTA-E-[c(RGDfK)]$_2$ (IC_{50} = 69.9 nM) and about six times higher compared to DOTA-E-c(RGDfK) (IC_{50} = 120 nM). Enhanced affinity of $\alpha_v\beta_3$ expressing cells for multiple RGD sequences on a protein backbone as compared to the monomeric RGD peptides was demonstrated by Kok et al. [15]. They postulated that the enhanced affinity was due to cooperative binding of multiple RGD units. Recently, Thumshirn et al. [20] synthesized multimeric RGD peptides by oxime ligation. These multimeric RGD peptides showed retained affinity for the $\alpha_v\beta_3$ integrin. Their tetrameric RGD compound with a Hegas spacer showed enhanced affinity as compared to the monomeric and the dimeric analog. However, the tetrameric RGD compound with an aminohexanoic acid spacer showed a lower affinity than the dimeric analog [20], indicating clearly the importance of the proper choice of the spacer unit.

In athymic mice with s.c. SK-RC-52 tumors, all three RGD peptides of this study showed specific uptake in the tumor: in the presence of an excess of unlabeled DOTA-E-[c(RGDfK)]$_2$, the specificity of the tumor targeting of the monomeric, dimeric, and tetrameric RGD peptide was clearly demonstrated. The tumor uptake of ^{111}In-DOTA-E{E[c(RGDfK)]$_2$}$_2$ beyond 2 h p.i. was significantly higher compared to that of ^{111}In-DOTA-E-[c(RGDfK)]$_2$. Similarly, the tumor uptake of ^{111}In-DOTA-E-[c(RGDfK)]$_2$ was significantly higher compared to ^{111}In-DOTA-E-c(RGDfK) at all time points (Figure 4).

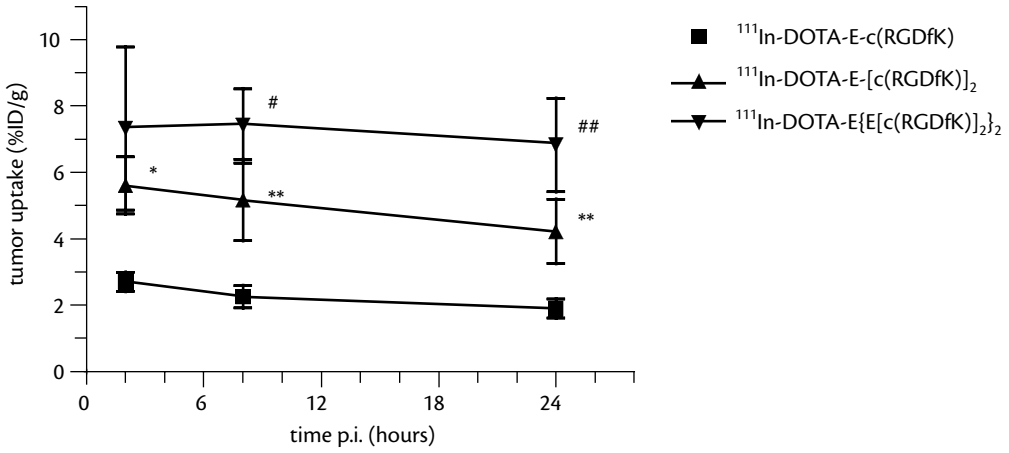

Figure 4. Tumor uptake of ^{111}In-DOTA-E-c(RGDfK), ^{111}In-DOTA-E-[c(RGDfK)]$_2$, and ^{111}In-DOTA-E{E[c(RGDfK)]$_2$}$_2$ at 2, 8, and 24 h after injection in athymic mice with s.c. SK-RC-52 tumors. Results are reflected as mean %ID/g ± SD. Values were analyzed using One-way Analysis of Variance, * = P<0.05, ** = P<0.01, $^{\#}$ = P<0.05, $^{\#\#}$ = P<0.01. P-values refer to differences in tumor uptake between ^{111}In-DOTA-E-c(RGDfK) and ^{111}In-DOTA-E-[c(RGDfK)]$_2$ or differences in tumor uptake between ^{111}In-DOTA-E-[c(RGDfK)]$_2$ and ^{111}In-DOTA-E{E[c(RGDfK)]$_2$}$_2$.

Thus, the higher the binding affinity for $\alpha_v\beta_3$, the higher the accumulation of the compound in $\alpha_v\beta_3$ expressing tumors. It appears that the enhanced uptake in the tumor of the tetrameric RGD peptide is mainly determined by early uptake in the tumor, while retention in the tumor at later time points of the monomer, dimer, and tetramer was similar.

Recently, Wu and coworkers tested ^{64}Cu-DOTA-E{E[c(RGDfK)]$_2$}$_2$ for PET imaging of $\alpha_v\beta_3$ expression in athymic nude mice with s.c. U87MG glioma xenografts [19]. ^{64}Cu-DOTA-E{E[c(RGDfK)]$_2$}$_2$ accumulated rapidly and efficiently in the tumor (9.93 ± 1.05 %ID/g at 30 min p.i.). At 2 h p.i. the uptake of this ^{64}Cu-labeled compound in the tumor was 7.61 ± 0.68 %ID/g, slowly decreasing to 4.56 ± 0.51 %ID/g at 24 h p.i.. Although our compound was labeled with another radionuclide and tested in another animal model, the uptake in the tumor during 24 h after injection was very similar. At 2 h p.i. the uptake in the tumor of ^{111}In-DOTA-E{E[c(RGDfK)]$_2$}$_2$ was 7.32 ± 2.45 %ID/g and decreased to 6.82 ± 1.41 %ID/g at 24 h p.i..

One may argue that the enhanced tumor uptake of ^{111}In-DOTA-E{E[c(RGDfK)]$_2$}$_2$ might be due to the higher molecular weight of the tetramer resulting in longer blood circulation time. However, not only the uptake in the tumor, but also the tumor-to-blood ratio of ^{111}In-DOTA-E{E[c(RGDfK)]$_2$}$_2$ (402 ± 96, 24 h p.i.) was significantly higher compared to that of ^{111}In-DOTA-E-[c(RGDfK)]$_2$ (287 ± 30) and ^{111}In-DOTA-E-c(RGDfK) (223 ± 39) ($P<0.05$ and $P<0.01$, respectively; Figure 5).

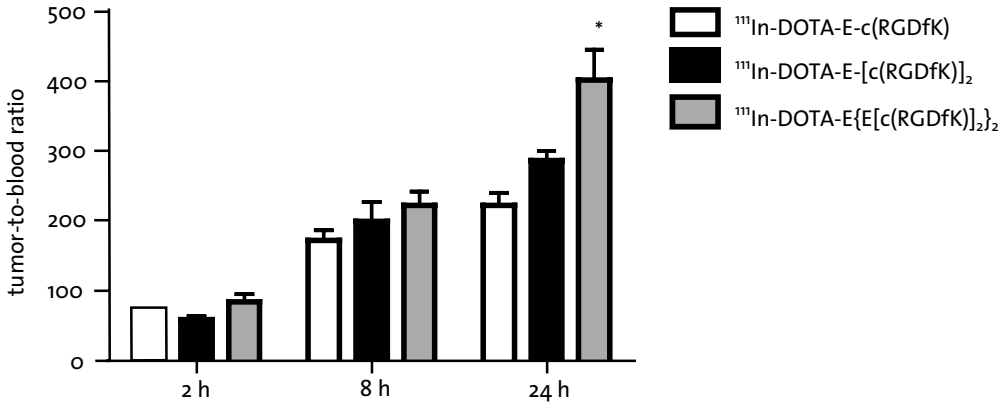

Figure 5. Tumor-to-blood ratios of ^{111}In-DOTA-E-c(RGDfK), ^{111}In-DOTA-E-[c(RGDfK)]$_2$, and ^{111}In-DOTA-E{E[c(RGDfK)]$_2$}$_2$ at 2, 8, and 24 h after injection in athymic mice with s.c. SK-RC-52 tumors. Each bar represents the mean values ± SD. Values were analyzed using One-way Analysis of Variance, * = $P<0.05$.

While the potential benefits of multivalency of targeting vehicles are universally accepted, the cause of the enhanced affinity is not yet clear [21]. Multivalent compounds could have enhanced affinity due to subsite binding, statistical rebinding, or due to receptor clustering [12, 22]. Subsite binding refers to binding of a ligand to sites other than the binding site. It is not likely that this mechanism is responsible for the enhanced uptake of RGD multimers in $\alpha_v\beta_3$ expressing tumors, because subsites have not been identified for these peptides.

Cells can form a cluster of many monovalent receptors on a small area of the cell surface [22] and multivalent ligands that can span the required distance between binding sites could then bind multiple receptors simultaneously. However, it is unlikely that the multivalent RGD peptides used in this study could bind multiple $\alpha_v\beta_3$ integrins simultaneously, because the distance between the RGD units is very short. Therefore, statistical rebinding might be the most likely explanation for the enhanced affinity of the multimeric RGD peptides. The receptor binding of one RGD unit will significantly enhance the local concentration of the other RGD unit in the vicinity of the receptor. This could lead to a higher "on rate" of receptor binding and/or a lower "off rate" of the RGD multimer [19].

The three RGD peptides showed a remarkable difference in uptake in the kidneys. The uptake of ^{111}In-DOTA-E{E[c(RGDfK)]$_2$}$_2$ is at all time points significantly higher compared to that of ^{111}In-DOTA-E-[c(RGDfK)]$_2$ and ^{111}In-DOTA-E-c(RGDfK). Uptake in the kidney was not $\alpha_v\beta_3$-mediated, thus the enhanced $\alpha_v\beta_3$ affinity can not explain the enhanced kidney uptake. Most likely, the difference in charge between the three peptides could cause the difference in renal uptake. It has been shown that positively charged peptides are more efficiently reabsorbed by the proximal renal tubular cell than neutral peptides [23]. Due to the presence of more guanidine groups, the tetrameric RGD peptide is more positively charged than the dimeric and monomeric RGD peptide.

In conclusion, the present study shows that multimeric RGD peptides have enhanced affinity for the $\alpha_v\beta_3$ integrin, most likely due to statistical rebinding of these RGD peptides. The tetrameric RGD peptide demonstrated improved tumor targeting compared to the dimeric RGD peptide. Analogously, the dimeric RGD peptide exhibits improved tumor targeting compared to the monomeric RGD peptide. The tetrameric RGD peptide is the favorable ligand for $\alpha_v\beta_3$ targeting in vivo. The uptake in the kidneys and intestines of this compound is relatively high and could hamper imaging of tumors in the abdomen.

References

1. Brooks PC. Role of integrins in angiogenesis. Eur J Cancer 1996;32A:2423-9.
2. Fiedler W, Graeven U, Ergun S, Verago S, Kilic N, Stockschlader M, et al. Vascular endothelial growth factor, a possible paracrine growth factor in human acute myeloid leukemia. Blood 1997;89:1870-5.
3. Foss HD, Araujo I, Demel G, Klotzbach H, Hummel M, Stein H. Expression of vascular endothelial growth factor in lymphomas and Castelman's disease. J Pathol 1997;183:44-50.
4. PerezAtayde AR, Sallan SE, Tedrow U, Conners S, Allred E, Folkman J. Spectrum of tumor angiogenesis in the bone marrow of children with acute lymphoblastic leukemia. Am J Pathol 1997;150:815-21.
5. Folkman J. Angiogenesis in cancer, vascular, rheumatoid and other disease. Nat Med 1995;1:27-31.
6. Plow EF, Haas TA, Zhang L, Loftus J, Smith JW. Ligands binding to integrins. J Biol Chem 2000;275:21785-8.

7. Haubner R, Finsinger D, Kessler H. Stereoisomeric Peptide Libraries and Peptidomimetics for Designing Selective Inhibitors of the $\alpha_v\beta_3$ Integrin for a New Cancer Therapy. Angew Chem Int Ed Engl 1997;36:1374-89.

8. Aumailley M, Gurrath M, Muller G, Calvete J, Timpl R, Kessler H. Arg-Gly-Asp constrained within cyclic pentapeptides. Strong and selective inhibitors of cell adhesion to vitronectin and laminin fragment P1. FEBS Let 1991;291:50-4.

9. Gurrath M, Muller G, Kessler H, Aumailley M, Timpl R. Conformation/activity studies of rationally designed potent anti-adhesive RDG peptides. Eur J Biochem 1992;210:911-21.

10. Janssen ML, Oyen WJ, Dijkgraaf I, Massuger LF, Frielink C, Edwards DS, Rajopadhye M, et al. Tumor targeting with radiolabeled alpha-v-beta-3 integrin binding peptides in a nude mouse model. Cancer Res 2002;62:6146-51.

11. Johansson SMC, Arnberg N, Elofsson M, Wadell G, Kihlberg J. Multivalent HSA Conjugates of 3'-Sialyllactose are Potent Inhibitors of Adenoviral Cell Attachment an Infection. Chembiochem 2005;6:358-64.

12. Mammen M, Choi SK, Whitesides GM. Polyvalent Interactions in Biological Systems: Implications for Design and Use of Multivalent Ligands and Inhibitors. Angew Chem Int Ed 1998;37:2754-94.

13. Joosten JAF, Loimaranta V, Appeldoorn CCM, Haataja S, Ait El Maate F, Liskamp RMJ, et al. Inhibition of *Streptococcus suis* Adhesion by Dendritic Galabiose Compounds at Low Nanomolar Concentration. J Med Chem 2004;47:6499-508.

14. Goel A, Baranowska-Kortylewicz J, Hinrichs SH, Wisecarver J, Pavlinkova G, Augustine S, et al. 99mTc-Labeled Divalent and Tetravalent CC49 Single-Chain Fv's: Novel Imaging Agents for Rapid In Vivo Localization of Human Colon Carcinoma. J Nucl Med 2001;42:1519-27.

15. Kok RJ, Schraa AJ, Bos EJ, Moorlag HE, Ásgeirsdóttir SA, Everts M, et al. Preparation and functional evaluation of RGD-modified proteins as $\alpha_v\beta_3$ integrin directed therapeutics. Bioconjugate Chem 2002;13:128-35.

16. Maheshwari G, Brown G, Lauffenburger DA, Wells A, Griffith LG. Cell adhesion and motility depend on nanoscale RGD clustering. J Cell Sci 2000;113:1677-86.

17. Dijkgraaf I, Boerman OC, Frielink C, Kruijtzer JAW, Liskamp RMJ, Oyen WJ, et al. Synthesis and preclinical evaluation of new $\alpha_v\beta_3$-integrin binding peptidomimetics for tumor targeting. Eur J Nucl Med Mol Imaging 2004;31 Suppl 2: S281.

18. Liu S, Cheung E, Ziegler M, Rajopadhye M, Edwards DS. ^{90}Y and ^{177}Lu labeling of a DOTA-conjugated vitronectin receptor antagonist useful for tumor therapy. Bioconjugate Chem 2001;12:559-68.

19. Wu Y, Zhang X, Xiong Z, Cheng Z, Fisher DR, Liu S, Gambhir SS, Chen X. microPET Imaging of Glioma Integrin $\alpha_v\beta_3$ Expression Using ^{64}Cu-Labeled Tetrameric RGD Peptide. J Nucl Med 2005;46:1707-18.

20. Thumshirn G, Hersel U, Goodman SL, Kessler H. Multimeric Cyclic RGD Peptides as Potential Tools for Tumor Targeting: Solid-Phase Peptide Synthesis and Chemoselective Oxime Ligation. Chem Eur J 2003;9:2717-25.

21. Vrasidas I, André S, Valentini P, Böck C, Lensch M, Kaltner H, et al. Rigified multivalent lactose molecules and their interactions with mammalian galectins: a route to selective inhibitors. Org Biomol Chem 2003;1:803-10.

22. Kiessling LL, Pohl NL. Strength in numbers: non-natural polyvalent carbohydrate derivatives. Chem Biol 1996;3: 71-7.

23. Behr TM, Goldenberg DM, Becker W. Reducing the renal uptake of radiolabeled antibody fragments and peptides for diagnosis and therapy: present status, future prospects and limitations. Eur J Nucl Med 1998;25:201-12.

Chapter 4

Synthesis of DOTA-conjugated multivalent cyclic RGD peptide dendrimers via 1,3-dipolar cycloaddition and their biological evaluation: implications for tumor targeting and tumor imaging purposes

Ingrid Dijkgraaf
Anneloes Y. Rijnders
Annemieke C. Soede
Annemarie C. Dechesne
G. Wilma van Esse
Arwin J. Brouwer
Frans H. M. Corstens
Otto C. Boerman
Dirk T. S. Rijkers
Rob M. J. Liskamp

Org Biomol Chem 2007, in press

Abstract

This chapter describes the design and synthesis of a series of $\alpha_v\beta_3$ integrin-directed monomeric, dimeric and tetrameric *cyclo*[Arg-Gly-Asp-D-Phe-Lys] dendrimers using "click chemistry". It was found that the unprotected *N*-ε-azido derivative of *cyclo*[Arg-Gly-Asp-D-Phe-Lys] underwent a highly chemoselective conjugation to amino acid-based dendrimers bearing terminal alkynes using a microwave-assisted Cu(I)-catalyzed 1,3-dipolar cycloaddition. The $\alpha_v\beta_3$ binding characteristics of the dendrimers were determined in vitro and their in vivo $\alpha_v\beta_3$ targeting properties were assessed in nude mice with subcutaneously growing human SK-RC-52 tumors. The multivalent RGD dendrimers were found to have enhanced affinity toward the $\alpha_v\beta_3$ integrin receptor as compared to the monomeric derivative as determined in an in vitro binding assay. In case of the DOTA-conjugated ^{111}In-labeled RGD dendrimers, it was found that the radiolabeled multimeric dendrimers showed specifically enhanced uptake in $\alpha_v\beta_3$ integrin expressing tumors in vivo. These studies showed that the tetrameric RGD dendrimer had better tumor targeting properties than its dimeric and monomeric congeners.

Introduction

Integrins are a class of heterodimeric transmembrane proteins [1] which play an important role in cell-signaling, cell-cell adhesion, apoptosis and cell-matrix interactions [2]. Integrin $\alpha_v\beta_3$, which binds to the Arg-Gly-Asp (RGD) tripeptide motif containing ligands [3], plays a pivotal role in tumor angiogenesis [2] and metastasis. $\alpha_v\beta_3$ Integrin expressed on endothelial cells modulate cell migration and survival during angiogenesis, while $\alpha_v\beta_3$ integrin expressed on carcinoma cells potentiate metastasis by facilitating invasion and movement across blood vessels. The $\alpha_v\beta_3$ integrin is expressed on activated endothelial cells during tumor-induced angiogenesis, whereas it is absent on quiescent endothelial cells and normal tissues. In addition, $\alpha_v\beta_3$ is expressed on various tumor cell types (e.g. breast, ovarian, and prostate cancers). Evidence exists that inhibition of $\alpha_v\beta_3$ integrin function prevents tumor growth and induces tumor regression by antagonizing angiogenesis [4]. Several peptidic [5] and peptidomimetic [6] $\alpha_v\beta_3$ antagonists have been synthesized. Among these, the *cyclo*[Arg-Gly-Asp-D-Phe-Val] (c[RGDfV]), as developed by Kessler and coworkers, is one of the most active and selective antagonists for the $\alpha_v\beta_3$ integrin [7]. Structure-activity relationship studies on this cyclic pentapeptide showed that the exchange of the valine by a lysine residue (Lys, K) did not significantly influence activity and selectivity [8]. Because the ε-amino moiety of the lysine residue can be easily modified, numerous applications of c[RGDfK] have been studied for tumor targeting and imaging [9].

Multivalency is a well accepted approach to increase the interaction of weakly interacting individual ligands with their respective receptors [10]. Dendrimers are macromolecules consisting of multiple perfectly branched monomers and this architecture makes them versatile constructs

for the simultaneous presentation of receptor binding ligands and other biologically relevant molecules [11]. Additionally, dendrimers might serve as promising molecular scaffolds containing a number of ligands thereby inducing an apparent increase of ligand concentration and increasing the probability of statistical rebinding [10b-e, 12]. Alternatively, dendrimers may align these ligands and induce multivalency when receptor clustering occurs or is initiated after initial monovalent binding [10b-e]. To improve tumor targeting efficacy and to obtain better in vivo imaging properties, several studies explored the multivalency effect by using dimeric and tetrameric RGD peptides with affinity toward the $\alpha_v\beta_3$ integrin [13]. These studies clearly demonstrated the multivalency effect, since the in vivo affinity significantly increased going from monomer via dimer to tetramer. Moreover, also with respect to tumor-uptake and tumor-to-organ ratios a similar increase was observed. These are promising results in view of the development of integrin targeted radionuclide therapy [12].

To decorate the dendrimer end-groups with biologically relevant peptides as ligands, it is of crucial importance to have the disposal of efficient and chemoselective conjugation chemistry to ensure the complete attachment of the ligands to the dendrimer. In cases of completely amino acid- or peptide-based dendrimers [14, 15], this is often achieved using peptide coupling reagents, however, in most cases, the peptide ligands are attached to dendrimers by chemoselective reaction of sulfhydryl groups of cysteine residues with maleimide or iodoacetamide functionalities [16], by thiol-disulfide exchange, by native chemical ligation [17] or via a chemoselective oxime [13d,l,m] respectively hydrazone [18] ligation. However, new bioconjugation reactions with mutually reactive conjugation partners with increased efficiency and chemoselectivity which are synthetically easily accessible would be very welcome.

Recently, the well-known reaction between an alkyne and an azide to yield 1,4-disubstituted 1,2,3-triazoles, was reinvestigated independently by Meldal [19a] and Sharpless [19b]. They found that an alkyne and an azide in the presence of Cu(I) undergo a 1,3-dipolar cycloaddition to the corresponding triazole under very mild reaction conditions with very high chemoselectivity and efficiency which make this reaction particularly suitable for bioconjugations. So far, this 1,3-dipolar cycloaddition denoted as "click reaction" [20] has led to a plethora of applications in the literature [21]. Recently, the synthesis of multivalent dendrimeric peptides [22a] (up to octa- and hexadecavalent systems) respectively triazole-linked glycodendrimers [22b] via a microwave-assisted 1,3-dipolar cycloaddition between azido peptides respectively glycosyl azides and dendrimeric alkynes was described as an alternative approach to functionalize dendrimers [22c].

Here we describe the synthesis of monomeric, dimeric and tetrameric c[RGDfK] dendrimers via a microwave-assisted 1,3-dipolar cycloaddition of dendrimeric alkynes with the *N*-ε-azido derivative of *cyclo*[Arg-Gly-Asp-D-Phe-Lys] and their subsequent evaluation as $\alpha_v\beta_3$ integrin antagonists. Additionally, the RGD dendrimers were conjugated with a 1,4,7,10-tetraazacyclododecane-*N*,*N*',*N*'',*N*'''-tetraacetic acid (DOTA)-moiety. These analogs were radiolabeled with ^{111}In to evaluate the in vitro receptor binding characteristics and in vivo tumor targeting properties.

Results and discussion

Synthesis

Scheme 1 and 2 illustrate the approach for the convergent synthesis of amino acid based dendrimers [23] and their corresponding DOTA-conjugated derivatives. The monovalent dendrimer **2** and the divalent dendrimer **3** respectively, were synthesized starting from 3-hydroxy benzoic acid or 3,5-dihydroxy benzoic acid via their corresponding methyl esters followed by alkylation in the presence of propargylbromide/K_2CO_3 and were obtained in 95 and 81% yield. Since these two dendrimers were also used as synthons in further syntheses, the resulting methyl esters **2** and **3** were treated with Tesser's base [24] to yield acids **4** and **5** in nearly quantitative yield. After treatment of the previously described **6** [23c] with TFA to remove both Boc-functionalities, the resulting bisamine TFA salt was coupled to acid **5** in the presence of BOP/DIPEA to give the tetravalent dendrimer **7** with 75% yield. To conjugate the tetravalent dendrimer with a DOTA-moiety at a later stage of the synthesis, its methyl ester was saponified with Tesser's base and acid **8** was obtained quantitatively.

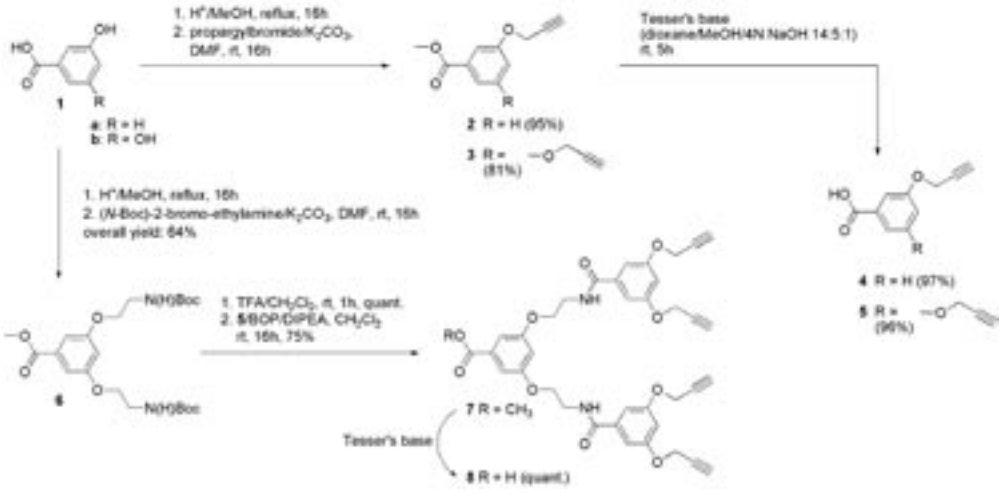

Scheme 1. Synthesis of the mono-, di- and tetravalent dendrimeric alkynes **2**, **3** and **7**.

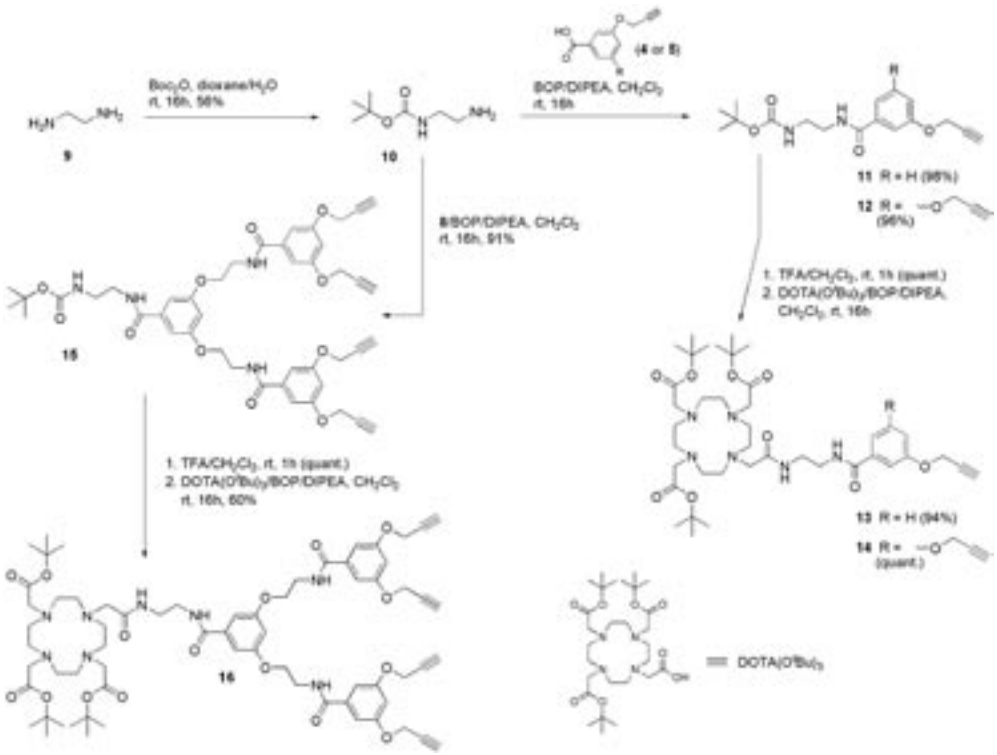

Scheme 2. Synthesis of the DOTA-conjugated dendrimeric alkynes **13**, **14** and **16**.

The DOTA-moiety was connected to the dendrimer core via a short ethylene spacer. For this purpose, 1,2-diaminoethane was converted into the mono-protected Boc derivative **10**, which was obtained in 56% yield. Unfortunately, although a large excess of the amine was used, the bis-protected side product was obtained in a considerable amount. Compound **10** was coupled in the presence of BOP/DIPEA to either the monovalent, divalent or tetravalent dendrimer acids **4**, **5** or **8** to obtain the corresponding amides **11**, **12** or **15**, respectively, generally in yields higher than 90%. The Boc-protected dendrimers were treated with TFA to obtain the corresponding amines and they were treated with BOP/DIPEA in the presence of 2-(4,7,10-tris(2-*tert*-butoxy-2-oxoethyl)-1,4,7,10-tetraazacyclododecan-1-yl) acetic acid (DOTA(O^tBu)$_3$) to give the DOTA-conjugated mono-, di- and tetravalent dendrimers **13**, **14** and **16** respectively. It is important to note that the solubility of the DOTA-conjugated dendrimer is an important factor that determines the yield of the coupling reaction. Compounds **13** and **14** were isolated in very high yields (>94%) but compound **16** was isolated with a modest yield of 60% due to its low solubility in solvents like EtOAc and CH_2Cl_2.

The next step in the synthesis was the preparation of the *N*-ε-azido *cyclo*(Arg-Gly-Asp-D-Phe-Lys) peptide **19** (Scheme 3). To obtain this compound, peptide resin **17** was synthesized using Fmoc/^{t}Bu SPPS based on the protocol of Liu *et al.* [25]. It was decided to cleave the protected

peptide acid from the resin by HFIP/CH_2Cl_2 [26] instead of AcOH/TFE to avoid premature acetylation during the BOP/DIPEA-mediated macrolactamization step. Cyclic peptide **18** was obtained in 36% overall yield based on the initial resin loading of 0.64 mmol/g. Subsequently, the ε-amine of the lysine residue was selectively converted into the azide moiety by a diazotransfer [27]. At pH 10, the ε-amine can be deprotonated in the presence of a guanidino functionality, since the latter is a much stronger base and will not act as nucleophile in the diazotransfer reaction. Finally, the peptide *N*-ε-azido *cyclo*(Arg-Gly-Asp-D-Phe-Lys) **19** was obtained in 21% yield after purification by HPLC and was characterized by ^{1}H-NMR (500 MHz) and mass spectrometry (LC-MS). Incorporation of Fmoc-Lys(N_3)-OH, to avoid the diazo transfer as the final reaction step, did not substantially improve the isolated yield.

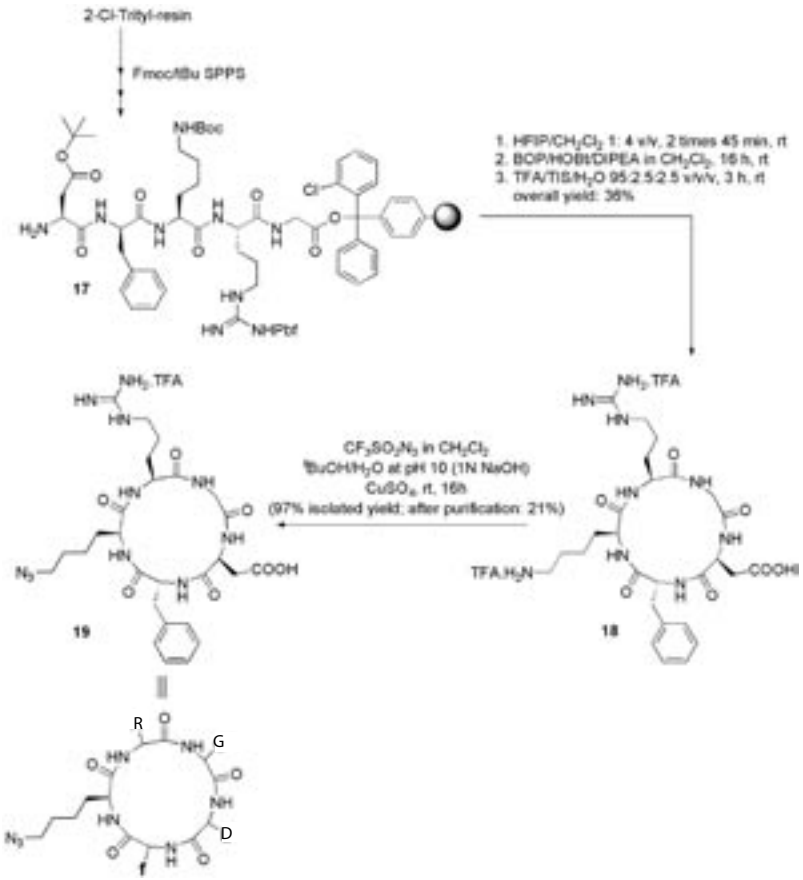

Scheme 3. Synthesis of the *N*-ε-azido *cyclo*[Arg-Gly-Asp-D-Phe-Lys] peptide **19**.

At this stage of the synthesis, the challenge was the chemoselective coupling of the different dendrimeric alkynes (**2**, **3**, **7**, **13**, **14**, or **16**) to the cyclic RGD azido peptide (**19**) to furnish the

DOTA-conjugated dendrimeric *cyclo*-RGD peptides as $\alpha_v\beta_3$ integrin antagonists as shown in Scheme 4. The first experiments were based on the literature procedure [19b] in which acetylene **3** was coupled to azido glycine ethyl ester (ethyl-2-azidoacetate) in the presence of $CuSO_4$/Na-ascorbate/Cu-wire in *tert*-BuOH/H_2O for 16 h at room temperature. Monitoring the reaction by TLC showed that formation of the monovalent cycloadduct proceeded rapidly, but the conversion into the divalent product was sluggish. However, a tremendous improvement was achieved by running this reaction under microwave irradiation. After 10 min at 100 °C using DMF/H_2O as solvent in the presence of $CuSO_4$/Na-ascorbate, the divalent cycloaddition product was obtained in 96% yield. This microwave-assisted cycloaddition of dendrimeric alkynes and azido peptides was recently reported as a versatile approach to obtain multivalent dendrimeric peptides [22a, c]. The optimized reaction conditions were used to couple the cyclic RGD azido peptide (**19**) to the different dendrimeric alkynes (**2**, **3**, **7**, **13**, **14**, or **16**).

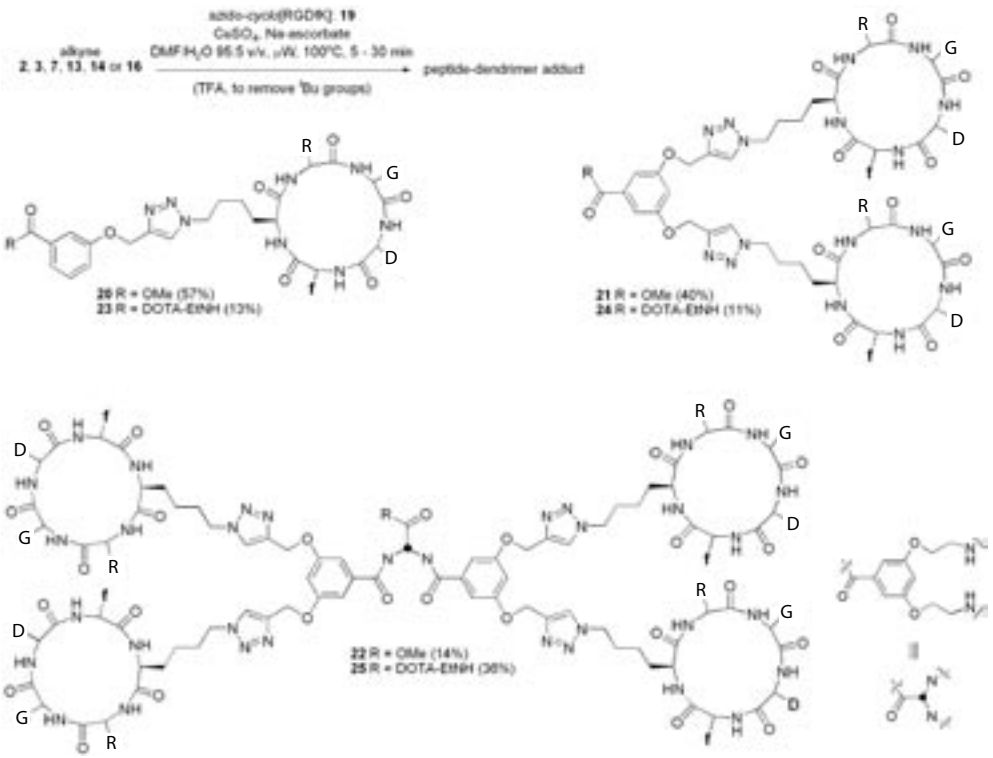

Scheme 4. Synthesis of the mono-, di- and tetravalent *cyclo*[RGDfK] peptide dendrimers **20**, **21** and **22** and their respective DOTA-conjugated counterparts **23**, **24** and **25**.

In case of alkynes **2**, **3** and **7** the formation of the cycloadducts **20**, **21** and **22** could be followed by TLC and LC-MS. It turned out that the formation of **20** and **21** was complete after 10 to 20 min microwave irradiation at 100 °C, whereas the formation of **22** was complete after 30 min.

Although HPLC analysis of the crude cycloaddition products evidenced a complete conversion as judged by the absence of the alkyne starting material, the RGD dendrimers **20** – **22** were obtained in yields varying between 14 to 57%. Then, the DOTA-conjugated alkyne dendrimers **13**, **14** and **16** were subjected to the cycloaddition reaction conditions in the presence of azido peptide **19**. It should be emphasized that the carboxyl functionalities of the DOTA-moiety needed to be protected by *tert*-butyl groups to avoid premature and irreversible sequestering of the Cu^{2+} ions. Chelated copper(II) will result in a lower efficiency of the Cu(II)/Cu(I) redox couple to generate the active Cu(I)-catalyst. More importantly, it will hamper the radiolabeling of the DOTA-moiety of compounds **23** – **25** with trivalent radiometals such as ^{111}In, ^{90}Y or ^{177}Lu. As a result, after the click reaction an additional reaction step was needed in which the partially protected cycloadducts were treated with TFA, in the presence of suitable scavengers, to give the unprotected DOTA-conjugated RGD dendrimers **23** – **25**.

The cycloaddition reaction of the DOTA-conjugated dendrimeric alkynes **13**, **14** and **16** was difficult to monitor by mass spectrometry. As was described above, reaction times of 10 to 30 min were used and the cycloaddition reaction was directly followed by a TFA-treatment without isolation of the cycloaddition intermediates. The isolated yield (13%) of monovalent **23** was rather disappointing. Recently, optimized conditions with respect to the generation of the catalytic active Cu(I) species were published [28] and these conditions were applied in the cycloaddition of **14** and **19**. Unfortunately, an increase of the isolated yield was not observed using these modified reaction conditions. As was mentioned earlier, the cycloaddition reaction was complete according to HPLC analysis, and the low isolated yield was mainly due to the difficult purification. The DOTA-conjugated RGD dendrimers were obtained in yields varying between 11 and 36%.

Radiolabeling of the RGD dendrimers

Dendrimers **23**, **24** and **25** were radiolabeled by dissolving these compounds in an NH_4OAc buffer of pH 6.0 and 22.2-37 MBq $^{111}InCl_3$ was added to each of the reaction mixtures. The reaction mixtures were degassed and subsequently heated at 100 °C for 15 min. Reversed-phase HPLC analysis showed a single peak for each of the three ^{111}In-labeled compounds with an elution time of 25.9 min, 29.5 min and 29.4 min for the ^{111}In-labeled monovalent **23**, divalent **24**, and tetravalent **25**, RGD peptide dendrimers respectively.

Solid-phase $\alpha_v\beta_3$ binding assay

The affinity of the DOTA-conjugated RGD dendrimers **23**, **24**, and **25** for the $\alpha_v\beta_3$ integrin was determined in a competitive binding assay. The results of these analyses are shown in Figure 1. Binding of the ^{111}In-labeled dimeric peptide, ^{111}In-DOTA-E-[c(RGDfK)]$_2$ [29], to $\alpha_v\beta_3$ was competed by unlabeled **23**, **24**, and **25** in a concentration dependent manner. The IC_{50} values were 212 nM for monovalent **23**, 356 nM for divalent **24**, and 50 nM for tetravalent **25**. The dendrimer containing four c[RGDfK] units (**25**) showed an increased affinity for $\alpha_v\beta_3$ compared to the dendrimers containing one (**23**) or two (**24**) c[RGDfK] units. Multimerization of c[RGDfK] resulted in enhanced affinity for $\alpha_v\beta_3$ as was evidenced by a decrease of the IC_{50} concentration.

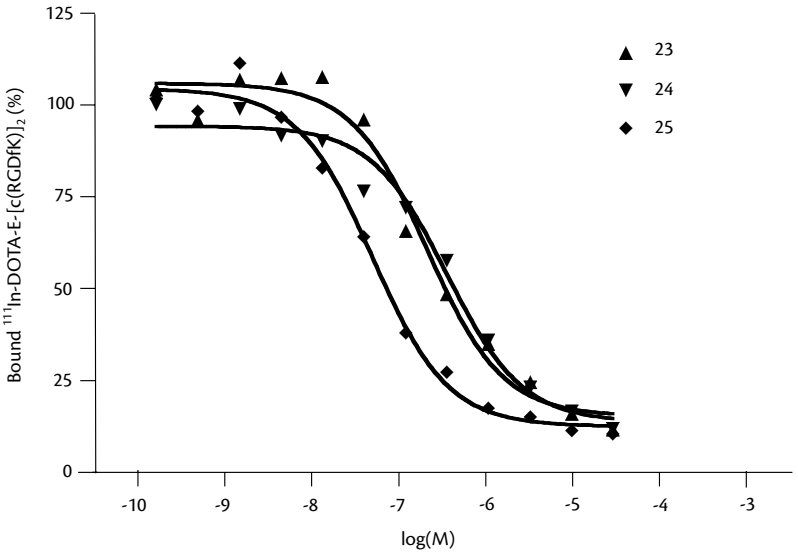

Figure 1. Competition of specific binding of ^{111}In-DOTA-E-[c(RGDfK)]$_2$ with RGD dendrimers **23**, **24**, and **25**.

Biodistribution studies

In athymic mice with subcutaneously (s.c.) growing SK-RC-52 renal cell carcinoma, the tumor uptake of the ^{111}In-labeled tetrameric RGD dendrimer **25** at 2 h postinjection (p.i.; 7.27 ± 2.06 %ID/g) was significantly higher ($P<0.05$) compared to that of the ^{111}In-labeled monomeric RGD dendrimer **23** (1.69 ± 0.41 %ID/g) as shown in Figure 2A. At 2 h p.i., the tumor uptake of tetrameric RGD dendrimer **25** was also significantly higher ($P<0.05$) than the dimeric analog **24** (3.15 ± 0.51 %ID/g). The tumor-to-blood ratios of the tetramer **25** (5.66 ± 1.74, 34.73 ± 5.95) were significantly higher ($P<0.05$) –both at 2 h p.i. and at 24 h p.i.– than those of the monomer **23** (3.12 ± 1.92, 19.65 ± 12.42) and dimer **24** (1.70 ± 0.50, 14.66 ± 0.25). At 24 h p.i., the tumor uptake of the tetrameric RGD dendrimer **25** (5.83 ± 1.18 %ID/g) was significantly higher compared to the dimeric RGD dendrimer **24** (2.82 ± 0.59 %ID/g, $P<0.05$) and the monomeric RGD dendrimer **23** (1.19 ± 0.31 %ID/g, $P<0.01$) which is shown in Figure 2B. Coinjection of an excess of non-radiolabeled RGD peptide (DOTA-E-[c(RGDfK)]$_2$) to saturate all $\alpha_v\beta_3$ receptors in vivo, resulted in a significantly reduced tumor uptake of each of the three compounds: **23**: 0.46 ± 0.04 %ID/g (2 h p.i.), 0.36 ± 0.31 %ID/g (24 h p.i.), **24**: 0.76 ± 0.09 %ID/g (2 h p.i.), not determined (24 h p.i.) and **24**: 1.56 ± 0.02 %ID/g (2 h p.i.), 1.19 ± 0.03 %ID/g (24 h p.i.), indicating that each of the three RGD dendrimers of this study showed receptor specific uptake in the tumor. These in vivo results were in line with the in vitro binding assay. The tetrameric RGD dendrimer showed enhanced affinity for $\alpha_v\beta_3$, as compared to the monomeric and dimeric RGD dendrimer, respectively. The results of this study correlated perfectly with the results observed in a previous study in which we evaluated multimeric RGD peptides in the same animal model [13o].

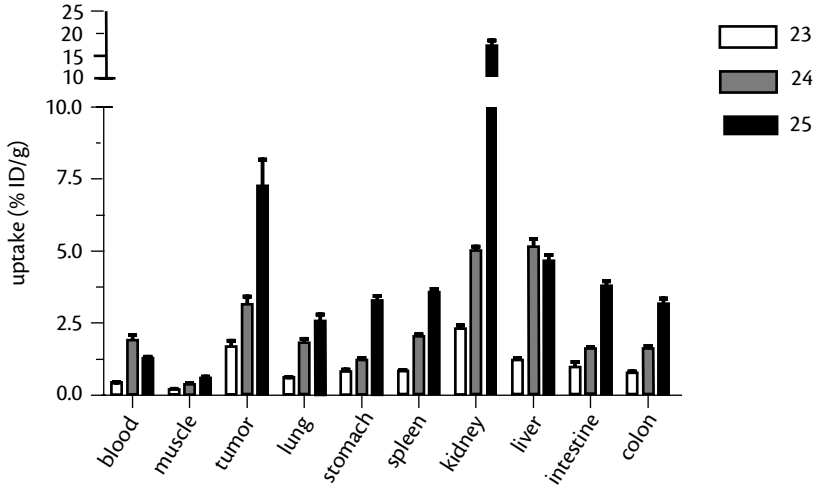

Figure 2A. Biodistribution of ^{111}In-labeled monomer **23**, dimer **24**, and tetramer **25** at 2 h p.i. in athymic mice with s.c. SK-RC-52 tumors.

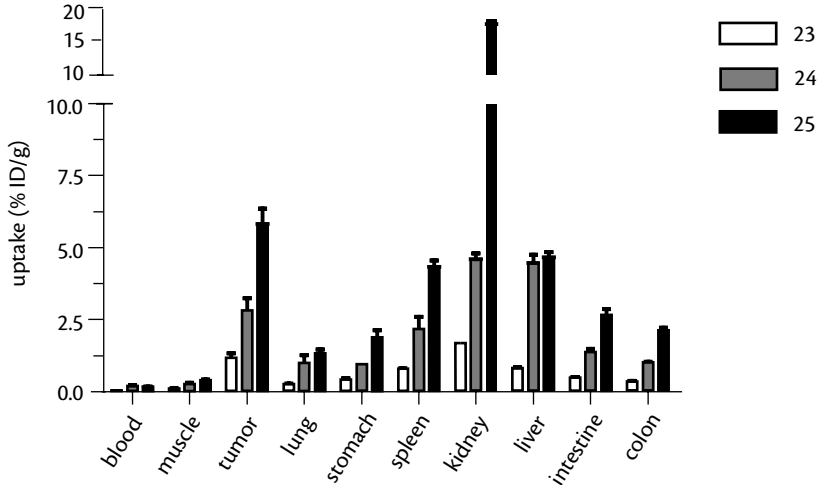

Figure 2B. Biodistribution of ^{111}In-labeled monomer **23**, dimer **24**, and tetramer **25** at 24 h p.i. in athymic mice with s.c. SK-RC-52 tumors.

The affinity of the dendrimers as determined in a vitro binding assay are in agreement with the results obtained from the in vivo experiment. The IC_{50} concentration of the tetrameric RGD dendrimer **25** was lower compared to those of the monomeric **23** and dimeric **24** analogs, resulting in a significant higher uptake of the former in $\alpha_v\beta_3$ expressing tumors and better tumor to blood ratios compared to the monomeric and dimeric RGD dendrimers.

In conclusion, a series of $\alpha_v\beta_3$ integrin-directed monomeric, dimeric and tetrameric *cyclo*[Arg-Gly-Asp-D-Phe-Lys] dendrimers using "click chemistry" was successfully synthesized, since

the unprotected *N*-ε-azido derivative of *cyclo*[Arg-Gly-Asp-D-Phe-Lys] underwent a highly chemoselective conjugation to amino acid-based dendrimers bearing terminal alkynes using a microwave-assisted Cu(I)-catalyzed 1,3-dipolar cycloaddition. The $\alpha_v\beta_3$ binding characteristics and $\alpha_v\beta_3$ targeting properties of the dendrimers were determined both in vitro and in vivo. In case of the DOTA-conjugated ^{111}In-labeled RGD dendrimers, it was found that the radiolabeled multimeric dendrimers showed specifically enhanced uptake in $\alpha_v\beta_3$ integrin expressing tumors in vivo. These studies showed that the tetrameric RGD dendrimer had better tumor targeting properties than its dimeric and monomeric congeners.

Experimental section

Instruments and methods

Peptides were synthesized on an ABI 433A automatic Peptide Synthesizer using the FastMoc solid-phase peptide synthesis protocols. Microwave-assisted reactions were carried out in a Biotage microwave reactor. Analytical HPLC runs were carried out on a Shimadzu HPLC system and preparative HPLC runs were performed on a Gilson HPLC workstation. Analytical HPLC runs were performed on Alltech Prosphere C4 or C8 and Adsorbosphere XL C18 columns (250 × 4.6 mm, pore size 300Å, particle size: 5 µm) or on a Merck LiChroCART CN column (250 × 4.6 mm, pore size 100Å, particle size: 5 µm) at a flow rate of 1.0 mL/min using a linear gradient of buffer B (0 – 100% in 25 min) in buffer A (buffer A: 0.1% TFA in H_2O, buffer B: 0.1 % TFA in CH_3CN/H_2O 95:5 v/v). Preparative HPLC runs were performed on an Alltech Prosphere C4 or C8 column (250 × 22 mm, pore size 300Å, particle size: 10 µm), and semi-prep HPLC runs were performed on an Alltech Adsorbosphere XL C18 column (250 × 10 mm, pore size 300Å, particle size: 10 µm) or on a Merck LiChroCART CN column (250 × 10 mm, pore size 100Å, particle size: 10 µm) at a flow rate of 10.0 mL/min (semi-prep HPLC: 4.0 mL/min) using a linear gradient of buffer B (0 – 100% in 50 min) in buffer A (buffer A: 0.1% TFA in H_2O, buffer B: 0.1 % TFA in CH_3CN/H_2O 95:5 v/v). Liquid chromatography electrospray ionization mass spectrometry was measured on a Shimadzu LCMS-QP8000 single quadrupole bench-top mass spectrometer operating in a positive ionization mode. LC/MS(MS) runs were performed on a Finnigan LCQ Deca XP MAX LC/MS equipped with a Shimadzu 10A VP analytical HPLC system. The samples were dissolved in 10% formic acid in CH_3CN/H_2O 1:1 v/v and analyzed using a Phenomenex Gemini C18 column (150 × 4.6 mm, particle size: 3 µm, pore size: 110Å) at a flow rate of 1.0 mL/min using a linear gradient of 100% buffer A (0.1% TFA in H_2O/CH_3CN 95:5 v/v) to 100% buffer B (0.1% TFA in CH_3CN/H_2O 95:5 v/v) in 50 min. MALDI-TOF analysis was performed on a Kratos Axima CFR apparatus with bradykinin(1-7) (monoisotopic $[M + H]^+$ 757.399), human ACTH(18-39) (monoisotopic $[M + H]^+$ 2465.198) and bovine insulin oxidized B chain (monoisotopic $[M + H]^+$ 3494.651) as external references and α-cyano-4-hydroxycinnamic acid or sinapinic acid as matrices. ^{1}H NMR spectra were recorded on a Varian G-300 (300 MHz) spectrometer and chemical shifts are given in ppm (δ) relative to TMS. ^{13}C

NMR spectra were recorded on a Varian G-300 (75.5 MHz) spectrometer and chemical shifts are given in ppm relative to $CDCl_3$ (77.0 ppm). The ^{13}C NMR spectra were recorded using the attached proton test (APT) sequence. ^1H NMR spectra in H_2O/D_2O 9:1 v/v were recorded on a Varian Inova-500 (500 MHz) spectrometer and chemical shifts are given in ppm (δ) relative to 3-(trimethylsilyl)-1-propanesulfonic acid sodium salt (0.00 ppm). Peak assignments are based on DQF-COSY, TOCSY (mixing times: 20 or 60 ms) and ROESY (mixing times: 150 or 250 ms) spectra. HSQC and HMBC spectra were measured on a Varian Inova-500 spectrometer and chemical shifts are given in ppm (δ) relative to 3-(trimethylsilyl)-1-propanesulfonic acid sodium salt (0.00 ppm). Fourier transform infrared spectra (FTIR) were measured on a Bio-Rad FTS-25 spectrophotometer. Melting points were measured on a Büchi Schmelzpunktbestimmungsapparat and are uncorrected. Elemental analyses were done by Kolbe Mikroanalytisches Labor (Mülheim/Ruhr, Germany). R_f values were determined by thin layer chromatography (TLC) on Merck precoated silica gel 60F254 plates. Spots were visualized by UV-quenching, ninhydrin or Cl_2/TDM [30]. The 2-chlorotrityl chloride resin (Hecheng Science & Technology Company) was used in all solid-phase syntheses. The coupling reagents 2-(1*H*-benzotriazol-1-yl)-1,1,3,3-tetramethyluronium hexafluorophosphate (HBTU) and benzotriazol-1-yloxy-tris-(dimethylamino)phosphonium hexafluorophosphate (BOP) were obtained from Biosolve. *N*-hydroxybenzotriazole (HOBt) was from Advanced ChemTech and *Nα*-9-fluorenylmethyloxycarbonyl (Fmoc) amino acids were obtained from MultiSynTech. The side chain protecting groups were chosen as *tert*-butyl for aspartic acid, *tert*-butyloxycarbonyl (Boc) for lysine and 2,2,4,6,7-pentamethyl-dihydrobenzofuran-5-sulfonyl (Pbf) for arginine. Peptide-grade *tert*-butanol (^{t}BuOH), dichloromethane, *N*,*N*-dimethylformamide (DMF), 1,1,1,3,3,3-hexafluoroisopropanol (HFIP) *tert*-butyl methylether (MTBE), *N*-methylpyrrolidone (NMP), and trifluoroacetic acid (TFA) and HPLC-grade acetronitrile were purchased from Biosolve. 2-(4,7,10-tris(2-*tert*-butoxy-2-oxoethyl)-1,4,7,10-tetraazacyclododecan-1-yl) acetic acid (DOTA(O^tBu)$_3$) was purchased from Macrocyclics. Piperidine, *N*,*N*-diisopropylethylamine (DIPEA), $CuSO_4$ and sodium ascorbate were obtained from Acros Organics. Triisopropylsilane (TIS) and HPLC-grade TFA were obtained from Merck. Triflic anhydride and propargylbromide were purchased from Aldrich.

Radiolabeling of the RGD dendrimers

Dendrimers **23** (25 µg, 20 nmol), **24** (25 µg, 13 nmol), and **25** (120 µg, 33 nmol) were radiolabeled by dissolving these compounds in 500 µL 0.5 M NH_4OAc buffer, pH 6.0, containing 0.6 mg/mL gentisic acid. Then 22.2-37 MBq $^{111}InCl_3$ was added to each of the reaction mixtures. The reaction mixtures were degassed and subsequently heated at 100 °C for 15 min. The ^{111}In-labeled dendrimers were further purified on a Waters C-18 SepPak cartridge (Milford, MA). After applying the sample on the methanol-activated cartridge, the cartridge was washed with 5 mL 25 mM NH_4OAc and eluted with 25% CH_3CN in 25 mM NH_4OAc. The radiochemical purity was determined by reversed-phase HPLC (HP 1100 series, Hewlett Packard, Palo Alto, CA, USA) using a Zorbax RX-C18 column (250 × 4.6 mm) eluted with a linear gradient of buffer B (8 – 20% in 25 min or 8 – 100% in 30 min in buffer A (buffer A: 25 mM NH_4OAc, buffer B: CH_3CN) at a flow rate of 1 mL/min. The radioactivity of the

eluate was monitored using an in-line radiodetector (Flo-One Beta series, Radiomatic, Meriden, CT, USA).

Solid-phase $\alpha_v\beta_3$ binding assay

The affinity of the DOTA-conjugated monovalent **23**, divalent **24** and tetravalent **25** RGD dendrimers for the $\alpha_v\beta_3$ integrin was determined using a solid-phase competitive binding assay. ^{111}In-labeled DOTA-E-[c(RGDfK)]$_2$ (3 MBq/µg) was prepared as described above and was used as the tracer in the assay. Microtiter 96-well vinyl assay plates (Corning B.V., Schiphol-Rijk, The Netherlands) were coated with 100 µL/well of a solution of purified human integrin $\alpha_v\beta_3$ (150 ng/mL) in Triton X-100 Formulation (Chemicon International, Temecula, CA, USA) in coating buffer (25 mM Tris-HCl, pH 7.4, 150 mM NaCl, 1 mM $CaCl_2$, 0.5 mM $MgCl_2$ and 1 mM $MnCl_2$) for 17 h at 4 °C. The plates were washed twice with binding buffer (0.1% bovine serum albumin (BSA) in coating buffer). The wells were blocked for 2 h with 200 µL blocking buffer (1% BSA in coating buffer). The plates were washed twice with binding buffer. Then 100 µL binding buffer containing 11.1 kBq of ^{111}In-DOTA-E-[c(RGDfK)]$_2$ and appropriate dilutions of non-labeled monovalent **23**, divalent **24** and tetravalent **25** RGD dendrimers in binding buffer were incubated in the wells at 37 °C for 1 h. After incubation, the plates were washed three times with binding buffer. The retained radioactivity in each well was determined in a γ-counter (1480 Wizard, Wallac, Turku, Finland). The IC_{50} values of the RGD dendrimers were calculated by non-linear regression using GraphPad Prism (GraphPad Prism 4.0 Software, San Diego, CA, USA). Each data point represents the average of three individual determinations.

Biodistribution studies

In the right flank of 6-8 weeks old female nude BALB/c mice, 0.2 mL of a cell suspension of 8.5 × 10^6 cells/mL SK-RC-52 cells was injected subcutaneously (s.c.). Two weeks after inoculation of the tumor cells, mice were randomly divided into three groups. The mice were injected with 0.25-0.29 MBq of the ^{111}In-labeled dendrimers **23**, **24**, or **25** via a tail vein. The mice were euthanized by CO_2 asphyxiation, 2 and 24 h postinjection (p.i.) (3-5 mice/group). Blood, tumor, and the major organs and tissues were collected, weighed, and counted in a γ-counter. The percentage injected dose per gram (%ID/g) was determined for each sample. To investigate whether the uptake of each of the three RGD dendrimers is $\alpha_v\beta_3$-mediated, a separate group of mice was coinjected with an excess (50 µg) of non-radiolabeled DOTA-E-[c(RGDfK)]$_2$ to saturate all the $\alpha_v\beta_3$ integrin receptors.

Statistical analysis

All mean values are given ± standard deviation (S.D.). Statistical analysis was performed using the One-way Analysis of Variance. Tukey corrections for multiple comparisons were applied. The level of significance was set at $P<0.05$.

Syntheses

methyl 3-(prop-2-ynyloxy)benzoate (2): methyl 3-hydroxy benzoate [23c] (2.35 g, 15.5 mmol) was dissolved in dry DMF (25 mL) and anhydrous K_2CO_3 (2.63 g, 19.8 mmol, 1.3 equiv) was added. To this suspension, a solution of propargylbromide in toluene (2 mL, 17.9 mmol, 1.15 equiv) was added dropwise. The reaction mixture was stirred for 16 h at room temperature. Then, DMF was removed by evaporation and the residue was redissolved in EtOAc (75 mL) and the organic phase was washed with H_2O (3 × 25 mL), 1N $KHSO_4$ (3 × 25 mL) and brine (3 × 25 mL), dried (Na_2SO_4) and evaporated *in vacuo*. Propargyl ether **2** was obtained as a pale brownish waxy solid in 95% yield (2.80 g). R_f(EtOAc/hexane 4:1 v/v): 0.69; ^{1}H-NMR ($CDCl_3$) δ 2.56 (t (*J* 2.47 Hz), 2H, CH), 3.90 (s, 3H, OCH_3), 4.72 (d (*J* 2.47 Hz), 4H, ~O-CH_2), 7.16 (m, 1H, arom H), 7.35 (d (*J* 7.81 Hz), 1H, arom H), 7.62 (s, 1H, arom H), 7.66 (d (*J* 7.81 Hz), 1H, arom H); ^{13}C-NMR ($CDCl_3$) δ 52.0, 55.8, 76.0, 75.8, 115.1, 120.0, 122.7, 131.4, 157.3; MS analysis: calcd for $C_{11}H_{10}O_3$ 190.20, found ES-MS 191.38 $[M + H]^+$.

methyl 3,5-bis(prop-2-ynyloxy)benzoate (3): This compound was synthesized as described for **2** on a 130 mmol scale (methyl 3,5-dihydroxy benzoate [23c], 21.4 g) in dry DMF (250 mL) in the presence of anhydrous K_2CO_3 (45 g, 330 mmol, 2.5 equiv) and a solution of propargylbromide in toluene (35 mL, 314 mmol, 2.5 equiv). Dipropargyl ether **3** was obtained as off-white crystals in 81% yield (25.2 g). M.p.: 110 °C; R_f(EtOAc/hexane 4:1 v/v): 0.76; R_f(CH_2Cl_2/MeOH 98:2 v/v): 0.87; R_f($CHCl_3$/MeOH/AcOH 95:20:3 v/v): 0.83; ^{1}H-NMR ($CDCl_3$) δ 2.55 (t (*J* 2.47 Hz), 2H, CH), 3.91 (s, 3H, OCH_3), 4.72 (d (*J* 2.47 Hz), 4H, ~O-CH_2), 6.81 (t (*J* 2.20 Hz), 1H, arom H4), 7.29 (d (*J* 2.20 Hz), 2H, arom H2/H6); ^{13}C-NMR ($CDCl_3$) δ 52.4, 56.0, 76.0, 77.9, 107.5, 108.8, 132.0, 157.8, 158.4; MS analysis: calcd for $C_{14}H_{12}O_4$ 244.24, found ES-MS 244.99 $[M + H]^+$; Elemental analysis: calcd for $C_{14}H_{12}O_4$ C 68.83, H 4.95, found C 68.76, H 4.95.

3-(prop-2-ynyloxy)benzoic acid (4): Compound **2** (1.0 g, 5.24 mmol) was dissolved in dioxane/MeOH (50 mL, 14:5 v/v) and 4N NaOH (2 mL, 1.5 equiv) was added in one portion. The obtained reaction mixture was stirred for 5 h at room temperature. Then, the reaction mixture was neutralized by the addition of 1N HCl and the solvents were removed by evaporation. The residue was redissolved in EtOAc (50 mL) and the organic phase was washed with 1N $KHSO_4$ (3 × 20 mL) and brine (3 × 20 mL), dried (Na_2SO_4) and evaporated *in vacuo*. The residual solid was obtained in 97% yield (900 mg) and used without further purification in the next synthesis step. M.p.: 126-131 °C; R_f(EtOAc/hexane 7:3 v/v): 0.65; ^{1}H NMR ($CDCl_3$) δ: 2.55 (s, 1H, CH), 4.77 (s, 2H, ~O-CH_2), 7.25 (m, 1H, arom H), 7.42 (t, 1H, arom H5), 7.72 (m, 1H, arom H), 7.77 (d, 1H, arom H); ^{13}C NMR ($CDCl_3$) δ: 56.0, 76.0, 78.0, 115.6, 121.2, 123.5, 129.6, 130.6, 157.5, 171.9; Elemental analysis: calcd for $C_{10}H_8O_3$ C 68.18, H 4.58, found C 67.87, H 4.70.

3,5-bis(prop-2-ynyloxy)benzoic acid (5): Methyl ester **3** (5.66 g, 23.2 mmol) was saponified as described for compound **4**. The acid **5** was obtained in 96% yield (5.13 g) and used without further purification in the next synthesis step. M.p.: 171-174 °C; R_f(CH_2Cl_2/MeOH 9:1 v/v): 0.26; ^{1}H-NMR (DMSO-d_6) δ: 3.59 (broad s, 2H, CH), 4.85 (d (*J* 2.20 Hz), 4H, ~O-CH_2), 6.86 (t (*J* 2.47 Hz), 1H, arom H4), 7.17 (d (*J* 2.47 Hz), 2H, arom H2/H6); ^{13}C-NMR (DMSO-d_6) δ: 55.8, 78.6, 78.9, 107.0, 108.4, 132.9, 158.2,

166.8; MS analysis: calcd for $C_{14}H_{12}O_4$ 230.22, found ES-MS 231.01 [M + H]$^+$; Elemental analysis: calcd for $C_{13}H_{10}O_4$ C 67.82, H 4.38, found C 67.56, H 4.11.

methyl 3,5-bis(2-(3,5-bis(prop-2-ynyloxy)benzamido)ethoxy)benzoate (7): To a solution of 3,5-bis-(2-*tert*-butyloxycarbonylamino-ethoxy) methyl benzoate [23c] (**6**; 2.27 g, 5.0 mmol) in CH_2Cl_2 (25 mL), TFA (25 mL) was added to remove the Boc functionalities. After 1 h of stirring at room temperature, the volatiles were removed by evaporation and the residue was coevaporated with CH_2Cl_2 to remove any residual TFA. The obtained solid was used without further purification. Acid **5** (2.53 g, 11 mmol, 2.2 equiv) was dissolved in CH_2Cl_2 (100 mL) and the TFA-salt (dissolved in 50 mL CH_2Cl_2) followed by DIPEA (3.53 mL, 25 mmol, 5 equiv) were added. Finally, BOP (4.86 g, 11 mmol) was added and the obtained reaction mixture was stirred for 16 h at room temperature. Then, the solvent was removed *in vacuo* and the residue was redissolved in EtOAc (150 mL) and this solution was subsequently washed with H_2O (3 × 75 mL), 1N $KHSO_4$ (3 × 75 mL), H_2O (3 × 75 mL), 5% $NaHCO_3$ (3 × 75 mL) and brine (3 × 75 mL), dried (Na_2SO_4) and evaporated to dryness. The residue was crystallized from MeOH and was obtained as a white solid in 75% yield (2.54 g). M.p.: 113-124 °C; R_f(EtOAc/hexane 4:1 v/v): 0.49; R_f(CH_2Cl_2/MeOH 98:2 v/v): 0.13; R_f($CHCl_3$/MeOH/AcOH 95:20:3 v/v): 0.80; ^{1}H NMR (DMSO-d_6) δ: 3.58 (s, 4H, CH), 3.65 (m, 4H, ~CH_2~), 3.84 (s, 3H, OCH_3), 4.19 (m, 4H, ~CH_2~), 4.85 (s, 8H, ~O-CH_2), 6.80 (s, 2H, arom H4'), 6.87 (s, 1H, arom H4), 7.12 (s, 2H, arom H2/H6), (s, 4H, arom H2'/H6'), 8.67 (m, 2H, NH amide); ^{13}C-NMR ($CDCl_3$) δ: 40.4, 53.2, 56.9, 57.6, 77.0, 78.8, 106.3, 107.1, 107.6, 109.0 132.9, 137.4, 159.6, 160.3, 167.4, 168.1; MS analysis: calcd for $C_{38}H_{34}N_2O_{10}$ 678.22, found ES-MS 679.40 [M + H]$^+$, 701.45 [M + Na]$^+$; MALDI-TOF 679.298 [M + H]$^+$, 701.245 [M + Na]$^+$; Elemental analysis: calcd for $C_{38}H_{34}N_2O_{10}$ C 67.25, H 5.05, N 4.13 found C 66.92, H 5.09, N 4.10.

3,5-bis(2-(3,5-bis(prop-2-ynyloxy)benzamido)ethoxy)benzoic acid (8): Methyl ester **7** (1.36 g, 2 mmol) was saponified as described for compound **4**. Acid **8** was obtained as a white powder with nearly quantitative yield (1.33 g). M.p.: 163-168 °C; R_f(CH_2Cl_2/MeOH 9:1 v/v): 0.23; ^{1}H NMR (DMSO-d_6) δ: 3.58 (s, 4H, CH), 3.65 (m, 4H, ~CH_2~), 4.19 (m, 4H, ~CH_2~), 4.85 (s, 8H, ~O-CH_2), 6.80 (s, 2H, arom H4'), 6.83 (s, 1H, arom H4), 7.11 (s, 2H, arom H2/H6), 7.15 (s, 4H, arom H2'/H6'), 8.66 (m, 2H, NH amide); ^{13}C-NMR (DMSO-d_6) δ: 38.9, 55.8, 66.3, 78.4, 78.9, 105.0, 105.8, 106.8, 107.8, 132.9, 136.3, 158.2, 159.6, 165.8, 166.9; MS analysis: calcd for $C_{37}H_{32}N_2O_{10}$ 664.66, found ES-MS 665.75 [M + H]$^+$, 687.60 [M + Na]$^+$; Elemental analysis: calcd for $C_{37}H_{32}N_2O_{10}$ C 66.86, H 4.85, N 4.21 found C 66.76, H 4.72, N 4.11.

tert-**butyl 2-aminoethylcarbamate (10):** To a solution of 1,2-diaminoethane (13.4 mL, 200 mmol) in dioxane (100 mL) a solution of Boc_2O (5.46 g, 25 mmol) in dioxane (100 mL) was added dropwise over a period of 2 h. After the addition was complete, the obtained reaction mixture was stirred for 16 h at room temperature. Then, the solvent was removed by evaporation and the residue was suspended in H_2O (100 mL) and the white precipitate (bis-substitution product) was removed by filtration. The aqueous solution was extracted with CH_2Cl_2 (3 × 50 mL), and the collected organic layers were washed with brine (1 × 50 mL), dried ($MgSO_4$) and evaporated to dryness. Compound **10** was obtained as a

yellowish oil with 56% yield (2.25 g). R_f(CH_2Cl_2/MeOH 94:6 v/v): 0.24 ^{1}H NMR ($CDCl_3$) δ: 1.45 (broad s, 11H, $(CH_3)_3$ Boc/~NH_2), 2.79 (m, 2H, ~C*H*$_2$-NH_2), 3.16 (m, 2H, ~NH-C*H*$_2$~), 5.32 (m, 1H, NH urethane); ^{13}C-NMR ($CDCl_3$) δ 28.2, 41.6, 43.1, 78.9, 156.2; MS analysis: calcd for $C_7H_{16}N_2O_2$ 160.12, found ES-MS 161.15 [M + H]$^+$.

tert-**butyl 2-(3-(prop-2-ynyloxy)benzamido)ethylcarbamate (11)**: Acid **4** (774 mg, 4.40 mmol) and amine **10** (704 mg, 4.40 mmol) were dissolved in CH_2Cl_2 (25 mL) and BOP (1.95 g, 4.41 mmol) followed by DIPEA (1.77 mL, 10 mmol, 2.27 equiv) were added and the obtained reaction mixture was stirred for 16 h. Then, the solvent was removed by evaporation and the residue was redissolved in EtOAc (50 mL) and subsequently washed with H_2O (3 × 20 mL), 1N $KHSO_4$ (3 × 20 mL), H_2O (3 × 20 mL), 5% $NaHCO_3$ (3 × 20 mL) and brine (3 × 20 mL), dried (Na_2SO_4) and evaporated to dryness. The residue was purified by column chromatography (eluens: EtOAc/hexane 1:1 v/v) and was obtained as a white solid with 98% yield (1.38 g). M.p.: 118-121 °C; R_f(EtOAc/hexane 1:1 v/v): 0.20; ^{1}H NMR ($CDCl_3$) δ: 1.42 (s, 9H, $(CH_3)_3$ Boc), 2.54 (s, 1H, CH), 3.38 (m, 2H, ~NH-C*H*$_2$-CH_2~), 3.54 (m, 2H, ~CH_2-C*H*$_2$-NH~), 4.70 (s, 2H, ~O-CH_2), 5.35 (m, 1H, NH urethane), 7.10 – 7.47 (broad m, 5H, arom H/NH amide); ^{13}C NMR ($CDCl_3$) δ: 28.3, 39.9, 41.7, 55.8, 75.7, 78.1, 79.7, 113.4, 118.3, 119.8, 129.4, 135.6, 157.3, 157.6, 167.5; MS analysis: calcd for $C_{17}H_{22}N_2O_4$ 318.16, found ES-MS 319.27 [M + H]$^+$, 341.33 [M + Na]$^+$; Elemental analysis: calcd for $C_{17}H_{22}N_2O_4$ C 64.13, H 6.97, N 8.80 found C 63.81, H 6.81, N 8.63.

tert-**butyl 2-(3,5-bis(prop-2-ynyloxy)benzamido)ethylcarbamate (12)**: This compound was synthesized using acid **5** (506 mg, 2.20 mmol) and amine **10** (352 mg, 2.20 mmol) as described for **11**. Compound **12** was obtained in 96% yield (760 mg) after column chromatography with EtOAc/hexane 8:2 v/v as eluens. M.p.: 128-134 °C; R_f(EtOAc/hexane 7:3 v/v): 0.31; ^{1}H NMR ($CDCl_3$) δ: 1.42 (s, 9H, $(CH_3)_3$ Boc), 2.55 (s, 2H, CH), 3.37 (m, 2H, ~NH-C*H*$_2$-CH_2~), 3.52 (m, 2H, ~CH_2-C*H*$_2$-NH~), 4.68 (s, 4H, ~O-CH_2), 5.30 (m, 1H, NH urethane), 6.72 (s, 1H, arom H4), 7.06 (s, 2H, arom H2/H6), 7.44 (m, 1H, NH amide); ^{13}C NMR (125 MHz, $CDCl_3$) δ: 28.3, 40.0, 41.7, 56.0, 75.9, 78.0, 79.8, 105.5, 106.6, 136.4, 157.3, 158.6, 167.2; MS analysis: calcd for $C_{20}H_{24}N_2O_5$ 372.17, found ES-MS 373.24 [M + H]$^+$, 395.27 [M + Na]$^+$; Elemental analysis: calcd for $C_{20}H_{24}N_2O_5$ C 64.50, H 6.50, N 7.52 found C 63.61, H 6.21, N 7.05.

tert-**butyl-2,2',2''-(10-(2-oxo-2-(2-(3-(prop-2-ynyloxy)benzamido)ethylamino)ethyl)-1,4,7,10-tetraazacyclododecane-1,4,7-triyl)triacetate (13)**: To a solution of compound **11** (100 mg, 0.31 mmol) in CH_2Cl_2 (5 mL), TFA (5 mL) was added to remove the Boc protecting group. After 1 h of stirring at room temperature, the volatiles were removed by evaporation and the residue was coevaporated with CH_2Cl_2 to remove any residual TFA. The obtained solid was used without further purification. Then, the TFA-salt was dissolved in CH_2Cl_2 (10 mL) and 2-(4,7,10-tris(2-*tert*-butoxy-2-oxoethyl)-1,4,7,10-tetraazacyclododecan-1-yl) acetic acid (DOTA(O^tBu)$_3$; 177 mg, 0.31 mmol), BOP (137 mg, 0.31 mmol) followed by DIPEA (220 µL, 1.24 mmol, 4 equiv) were added and the obtained reaction mixture was stirred for 16 h at room temperature. Subsequently, the solvent was removed by evaporation and the residue was redissolved in EtOAc (50 mL) and this solution was washed with H_2O (3 × 20 mL), 1N

$KHSO_4$ (3 × 20 mL), H_2O (3 × 20 mL), 5% $NaHCO_3$ (3 × 20 mL), brine (3 × 20 mL) and dried (Na_2SO_4). Finally, the solvent was evaporated in vacuo after which **13** was obtained as a pale yellow oil with 94% yield (227 mg). R_f(CH_2Cl_2/MeOH 9:1 v/v): 0.49; R_t: 18.10 min (C8); ^{1}H NMR ($CDCl_3$) δ: 1.42 (s, 27H, $(CH_3)_3$ ^{t}Bu), 2.20 – 3.70 (broad s, 28H, CH_2 DOTA (24H)/~NH-C*H*$_2$-C*H*$_2$-NH~(4H)), 2.52 (s, 1H, CH), 4.75 (s, 2H, ~O-CH_2), 6.85 (m, 1H, NH), 7.08 (m, 1H, arom H), 7.25 – 7.32 (m, 2H, arom H), 7.51 (m, 2H, arom H/NH); ^{13}C NMR ($CDCl_3$) δ: 27.9, 39.6, 39.7, 55.6, 55.8, 56.0, 75.5, 78.4, 81.8, 112.9, 118.9, 120.3, 129.6, 135.5, 157.6, 167.4, 172.0, 172.4; MS analysis: calcd for $C_{40}H_{64}N_6O_9$, 772.47, found ES-MS 773.90 [M + H]$^+$.

tert-**butyl 2,2',2''-(10-(2-(2-(3,5-bis(prop-2-ynyloxy)benzamido)ethylamino)-2-oxoethyl)-1,4,7,10-tetraazacyclododecane-1,4,7-triyl)triacetate (14)**: This compound was synthesized as described for **13** starting from **12** (107 mg, 0.30 mmol). Compound **14** was obtained as a yellowish solid with nearly quantitative yield (250 mg). M.p.: 74-84 °C; R_f($CHCl_3$/MeOH/AcOH 95:20:3 v/v/v): 0.45; R_t: 18.70 min (C8); ^{1}H NMR ($CDCl_3$) δ: 1.43 (s, 27H, $(CH_3)_3$ ^{t}Bu), 2.04 – 3.70 (broad s, 28H, CH_2 DOTA (24H)/~NH-C*H*$_2$-C*H*$_2$-NH~(4H)), 2.52 (s, 2H, CH), 4.73 (s, 4H, ~O-CH_2), 6.73 (m, 2H, arom H4/NH), 7.10 (s, 2H, arom H2/H6), 7.11 (m, 1H, NH); ^{13}C NMR ($CDCl_3$) δ: 27.9, 39.6, 50.0*, 55.6, 55.8, 56.2, 75.6, 78.4, 81.9, 106.4, 106.5, 136.4, 158.7, 167.2, 172.0, 172.4 (*broad signal: CH_2 DOTA); MS analysis: calcd for $C_{43}H_{66}N_6O_{10}$, 826.48, found ES-MS 827.65 [M + H]$^+$; Elemental analysis: calcd for $C_{43}H_{66}N_6O_{10}$·K_2SO_4 C 51.58, H 6.64, N 8.39 found C 52.05, H 6.54, N 8.04.

tert-**butyl-2 (3,5-bis(2-(3,5-bis(prop-2-ynyloxy)benzamido)ethoxy)benzamido)ethylcarbamate (15)**: This compound was synthesized as described for **11** using amine **10** (292 mg, 2.0 mmol) and acid **8** (460 mg, 2.0 mmol). Compound **15** was obtained as a pale yellow solid with 91% yield (1.46 g). M.p.: 110 °C; R_f(EtOAc/hexane 4:1 v/v): 0.53; R_t: 18.38 min (C8); ^{1}H NMR (DMSO-d_6) δ: 1.37 (s, 9H, $(CH_3)_3$ Boc), 3.10 (m, 2H, ~NH-C*H*$_2$-CH_2-NH~), 3.28 (m, 2H, ~NH-CH_2-C*H*$_2$-NH~), 3.58 (s, 4H, CH), 3.65 (m, 4H, ~O-CH_2-C*H*$_2$-NH~), 4.17 (m, 4H, ~O-C*H*$_2$-CH_2-NH~), 4.85 (s, 8H, ~O-CH_2), 6.72 (m, 1H, arom H4), 6.80 (m, 2H, arom H2/H6), 6.90 (m, 1H, NH urethane), 7.05 (m, 2H, arom H4'), 7.15 (m, 4H, arom H2'/H6'), 8.44 (m, 1H, NH amide), 8.68 (m, 2H, NH amide); ^{13}C NMR (DMSO-d_6) δ: 28.0, 39.2, 55.9, 75.8, 75.9, 77.8, 79.6, 104.7, 105.4, 105.9, 106.7, 135.9, 136.1, 157.2, 158.5, 159.5, 167.7, 167.8, 168.0, 168.1; MS analysis: calcd for $C_{44}H_{46}N_4O_{11}$, 806.32, found ES-MS 807.65 [M + H]$^+$, 707.55 [(M – $C_5H_8O_2$) + H]$^+$; Elemental analysis: calcd for $C_{44}H_{46}N_4O_{11}$ C 65.50, H 5.75, N 6.94 found C 65.28, H 5.71, N 6.80.

tert-**butyl 2,2',2''-(10-(2-(2-(3,5-bis(2-(3,5-bis(prop-2-ynyloxy)benzamido)ethoxy)benzamido)ethylamino)-2-oxyethyl)-1,4,7,10-tetraazacyclododecane-1,4,7-triyl)triacetate (16)**: Compound **16** was synthesized as described for **13** starting from **15** (242 mg, 0.30 mmol). After workup, the crude product was purified by column chromatography (eluens DCM/MeOH 98:2 v/v DCM/MeOH 9:1 v/v) to yield a white solid (227 mg, 60%). M.p.: 108-114 °C; R_f(CH_2Cl_2/MeOH 9:1 v/v): 0.30; R_t: 19.70 min (C8); ^{1}H NMR ($CDCl_3$) δ: 1.45 (s, 27H, $(CH_3)_3$ ^{t}Bu), 2.04 – 4.50 (broad s, 36H, CH_2 DOTA (24H)/~NH-C*H*$_2$-C*H*$_2$-NH~(4H)/~O-C*H*$_2$-C*H*$_2$-NH~(8H)), 2.55 (s, 4H, CH), 4.72 (m, 8H, ~O-CH_2), 6.60 (m, 1H, arom H4), 6.70 (m, 2H, arom H2/H6), 7.18 – 7.33 (m, 6H, arom H2'/H4'/H6'), 7.80 (m, 2H, NH), 8.75 (m, 2H, NH); ^{13}C

NMR ($CDCl_3$) δ: 27.9, 28.0, 38.8, 39.3, 39.7, 55.7, 55.9, 56.2, 66.5, 75.8, 76.0, 78.3, 82.0, 106.0, 106.3, 106.5, 106.7, 136.3, 136.8, 158.6, 159.4, 166.7, 166.9, 171.5, 172.3; MS analysis: calcd for $C_{67}H_{88}N_8O_{16}$, 1260.63, found ES-MS 1261.75 $[M + H]^+$; Elemental analysis: calcd for $C_{67}H_{88}N_8O_{16}{\cdot}H_2SO_4$ C 59.19, H 6.67, N 8.24 found C 59.60, H 6.82, N 7.71.

H-Asp(O^{t}Bu)-D-Phe-Lys(Boc)-Arg(Pbf)-Gly-O-**2-chlorotrityl resin (17)**: The 2-chlorotrityl chloride resin was treated with $SOCl_2/CH_2Cl_2$ (1:1 v/v; 2 × 6 mL, 10 min) to convert it completely into the chloride form prior loading of the first amino acid. To remove any residual $SOCl_2$, the resin was extensively washed with CH_2Cl_2 (6 × 10 mL, 10 min). Then, Fmoc-Gly-OH (430 mg, 1.44 mmol) was dissolved in CH_2Cl_2 (10 mL) and DIPEA (510 µL, 2.88 mmol) followed by the 2-chlorotrityl chloride resin (360 mg (1 mmol/g), 0.36 mmol) were added and the obtained slurry was gently swirled for 2 h at room temperature. The resin was subsequently washed with CH_2Cl_2/MeOH/DIPEA (17:2:1 v/v/v; 3 × 10 mL, 10 min) to cap any remaining linked tritylchloride, followed by CH_2Cl_2 (3 × 10 mL, 2 min), DMF (3 × 10 mL, 2 min) and CH_2Cl_2 (3 × 10 mL, 2 min). The loading of the resin, as calculated from an Fmoc determination, was 64% (0.64 mmol/g). The linear peptide sequence H-Asp(O^{t}Bu)-D-Phe-Lys(Boc)-Arg(Pbf)-Gly-OH was synthesized according to the Fast*Moc* solid-phase peptide synthesis protocols [31] and the final Fmoc-group was removed to obtain peptide resin **17**.

cyclo**(Arg-Gly-Asp-D-Phe-Lys) (18)**: Peptide resin **17** was treated twice with HFIP/CH_2Cl_2 (32 mL, 1:4 v/v) for 45 min each to cleave the protected peptide acid from the resin. After this, the resin was washed with CH_2Cl_2 (3 × 20 mL, 10 min) and all fractions were collected and evaporated to dryness. The crude protected peptide acid (MS analysis: calcd for $C_{49}H_{75}N_9O_{13}S$, 1030.24, found ES-MS 1031.55 $[M + H]^+$) was obtained with 85% yield (202 mg, 0.20 mmol). This crude peptide was dissolved in CH_2Cl_2 (30 mL) and HOBt (30 mg, 0.20 mmol), BOP (41 mg, 0.20 mmol) followed by DIPEA (80 µL, 0.45 mmol, 2.25 equiv) were added and the obtained reaction mixture was stirred for 16 h at room temperature. Subsequently, the solvent was partly removed by evaporation and the oily residue was dissolved in $CHCl_3$ (50 mL) and washed with 1N $KHSO_4$ (3 × 20 mL), H_2O (3 × 20 mL) and brine (3 × 20 mL). After the final wash steps, the solvent was removed *in vacuo* a white solid was obtained. This compound was dissolved in TFA/H_2O/TIS (10 mL; 95:2.5:2.5 v/v/v) and stirred for 3 h to remove the side chain protecting groups. The crude cyclic peptide was isolated by precipitation with MTBE/hexane 1:1 v/v at −20°C. After centrifugation, the pellet was dissolved in *tert*-BuOH/H_2O 1:1 v/v, lyophilized and subsequently purified by HPLC (C8). Cyclic peptide **18** was obtained in 42% (51 mg) yield. R_t: 9.97 min (C4); R_t: 15.26 min (CN); MS analysis: calcd for $C_{27}H_{41}N_9O_7$, 603.31, found ES-MS 604.60 $[M + H]^+$.

N-ε-**azido** cyclo**(Arg-Gly-Asp-D-Phe-Lys) (19)**: Cyclic peptide **18** (200 mg, 0.33 mmol) was dissolved in *tert*-BuOH/H_2O (5 mL; 1:1 v/v) and the pH was adjusted to 10 by the addition of 1N NaOH. To this solution were added: $CuSO_4.5H_2O$ (8 mg, 0.03 mmol, 0.1 equiv) and a solution of triflic azide (587 mg, 3.3 mmol, 10 equiv) in CH_2Cl_2 (freshly prepared from triflic anhydride (555 µL, 3.3 mmol, 10 equiv) and NaN_3 (975 mg, 15 mmol, 4.5 equiv) in CH_2Cl_2/H_2O (13 mL; 10:3 v/v) [27]. The obtained two-phase

reaction mixture was firmly stirred for 16 h at room temperature. Then, the solvents were removed by evaporation and the residue was mixed with *tert*-BuOH/H_2O and subsequently lyophilized to yield 202 mg (97%) crude reaction product. Pure azido peptide **19** was obtained in 21% yield (44 mg) after purification by HPLC (C8). R_f($CHCl_3$/MeOH/AcOH 90:20:3 v/v/v): 0.25; R_t: 16.81 min (C4); R_t: 17.33 min (CN); FTIR (KBr) υ: 2100 cm^{-1}; ^{1}H NMR (500 MHz, H_2O/D_2O 9:1 v/v, 293 K, 6.4 mM, pH 4): Arg, δ: 1.43 (m, 2H, γCH_2), 1.65/1.86 (double m, 2H, βCH_2), 3.18 (m, 2H, δCH_2), 4.36 (m, 1H, αCH), 7.20 (t (*J* 5.8 Hz), 1H, δNH), 8.04 (d (*J* 8.7 Hz), 1H, αNH); Gly, δ: 3.49 (dd (*J* 4.5 Hz, *J* 14.8 Hz), 1H, αCH_2), 4.21 (dd (*J* 7.7 Hz, *J* 14.8 Hz), 1H, αCH_2), 8.33/8.36 (dd, (*J* 4.7 Hz, *J* 7.4 Hz), 1H, αNH); Asp, δ: 2.63/2.66 (dd (*J* 6.7 Hz, *J* 16.4 Hz), 1H, βCH_2), 2.79/2.83 (dd (*J* 7.7 Hz, *J* 16.4 Hz), 1H, βCH_2), 4.73 (m, 1H, αCH), 8.12 (d, (*J* 8.8 Hz), 1H, αNH); D-Phe, δ: 2.93/2.98 (dd (*J* 10.3 Hz, *J* 13.2 Hz), 1H, βCH_2), 3.07/3.10 (dd (*J* 5.9 Hz, *J* 13.2 Hz), 1H, βCH_2), 4.45 (m, 1H, αCH), 7.25 (d (*J* 7.3 Hz), 2H, arom H), 7.33-7.38 (m, 3H, arom H), 8.42 (d (*J* 5.9 Hz), 1H, αNH); azido Lys, δ: 0.95 (m, 2H, γCH_2), 1.46/1.65 (double m, 2H, βCH_2), 1.49 (m, 2H, δCH_2), 3.24 (t (*J* 7.1 Hz), 2H, εCH_2), 3.85 (m, 1H, αCH), 8.44 (d (*J* 5.6 Hz), 1H, αNH); ^{13}C NMR (H_2O/D_2O 9:1 v/v, 293 K, 6.4 mM, pH 4): Arg, δ: 29.8 γC, 30.0 βC, 43.3 δC, 55.2 αC, 176.0 αCO, 176.3 guanidino C; Gly, δ: 46.3 αC, 172.9 αCO; Asp, δ: 38.5 βC, 52.9 αC, 175.1 αCO, 178.6 βCO; D-Phe, δ: 39.6 βC, 58.1 αC, 130.0 arom CH, 131.5 arom CH, 131.9 arom CH, 138.8 arom qC, 176.5 αCO; azido Lys, δ: 25.1 γC, 27.2 δC, 32.6 βC, 53.3 εC, 58.2 αC, 177.9 αCO; MS analysis: calcd for $C_{27}H_{39}N_{11}O_7$, 629.30, found ES-MS 630.55 $[M + H]^+$, 652.70 $[M + Na]^+$, 668.25 $[M + K]^+$.

General procedure for the microwave-assisted click reaction: [22] the alkyne (1 equiv) and the azide (1.3 equiv per arm) were dissolved in DMF/H_2O. To this solution, $CuSO_4.5H_2O$ (0.05 equiv) and Na-ascorbate (0.50 equiv) were added. The reaction mixture was placed in a microwave reactor and irradiated during 10 – 30 min at 100°C. The cycloaddition was monitored on TLC and LC-MS for completion of the reaction.

monovalent cyclo**[RGDfK] peptide dendrimer (20)**: Alkyne **2** (1.3 mg, 6.6 μmol) and azido peptide **19** (5.4 mg, 7.3 μmol, 1.1 equiv) were dissolved in DMF (500 μL) and 0.05 M Na-ascorbate (66 μL, 3.3 μmol, 0.50 equiv) followed by 6 mM $CuSO_4.5H_2O$ (55 μL, 0.33 μmol, 0.05 equiv) were added. The reaction mixture was placed in the microwave reactor and irradiated for 30 min at 100°C. Then, the solvents were removed under reduced pressure and the residue was dissolved in *tert*-BuOH/H_2O 1:1 v/v and lyophilized and subsequently purified by semi-prep HPLC (C18). Yield: 3.1 mg (57%). R_t: 18.85 min (CN); MS analysis: calcd for $C_{38}H_{49}N_{11}O_{10}$, 819.366, found ES-MS 820.60 $[M + H]^+$, found MALDI-TOF 820.641 $[M + H]^+$, 842.620 $[M + Na]^+$.

divalent cyclo**[RGDfK] peptide dendrimer (21)**: For this synthesis, alkyne **3** (0.8 mg, 3.3 μmol) and azido peptide **19** (6.3 mg, 8.5 μmol, 1.3 equiv) were used. After purification by semi-prep HPLC compound **21** was obtained with 40% yield (1.9 mg). R_t: 18.97 min (C4); R_t: 20.30 min (CN); MS analysis: calcd for $C_{68}H_{90}N_{22}O_{18}$, 1502.680, found MALDI-TOF 1503.646 $[M + H]^+$.

tetravalent cyclo**[RGDfK] peptide dendrimer (22)**: For this synthesis, alkyne **7** (1.10 mg, 1.6 µmol) and azido peptide **19** (6.3 mg, 8.5 µmol, 1.3 equiv) were used. After purification by semi-prep HPLC compound **22** was obtained with 14% yield (0.7 mg). R_t: 21.23 min (CN); MS analysis: calcd for $C_{146}H_{190}N_{46}O_{38}$, 3195.435 ($M_{ave}$), found MALDI-TOF 3196.573 $[M + H]_{ave}^+$.

DOTA-conjugated monovalent cyclo**[RGDfK] peptide dendrimer (23)**: Alkyne **13** (5.5 mg, 7.1 µmol) and azido peptide **19** (6.0 mg, 8.1 µmol, 1.1 equiv) were dissolved in DMF (500 µL) and 0.05 M Na-ascorbate (72 µL, 3.6 µmol, 0.50 equiv) followed by 6 mM $CuSO_4.5H_2O$ (60 µL, 0.36 µmol, 0.05 equiv) were added. The reaction mixture was placed in the microwave reactor and irradiated for 3 × 5 min at 100°C. Then, the solvents were removed under reduced pressure and the residue was dissolved in *tert*-BuOH/H_2O 1:1 v/v and lyophilized. The obtained fluffy solid was dissolved in TFA/H_2O (1 mL; 95:5 v/v) and stirred for 4 h at room temperature. Subsequently, the reaction mixture was concentrated *in vacuo* and the residue was redissolved in *tert*-BuOH/H_2O 1:1 v/v, lyophilized and purified by semi-prep HPLC (C18) to give compound **23** in 13% yield (1.1 mg). R_t: 10.27 min (C18); MS analysis: calcd for $C_{55}H_{79}N_{17}O_{16}$, 1234.340 (M_{ave}), found MALDI-TOF 1234.807 $[M + H]_{ave}^+$.

DOTA-conjugated divalent cyclo**[RGDfK] peptide dendrimer (24)** [28]: Alkyne **14** (4.9 mg, 5.9 µmol) and azido peptide **19** (11 mg, 14.8 µmol, 1.3 equiv) were dissolved in DMF/2,6-lutidine (1 mL, 7:3 v/v) and to this solution the following reagents were subsequently added: CuOAc (1.8 mg, 14.7 µmol, 2.5 equiv), Na-ascorbate (5.9 mg, 29.8 µmol, 5.1 equiv) and DIPEA (9.8 µL, 7.1 µmol, 1.2 equiv). The obtained reaction mixture was heated by microwave irradiation to 100°C for 3 × 5 min. Then, the solvents were removed under reduced pressure and the residue was dissolved in *tert*-BuOH/H_2O 1:1 v/v and lyophilized. The obtained fluffy solid was dissolved in TFA/H_2O (1 mL; 95:5 v/v) and stirred for 4 h at room temperature. Subsequently, the reaction mixture was concentrated *in vacuo* and the residue was redissolved in *tert*-BuOH/H_2O 1:1, lyophilized and purified by semi-prep HPLC (C18) to obtain compound **24** in 11% yield (1.3 mg). R_t: 12.08 min (C18); MS analysis: calcd for $C_{85}H_{120}N_{28}O_{24}$, 1918.067 ($M_{ave}$), found MALDI-TOF 1918.516 $[M + H]_{ave}^+$.

DOTA-conjugated tetravalent cyclo**[RGDfK] peptide dendrimer (25)**: Alkyne **16** (3.8 mg, 3.0 µmol) and azido peptide **19** (11 mg, 14.8 µmol, 1.2 equiv) were dissolved in DMF (500 µL) and to this solution, 0.05 M Na-ascorbate (30 µL, 1.5 µmol, 0.50 equiv) followed by 6 mM $CuSO_4.5H_2O$ (25 µL, 0.15 µmol, 0.05 equiv) were added. The obtained reaction mixture was heated by microwave irradiation to 100°C for 2 × 5 min. Then, the solvents were removed under reduced pressure and the residue was dissolved in *tert*-BuOH/H_2O 1:1 v/v and lyophilized. The obtained fluffy solid was dissolved in TFA/H_2O (1 mL; 95:5 v/v) and stirred for 4 h at room temperature. Subsequently, the reaction mixture was concentrated *in vacuo* and the residue was redissolved in *tert*-BuOH/H_2O 1:1 v/v, lyophilized and purified by semi-prep HPLC (C18) to give compound **25** in 36% yield (3.9 mg). R_t: 11.6 min (C18); MS analysis: calcd for $C_{163}H_{220}N_{52}O_{44}$, 3611.873 ($M_{ave}$), found MALDI-TOF 3612.530 $[M + H]_{ave}^+$.

References and notes

1. (*a*) E. F. Plow, T. A. Haas, L. Zhang, J. Loftus and J. W. Smith, *J. Chem. Biol.*, 2000, **275**, 21785; (*b*) K.-E. Gottschalk and H. Kessler, *Angew. Chem. Int. Ed.*, 2002, **41**, 3767.

2. (*a*) R. O. Hynes, *Cell*, 1992, **69**, 11; (*b*) P. C. Brooks, R. A. Clark and D. A. Cheresh, *Science*, 1994, **264**, 569; (*c*) R. O. Hynes, *Nat. Med.*, 2002, **8**, 918.

3. J.-P. Xiong, T. Stehle, R. Zhang, A. Joachimiak, M. Frech, S. L. Goodman and M. A. Arnaout, *Science*, 2002, **296**, 151.

4. P. C. Brooks, A. M. P. Montgomery, M. Rosenfeld, R. A. Reisfeld, T. Hu, G. Klier and D. A. Cheresh, *Cell*, 1994, **79**, 1157.

5. R. Haubner, D. Finsinger and H. Kessler, *Angew. Chem. Int. Ed.*, 1997, **36**, 1374.

6. (*a*) R. M. Keenan, W. H. Miller, C. Kwon, F. E. Ali, J. E. Callahan, R. R. Calvo, S.-M. Hwang, K. D. Kopple, C. E. Peishoff, J. M. Samanen, A. S. Wong, C.-K. Yuan and W. F. Huffman, *J. Med. Chem.*, 1997, **40**, 2289; (*b*) C. P. Carron, D. M. Meyer, J. A. Pegg, V. W. Engelman, M. A. Nickols, S. L. Settle, W. F. Westlin, P. G. Ruminski and G. A. Nickols, *Cancer Res.*, 1998, **58**, 1930; (*c*) J. D. Hood, M. Bednarski, R. Frausto, S. Guccione, R. A. Reisfeld, R. Xiang, D. A. Cheresh, *Science*, 2002, **296**, 2404; (*d*) C. A. Burnett, J. Xie, J. Quijano, Z. Shen, F. Hunter, M. Bur, K. C. P. Li and S. N. Danthi, *Bioorg. Med. Chem.*, 2005, **13**, 3763; (*e*) I. Dijkgraaf, J. A. W. Kruijtzer, C. Frielink, A. C. Soede, H. W. Hilbers, W. J. G. Oyen, F. H. M. Corstens, R. M. J. Liskamp and O. C. Boerman, *Nucl. Med. Biol.*, 2006, **33**, 953.

7. M. Gurrath, G. Müller, H. Kessler, M. Aumailley and R. Timpl, *Eur. J. Biochem.*, 1992, **210**, 911.

8. R. Haubner, R. Gratias, B. Diefenbach, S. L. Goodman, A. Jonczyk and H. Kessler, *J. Am. Chem. Soc.*, 1996, **118**, 7461.

9. (*a*) R. Haubner, H.-J. Wester, U. Reuning, R. Senekowitsch-Schmidtke, B. Diefenbach, H. Kessler, G. Stöcklin and M. Schwaiger, *J. Nucl. Med.*, 1999, **40**, 1061; (*b*) R. Haubner, H.-J. Wester, F. Burkhart, R. Senekowitsch-Schmidtke, W. Weber, S. L. Goodman, H. Kessler and M. Schwaiger, *J. Nucl. Med.*, 2001, **42**, 326; (*c*) W. Wang, Q. Wu, M. Pasuelo, J. S. McMurray and C. Li, *Bioconjugate Chem.*, 2005, **16**, 729; (*d*) J. Auernheimer, D. Zukowski, C. Dahmen, M. Kantlehner, A. Enderle, S. L. Goodman and H. Kessler, *ChemBioChem*, 2005, **6**, 2034; (*e*) S. Achilefu, S. Bloch, M. A. Markiewicz, T. Zhong, Y. Ye, R. B. Dorshow, B. Chance and K. Liang, *Proc. Natl. Acad. Sci. USA*, 2005, **102**, 7976; (*f*) J. Auernheimer and H. Kessler, *Bioorg. Med. Chem. Lett.*, 2006, **16**, 271 (*g*) W. J. M. Mulder, R. Koole, R. J. Brandwijk, G. Storm, P. T. K. Chin, G. J. Strijkers, C. De Mello Donegá, K. Nicolay and A. W. Griffioen, *Nano Lett.*, 2006, **6**, 1; (*h*) W. Cai, D.-W. Shin, K. Chen, O. Gheysens, Q. Cao, S. X. Wang, S. S. Gambhir and X. Chen, *Nano Lett.*, 2006, **6**, 669.

10. (*a*) A. Varki, *Glycobiology*, 1993, *3*, 97; (*b*) M. Mammen, S.-K. Choi and G. M. Whitesides, *Angew. Chem. Int. Ed.*, 1998, **37**, 2754; (*c*) R. H. Kramer and J. W. Karpen, *Nature*, 1998, **395**, 710; (*d*) A. Mulder, J. Huskens and D. N. Reinhoudt, *Org. Biomol. Chem.*, 2004, **2**, 3409; (*e*) L. L. Kiessling, J. E. Gestwicki and L. E. Strong, *Angew. Chem. Int. Ed.*, 2006, **45**, 2348.

11. (*a*) G. R. Newkome, C. N. Moorefield and F. Vögtle, *Dendrimers and Dendrons: Concept, Synthesis, Applications*, Wiley, New York, 2001; (*b*) J. M. J. Fréchet, *Proc. Natl. Acad. Sci. USA*, 2002, **99**, 4782; (*c*) C. C. Lee, J. A. MacKay, J. M. J. Fréchet and F. C. Szoka, *Nat. Biotechnol.*, 2005, **23**, 1517.

12. H.-J. Wester and H. Kessler, *J. Nucl. Med.*, 2005, **46**, 1940.

13. (*a*) M. L. Janssen, W. J. Oyen, I. Dijkgraaf, L. F. Massuger, C. Frielink, D. S. Edwards, M. Rajopadhye, H. Boonstra, F. H. Corstens and O. C. Boerman, *Cancer Res.*, 2002, **62**, 6146; (*b*) R. J. Kok, A. J. Schraa, E. J. Bos, H. E. Moorlag, S. A. Ásgeirsdóttir, M. Everts, D. K. F. Meijer and G. Molema, *Bioconjugate Chem.*, 2002, **13**, 128; (*c*) M. Janssen, W. J. G. Oyen, L. F. A. G. Massuger, C. Frielink, I. Dijkgraaf, D. S. Edwards, M. Radjopadhye, F. H. M. Corstens and O. C. Boerman, *Cancer Biother. Radiopharm.*, 2002, **17**, 641; (*d*) G. Thumshirn, U. Hersel, S. L. Goodman and H. Kessler, *Chem. Eur. J.*, 2003, **9**, 2717; (*e*) M. Janssen, C. Frielink, I. Dijkgraaf, W. Oyen, D. S. Edwards, S. Liu, M. Rajopaghye, L.

Massuger, F. Corstens and O. Boerman, *Cancer Biother. Radiopharm.*, 2004, **19**, 399; (*f*) B. R. Line, A. Mitra, A. Nan, H. Ghandehari, *J. Nucl. Med.*, 2005, **46**, 1552; (*g*) Y. Wu, X. Zhang, Z. Xiong, Z. Cheng, D. R. Fisher, S. Liu, S. S. Gambhir and X. Chen, *J. Nucl. Med.*, 2005, **46**, 1707; (*h*) Z. Cheng, Y. Wu, Z. Xiong, S. S. Gambhir and X. Chen, *Bioconjugate Chem.*, 2005, **16**, 1433; (*i*) S. Liu, W.-Y. Hsieh, Y.-S. Kim and S. I. Mohammed, *Bioconjugate Chem.*, 2005, **16**, 1508; (*j*) R. Shukla, T. P. Thomas, J. Peters, A. Kotlyar, A. Myc and J. R. Baker, Jr., *Chem. Commun.*, 2005, 5739; (*k*) X. Chen, C. Plasencia, Y. Hou and N. Neamati, *J. Med. Chem.*, 2005, **48**, 1098; (*l*) E. Garanger, D. Boturyn, O. Renaudet, E. Defrancq and P. Dumy, *J. Org. Chem.*, 2006, **71**, 2402; (*m*) E. Garanger, D. Boturyn, J.-L. Coll, M.-C. Favrot and P. Dumy, *Org. Biomol. Chem.*, 2006, **4**, 1958; (*n*) Y. Ye, S. Bloch, B. Xu and S. Achilefu, *J. Med. Chem.*, 2006, **49**, 2268; (*o*) I. Dijkgraaf, J. A. W. Kruijtzer, S. Liu, A. C. Soede, W. J. G. Oyen, F. H. M. Corstens, R. M. J. Liskamp and O. C. Boerman, *Eur. J. Nucl. Med. Mol. Imaging*, 2007, **34**, 267.

14. (*a*) R. G. Denkewalter, J. Kolc and W. J. Lukasavage, *US Patent 4,289,872*, September 15, 1981; (*b*) R. G. Denkewalter, J. F. Kolc and W. J. Lukasavage, *US Patent 4,410,688*, October 18, 1983; (*c*) J. P. Tam, *Proc. Natl. Acad. Sci. USA*, 1988, **85**, 5409.

15. (*a*) A. Herrmann, G. Mihov, G. W. M. Vandermeulen, H.-A. Klok and K. Müllen, *Tetrahedron*, 2003, **59**, 3925; (*b*) L. Crespo, G. Sanclimens, M. Pons, E. Giralt, M. Royo and F. Albericio, *Chem. Rev.*, 2005, **105**, 1663; (*c*) P. Niederhafner, J. Šebestík and J. Ježek, *J. Peptide Sci.*, 2005, **11**, 757.

16. J. P. Tam and Y.-A. Lu, *Proc. Natl. Acad. Sci. USA*, 1989, **86**, 9084.

17. (*a*) A. Dirksen, S. Langereis, B. F. M. de Waal, M. H. P. van Genderen, T. M. Hackeng and E. W. Meijer, *Chem. Commun.*, 2005, 2811; (*b*) S. Langereis, A. Dirksen, B. F. M. de Waal, M. H. P. van Genderen, Q. G. De Lussanet, T. M. Hackeng and E. W. Meijer, *Eur. J. Org. Chem.*, 2005, 2534; (*c*) I. van Baal, H. Malda, S. A. Synowsky, J. L. J. van Dongen, T. M. Hackeng, M. Merkx and E. W. Meijer, *Angew. Chem. Int. Ed.*, 2005, **44**, 5052.

18. H. F. Gaertner, K. Rose, R. Cotton, D. Timms, R. Camble and R. E. Offord, *Bioconjugate Chem.*, 1992, **3**, 262.

19. (*a*) C. W. Tornøe, C. Christensen and M. Meldal, *J. Org. Chem.*, 2002, **67**, 3057; (*b*) V. V. Rostovtsev, L. G. Green, V. V. Fokin and K. B. Sharpless, *Angew. Chem. Int. Ed.*, 2002, **41**, 2596.

20. H. C. Kolb, M. G. Finn and K. B. Sharpless, *Angew. Chem. Int. Ed.*, 2001, **40**, 2004.

21. For recent reviews on the applications of click reactions, see: (*a*) R. Breinbauer and M. Köhn, *ChemBioChem*, 2003, **4**, 1147; (*b*) V. D. Bock, H. Hiemstra and J. H. van Maarseveen, *Eur. J. Org. Chem.*, 2006, 51.

22. (*a*) D. T. S. Rijkers, G. W. van Esse, R. Merkx, A. J. Brouwer, H. J. F. Jacobs, R. J. Pieters and R. M. J. Liskamp, *Chem. Commun.*, 2005, 4581; (*b*) J. A. F. Joosten, N. T. H. Tholen, F. Ait El Maate, A. J. Brouwer, G. W. van Esse, D. T. S. Rijkers, R. M. J. Liskamp and R. J. Pieters, *Eur. J. Org. Chem.*, 2005, 3182; (*c*) R. M. J. Liskamp, D. T. S. Rijkers, R. J. Pieters, A. J. Brouwer and J. A. F. Joosten, International Patent Application: P73572PC00, 2005, Dendrimers multivalently substituted with active groups.

23. (*a*) S. J. E. Mulders, A. J. Brouwer, P. G. J. van der Meer and R. M. J. Liskamp, *Tetrahedron Lett.*, 1997, **38**, 631; (*b*) S. J. E. Mulders, A. J. Brouwer and R. M. J. Liskamp, *Tetrahedron Lett.*, 1997, **38**, 3085; (*c*) A. J. Brouwer, S. J. E. Mulders and R. M. J. Liskamp, *Eur. J. Org. Chem.*, 2001, 1903; (*d*) A. J. Brouwer and R. M. J. Liskamp, *Eur. J. Org. Chem.*, 2005, 487.

24. Tesser's base is a mixture of dioxane, methanol and aqueous NaOH, see: G. I. Tesser and I. C. Balvert-Geers, *Int. J. Peptide Protein Res.*, 1975, **7**, 295.

25. X. Dai, Z. Su and J. O. Liu, *Tetrahedron Lett.*, 2000, **41**, 6295.

26. R. Bollhagen, M. Schmiedberger, K. Barlos and E. Grell, *J. Chem. Soc., Chem. Commun.*, 1994, 2559.

27. (*a*) J. T. Lundquist, IV and J. C. Pelletier, *Org. Lett.*, 2001, **3**, 781; (*b*) D. T. S. Rijkers, H. R. R. van Vugt, H. J. F. Jacobs and R. M. J. Liskamp, *Tetrahedron Lett.*, 2002, **43**, 3657.

28. Z. Zhang and E. Fan, *Tetrahedron Lett.*, 2005, **47**, 665.

29. S. Liu, E. Cheung, M. C. Ziegler, M. Rajopadhye and D. S. Edwards, *Bioconjugate Chem.*, 2001, **12**, 559.

30. E. von Arx, M. Faupel and M. J. Brugger, *J. Chromatogr.*, 1976, **120**, 224.

31. C. G. Fields, D. H. Lloyd, R. L. Macdonald, K. M. Otteson and R. L. Noble, *Peptide Res.*, 1991, **4**, 95.

Chapter 5

Effect of linker variation on the in vitro and in vivo characteristics of an ^{111}In-labeled RGD peptide

Ingrid Dijkgraaf
Shuang Liu
John A. W. Kruijtzer
Annemieke C. Soede
Wim J. G. Oyen
Rob M. J. Liskamp
Frans H. M. Corstens
Otto C. Boerman

Nucl Med Biol 2007:34;29-35

Abstract

Due to selective expression of $\alpha_v\beta_3$ integrin in tumors, radiolabeled RGD peptides are attractive candidates for tumor targeting. Minor modifications of these peptides could have major impact on the in vivo characteristics. In this study, the effect of linker modification between two cyclic RGD sequences and DOTA on the in vitro and in vivo characteristics of the tracer was systematically investigated.

Methods: A dimeric RGD peptide was synthesized and conjugated either directly with DOTA or via different linkers: PEG_4, glutamic acid, and lysine. The RGD peptides were radiolabeled with ^{111}In and their in vitro and in vivo $\alpha_v\beta_3$ binding characteristics were determined.

Results: LogP values varied between -2.82 ± 0.06 and −3.95 ± 0.33. IC_{50} values for DOTA-E-$[c(RGDfK)]_2$, DOTA-PEG_4-E-$[c(RGDfK)]_2$, DOTA-E-E-$[c(RGDfK)]_2$, and DOTA-K-E-$[c(RGDfK)]_2$ were comparable. 2 h p.i. Tumor uptake of the ^{111}In-labeled compounds was not significantly different. Kidney accumulation of ^{111}In-DOTA-K-E-$[c(RGDfK)]_2$ (4.05 ± 0.20 %ID/g) was significantly higher compared to ^{111}In-DOTA-E-$[c(RGDfK)]_2$ (2.63 ± 0.19 %ID/g, $P<0.05$) and ^{111}In-DOTA-E-E-$[c(RGDfK)]_2$ (2.16 ± 0.21 %ID/g, $P<0.01$). Liver uptake of ^{111}In-DOTA-E-E-$[c(RGDfK)]_2$ (2.12 ± 0.09 %ID/g) was significantly higher compared to ^{111}In-DOTA-E-$[c(RGDfK)]_2$ (1.64 ± 0.1 %ID/g, $P<0.05$) and ^{111}In-DOTA-K-E-$[c(RGDfK)]_2$ (1.52 ± 0.04 %ID/g, $P<0.01$).

Conclusions: Linker variation did not affect the affinity for $\alpha_v\beta_3$ and the tumor uptake. Insertion of K caused enhanced kidney retention, while insertion of E resulted in enhanced retention in the kidneys. PEG_4 appeared to be the most suitable linker compared to E and K, because of the highest tumor-to-blood ratio and the lowest uptake in kidney and liver.

Introduction

Integrins are a group of adhesion molecules consisting of two non-covalently bound subunits, α and β. They are involved in signal transduction as well as in cell/cell- and cell/matrix-interactions [1]. A prominent member of this receptor class is the $\alpha_v\beta_3$ integrin. The $\alpha_v\beta_3$ integrin is preferentially expressed on proliferating endothelial cells [2], whereas it is absent on quiescent endothelial cells. For growth beyond the size of 1-2 mm in diameter, tumors require the formation of new blood vessels. Consequently, $\alpha_v\beta_3$ expression on tumor vasculature is considered to be a marker of tumor-induced angiogenesis [3-5]. In addition, $\alpha_v\beta_3$ is expressed on the cell membrane of various tumor cell types. Due to this restricted expression of $\alpha_v\beta_3$ in tumors, $\alpha_v\beta_3$ is considered a suitable target for tumor targeting [6]. This $\alpha_v\beta_3$ integrin interacts with the arginine-glycine-aspartic acid (RGD) amino acid sequence present in extracellular matrix proteins such as vitronectin, fibrinogen, and laminin [7]. Based on the RGD tripeptide sequence a series of small cyclic peptides have been designed that have a high and specific affinity for the $\alpha_v\beta_3$ integrin [8]. Several radiolabeled RGD peptides as radiopharmaceuticals for SPECT and PET imaging applications have been developed to visualize and quantify $\alpha_v\beta_3$ expression non-invasively [9, 10].

It is important for a peptide-based radiopharmaceutical to clear rapidly from the blood and non-target organs, preferably via the kidneys. One method to modify the route and rate of excretion of these peptides is glycosylation. For example, the radioiodinated RGD peptide [^{125}I]-3-iodo-D-Tyr^4-cyclo(-Arg-Gly-Asp-D-Tyr-Val-) cleared mainly via the hepatobiliary route, which limited its further application [11]. Glycosylation of this compound resulted in a more hydrophilic compound that cleared mainly via the renal route [12]. The hydrophilicity of peptides can also be enhanced by linking them to polyethylene glycol (PEG) chains, an approach called PEGylation. Furthermore, peptides can be modified by introduction of specific hydrophilic or lipophilic amino acids into the peptide chain [13]. In addition, by altering the overall charge of a peptide by inserting basic or acidic amino acids, the route of excretion and/or kidney retention can be modified. Modification of a peptide by PEGylation, glycosylation or addition or substitution of amino acids could affect the affinity of a peptide for the receptor.

To improve the efficacy of tumor targeting and to obtain better in vivo imaging properties, several research groups have applied multivalent RGD peptides to enhance the targeting between the ligand and the $\alpha_v\beta_3$ expressing tumor. In a previous study, we demonstrated enhanced tumor retention of a dimeric RGD peptide compared to its monomeric counterpart [14].

The aim of the present study is to systematically study the effect of modification of the linker between the two cyclic RGD sequences and the DOTA chelator on the in vitro and in vivo characteristics. To investigate the effect of a hydrophilic linker, PEG_4 was used as a linker. Furthermore, to investigate the effect of charge the amino acids glutamic acid and lysine were inserted as a linker, because of their different charge under physiological conditions. Here, we synthesized a dimeric RGD peptide and conjugated this peptide either directly to 1,4,7,10-tetraazacyclododecane-N,N',N'',N'''-tetraacetic acid (DOTA) or via a hydrophilic, acidic, or basic linker: PEG_4, glutamic acid, or lysine, respectively. Subsequently, the RGD peptides were radiolabeled with ^{111}In and the in vivo tumor targeting characteristics of the peptides to $\alpha_v\beta_3$ expressing tumors were determined.

Materials and methods

Synthesis of DOTA-conjugated RGD peptides

The synthesis of the dimeric cyclic RGD peptide E-[c(RGDfK)]$_2$ conjugated with DOTA was described previously [15]. For the coupling of each of the linkers to E-[c(RGDfK)]$_2$, (0.51 mmol) of Boc-PEG_4-OH, Boc-Glu(OtBu)-OH, or H-Lys(Boc)-OH and 57.4 mg (0.50 mmol) N-hydroxysuccinimide were placed in a rondbottom flask. Then, 109 mg (0.53 mmol) 1,3-Dicyclohexylcarbodiimide (DCC) was dissolved in 5 mL dichloromethane (DCM) and added to each of the Boc-protected linker and N-hydroxysuccinimide (HOSu). After stirring for 2 h at room temperature, the reaction mixtures were concentrated in vacuo and the residues were titurated in EtOAc. These were filtrated and the filtrates were concentrated in vacuo. The residues were redissolved in 5 mL DCM. The unprotected dimeric RGD peptide, E-[c(RGDfK)]$_2$, and 131 µL N,N-diisopropylethylamine (DiPEA) (0.75 mmol)

were dissolved in 5 mL dimethylformamide (DMF). Subsequently, this mixture was added to each of the Boc-protected succinimydyl ester dissolved in 5 mL DCM.

DOTA-conjugation

The protected compounds were deprotected by dissolving the compound in DCM/trifluoroacetic acid (TFA; 1:1). After stirring for 2.5 h at room temperature, the reaction mixtures were concentrated in vacuo and coevaporated with $CHCl_3$. 84.8 mg (0.22 mmol) 2-(1H-benzotriazol-1-yl) -1,1,3,3-tetramethyluroniumhexafluorophosphate (HBTU) and 70 µL (0.40 mmol) DiPEA were dissolved in 10 mL dry DMF. 1 mL of this solution was added to 14 mg (24 µmol) DOTA-tris(tertBu) (Macrocyclics, Dallas, TX, USA) and stirred for 5 minutes at room temperature. PEG_4-E-[c(RGDfK)]$_2$, E-E-[c(RGDfK)]$_2$ or K-E-[c(RGDfK)]$_2$ was added and the mixtures were stirred for 4.5 h under nitrogen at room temperature. Then, the reaction mixture was concentrated in vacuo and the residue was dissolved in 4.75 mL TFA and 250 µL H_2O for deprotection of the Boc-group. These reaction mixture were stirred under nitrogen for 5 h. Subsequently, the reaction mixtures were concentrated in vacuo and the residues were dissolved in MeCN/H_2O (1/1) and lyophilized to afford a fluffy solid. The crude DOTA-conjugated PEG_4-E-[c(RGDfK)]$_2$, E-E-[c(RGDfK)]$_2$, and K-E-[c(RGDfK)]$_2$ were purified by preparative RP-HPLC and analyzed by analytical HPLC and mass spectrometry. The structures of the DOTA-conjugated RGD peptide analogs are shown in Figure 1.

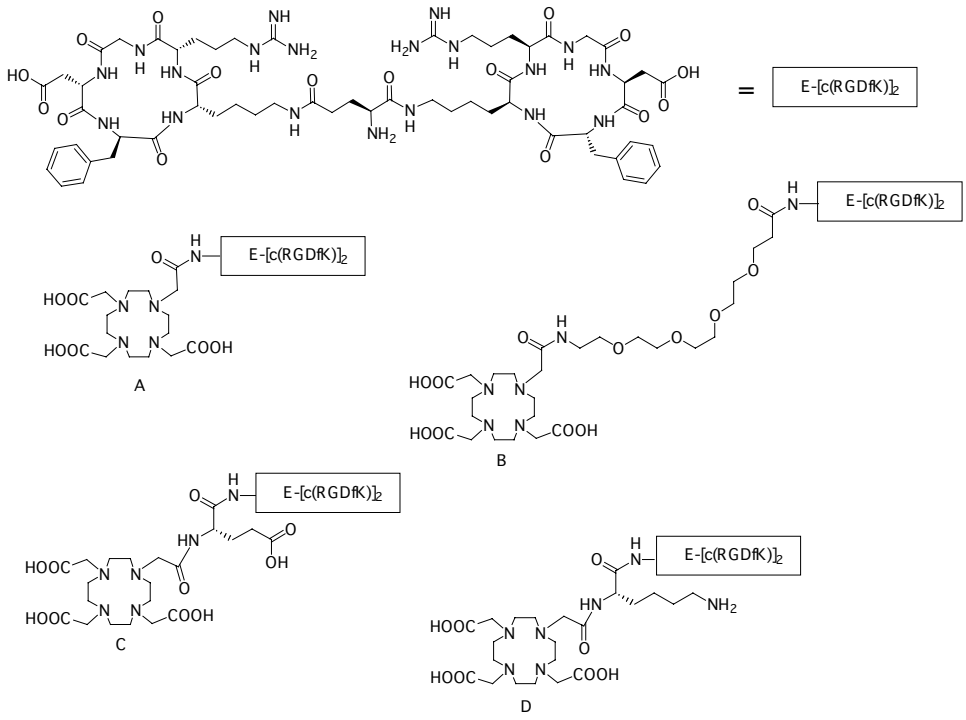

Figure 1. Structural formula of the DOTA-conjugated dimeric RGD peptide, DOTA-E-[c(RGDfK)]$_2$ (**A**), and its analogs containing different linkers: DOTA-PEG_4-E-[c(RGDfK)]$_2$ (**B**), DOTA-E-E-[c(RGDfK)]$_2$ (**C**), and DOTA-K-E-[c(RGDfK)]$_2$ (**D**).

Radiolabeling of the RGD peptides

DOTA-E-$[c(RGDfK)]_2$ was radiolabeled with $InCl_3$ by adding 20.2 MBq $InCl_3$ (Mallinckrodt, Petten, The Netherlands) to 28 µg (16.4 nmol) DOTA-E-$[c(RGDfK)]_2$ dissolved in 500 µL 0.5 M ammonium acetate buffer pH 6.0, containing 0.6 mg/mL gentisic acid. The compounds containing the linkers were radiolabeled analogously with minor modifications. These compounds were prepared by adding 7.4 to 11.1 MBq $InCl_3$ to 5.1 to 8.2 nmol of DOTA-PEG_4-E-$[c(RGDfK)]_2$, DOTA-E-E-$[c(RGDfK)]_2$, or DOTA-K-E-$[c(RGDfK)]_2$ dissolved in 200 to 300 µL ammonium acetate buffer, pH 6.0, containing 0.6 mg/mL gentisic acid.

The reaction mixtures were degassed and subsequently the mixtures were heated at 100 ºC for 15 minutes. ^{111}In-DOTA-PEG_4-E-$[c(RGDfK)]_2$, and ^{111}In-DOTA-K-E-$[c(RGDfK)]_2$ were further purified on a C-18 SepPak cartridge (Waters, Milford, MA). After applying the sample on the methanol-activated cartridge, the cartridge was washed with 5 mL 25 mM ammonium acetate and eluted with 5 mL 25% acetonitrile in 25 mM ammonium acetate. The radiochemical purity was determined by reversed-phase high-performance liquid chromatography (RP-HPLC) (HP 1100 series, Hewlett Packard, Palo Alto, CA, USA) using a C18 column (RX-C18, 4.6 mm × 250 mm, Zorbax) eluted with a gradient mobile phase (8-20% B over 25 min or 8-100% B over 30 min, solvent A = 25 mM ammonium acetate buffer, solvent B = acetonitrile) at 1 mL/min. The radioactivity of the eluate was monitored using an in-line radiodetector (Flo-One Beta series, Radiomatic, Meriden, CT, USA).

Octanol-water partition coefficient

To determine the lipophilicity of ^{111}In-DOTA-E-$[c(RGDfK)]_2$, ^{111}In-DOTA-PEG_4-E-$[c(RGDfK)]_2$, ^{111}In-DOTA-E-E-$[c(RGDfK)]_2$, and ^{111}In-DOTA-K-E-$[c(RGDfK)]_2$, approximately 300,000 cpm of each of the preparations were diluted with phosphate-buffered saline (PBS) to a total volume of three mL. An equal volume of octanol was added and the resulting biphasic system was mixed vigorously for one minute and gently for another ten minutes. The two phases were separated by centrifugation (5 min, 1000 rpm) and the counts in 250 µL aliquots (n=3) of the organic and the inorganic layer were determined by use of a γ-counter (1480 Wizard, Wallac, Turku, Finland). The logP values of the compounds were determined in at least two independent experiments.

Solid-phase $\alpha_v\beta_3$ binding assay

The affinity of DOTA-E-$[c(RGDfK)]_2$, DOTA-PEG_4-E-$[c(RGDfK)]_2$, DOTA-E-E-$[c(RGDfK)]_2$, and DOTA-K-E-$[c(RGDfK)]_2$ for $\alpha_v\beta_3$ was determined using a solid-phase competitive binding assay. ^{111}In-labeled DOTA-E-$[c(RGDfK)]_2$ (3 MBq/µg) was prepared as described above and was used as the tracer in this assay. Microtiter 96-well vinyl assay plates (Corning B.V., Schiphol-Rijk, The Netherlands) were coated with 100 µL/well of a solution of purified human integrin $\alpha_v\beta_3$ (150 ng/mL) in Triton X-100 Formulation (Chemicon International, Temecula, CA, USA) in coating buffer (25 mM Tris-HCl, pH 7.4, 150 mM NaCl, 1 mM $CaCl_2$, 0.5 mM $MgCl_2$ and 1 mM $MnCl_2$) for 17 h at 4 ºC. The plates were washed twice with binding buffer (0.1% bovine serum albumin (BSA) in coating buffer). The wells were blocked for 2 h with 200 µL blocking buffer (1% BSA in coating

buffer) at room temperature. The plates were washed twice with binding buffer. Then 100 µL binding buffer containing 11.1 kBq of ^{111}In-DOTA-E-[c(RGDfK)]$_2$ and appropiate dilutions of non-labeled DOTA-E-[c(RGDfK)]$_2$, DOTA-PEG$_4$-E-[c(RGDfK)]$_2$, DOTA-E-E-[c(RGDfK)]$_2$, and DOTA-K-E-[c(RGDfK)]$_2$ in binding buffer were incubated in the wells at 37 °C for 1 h. After incubation, the plates were washed three times with binding buffer. The retained radioactivity in each well was determined in a γ-counter. IC_{50} values of the RGD peptides were calculated by non-linear regression using GraphPad Prism (GraphPad Prism 4.0 Software, San Diego, CA, USA). Each data point is the average of three determinations. K_i values were calculated from IC_{50} values using the Cheng-Prusoff equation as described by Cheng [16, 17]. The Hill slope (K) of DOTA-E-[c(RGDfK)]$_2$ concentration-response curve was 0.6.

Biodistribution studies

In the right flank of 6-8 weeks old female nude BALB/c mice, 0.2 mL of a cell suspension of 10 × 10^6 cells/mL SK-RC-52 cells was injected subcutaneously (s.c.). Two weeks after inoculation of the tumor cells mice were randomly divided into four groups (3 mice/group).

Mice received 0.5 µg/mouse of ^{111}In-DOTA-E-[c(RGDfK)]$_2$ (0.38 MBq), ^{111}In-DOTA-PEG$_4$-E-[c(RGDfK)]$_2$ (0.48 MBq), ^{111}In-DOTA-E-E-[c(RGDfK)]$_2$ (0.36 MBq), or ^{111}In-DOTA-K-E-[c(RGDfK)]$_2$ (0.29 MBq) via a tail vein. Mice were killed by CO_2 asphyxiation 2 h postinjection (p.i.). Blood, tumor, and the major organs and tissues were collected, weighed, and counted in a γ-counter. The percentage injected dose per gram (%ID/g) was determined for each sample. All animal experiments were approved by the local animal welfare committee in accordance with the Dutch legislation and carried out in accordance with their guidelines.

Statistical analysis

All mean values are given ± standard deviation (S.D.). Statistical analysis was performed using the One-way Analysis of Variance. Bonferroni corrections for multiple comparisons were applied. The level of significance was set at $P<0.05$.

Results

Radiolabeling

The RP-HPLC elution profile of ^{111}In-DOTA-E-[c(RGDfK)]$_2$, ^{111}In-DOTA-PEG$_4$-E-[c(RGDfK)]$_2$, ^{111}In-DOTA-E-E-[c(RGDfK)]$_2$, and ^{111}In-DOTA-K-E-[c(RGDfK)]$_2$ showed a single peak for each of the four compounds with an elution time of 26 min, 29 min, and 22 min for ^{111}In-DOTA-E-[c(RGDfK)]$_2$, ^{111}In-DOTA-PEG$_4$-E-[c(RGDfK)]$_2$, and ^{111}In-DOTA-E-E-[c(RGDfK)]$_2$, respectively. The retention time of ^{111}In-DOTA-K-E-[c(RGDfK)]$_2$ was 14 min. Note that different gradients were used for elutions.

Octanol-water partition coefficient

All the compounds were relatively hydrophilic, as indicated from octanol-water partition coefficient measurements. The dimeric RGD peptide with no additional linker was the most hydrophilic compound. The PEGylated dimeric RGD peptide was the most hydrophobic compound. LogP values for ^{111}In-DOTA-E-[c(RGDfK)]$_2$, ^{111}In-DOTA-PEG$_4$-E-[c(RGDfK)]$_2$, ^{111}In-DOTA-E-E-[c(RGDfK)]$_2$, and ^{111}In-DOTA-K-E-[c(RGDfK)]$_2$ are given in Table 1.

Table 1. The LogP values of ^{111}In-DOTA-E-[c(RGDfK)]$_2$, ^{111}In-DOTA-PEG$_4$-E-[c(RGDfK)]$_2$, ^{111}In-DOTA-E-E-[c(RGDfK)]$_2$, and ^{111}In-DOTA-K-E-[c(RGDfK)]$_2$.

Compound	LogP value
DOTA-E-[c(RGDfK)]$_2$	-3.95 ± 0.33
DOTA-PEG$_4$-E-[c(RGDfK)]$_2$	-2.82 ± 0.06
DOTA-E-E-[c(RGDfK)]$_2$	-3.55 ± 0.03
DOTA-K-E-[c(RGDfK)]$_2$	-3.06 ± 0.13

Solid-phase $\alpha_v\beta_3$ binding assay

The affinity of DOTA-E-[c(RGDfK)]$_2$, DOTA-PEG$_4$-E-[c(RGDfK)]$_2$, DOTA-E-E-[c(RGDfK)]$_2$, and DOTA-K-E-[c(RGDfK)]$_2$ for the $\alpha_v\beta_3$ integrin was determined in a competitive binding assay. The results of these assays are summarized in Figure 2.

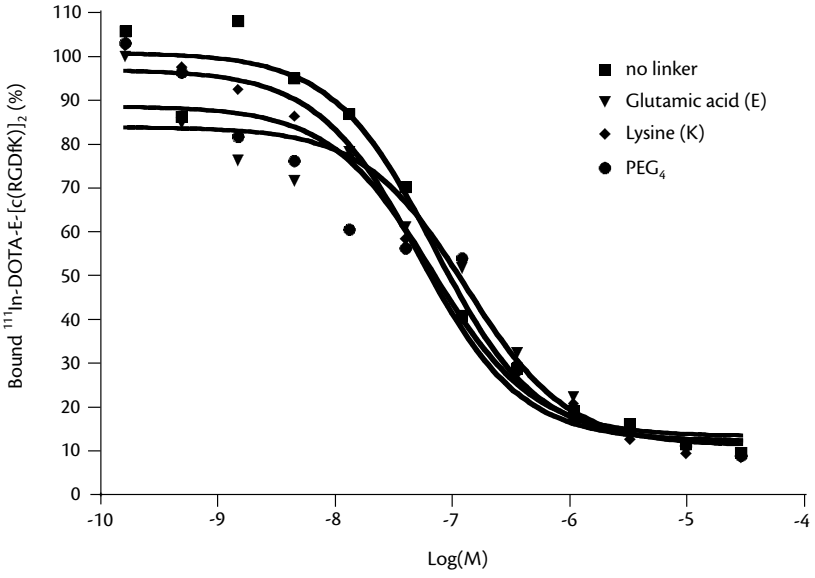

Figure 2. Competition of specific binding of ^{111}In-DOTA-E-[c(RGDfK)]$_2$ with DOTA-E-[c(RGDfK)]$_2$ (■), DOTA-PEG$_4$-E-[c(RGDfK)]$_2$ (●), DOTA-E-E-[c(RGDfK)]$_2$ (▼), and DOTA-K-E-[c(RGDfK)]$_2$ (◆).

Binding of ^{111}In-labeled dimeric peptide, ^{111}In-DOTA-E-[c(RGDfK)]$_2$, to $\alpha_v\beta_3$ was competed by DOTA-E-[c(RGDfK)]$_2$, DOTA-PEG$_4$-E-[c(RGDfK)]$_2$, DOTA-E-E-[c(RGDfK)]$_2$, and DOTA-K-E-[c(RGDfK)]$_2$ in a concentration dependent manner. The IC_{50} values were 69.9 nM for DOTA-E-[c(RGDfK)]$_2$, 66.8 nM for DOTA-PEG$_4$-E-[c(RGDfK)]$_2$, 129.5 nM for DOTA-E-E-[c(RGDfK)]$_2$, and 51.9 nM for DOTA-K-E-[c(RGDfK)]$_2$. Calculated K_i values using Cheng-Prusoff equation were 1.63 nM for DOTA-E-[c(RGDfK)]$_2$, 1.56 nM for DOTA-PEG$_4$-E-[c(RGDfK)]$_2$, 3.01 nM for DOTA-E-E-[c(RGDfK)]$_2$, and 1.21 nM for DOTA-K-E-[c(RGDfK)]$_2$.

Biodistribution studies

The results of the biodistribution studies of ^{111}In-DOTA-E-[c(RGDfK)]$_2$, ^{111}In-DOTA-PEG$_4$-E-[c(RGDfK)]$_2$, ^{111}In-DOTA-E-E-[c(RGDfK)]$_2$, and ^{111}In-DOTA-K-E-[c(RGDfK)]$_2$ in athymic mice with s.c. SK-RC-52 tumors at 2 h p.i. are summarized in Table 2. All compounds cleared rapidly from the blood and had similar uptake in the tumor at 2 h p.i. (4.65 ± 0.33 %ID/g, 5.15 ± 1.05 %ID/g, 4.36 ± 0.95 %ID/g, and 4.04 ± 0.05 %ID/g, respectively). Coinjection of an excess of non-radiolabeled DOTA-E-[c(RGDfK)]$_2$ with ^{111}In-DOTA-E-[c(RGDfK)]$_2$, ^{111}In-DOTA-PEG$_4$-E-[c(RGDfK)]$_2$, ^{111}In-DOTA-E-E-[c(RGDfK)]$_2$, or ^{111}In-DOTA-K-E-[c(RGDfK)]$_2$ resulted in a significant decrease of radioactivity in tumor for all four compounds, indicating that uptake in the tumor is $\alpha_v\beta_3$-mediated. In addition, uptake of all compounds in normal organs such as spleen, liver, intestine, and colon was significantly reduced in the presence of an excess non-radioactive DOTA-E-[c(RGDfK)]$_2$, indicating that uptake in these organs is at least partly $\alpha_v\beta_3$-mediated.

Table 2. Biodistribution data of ^{111}In-DOTA-E-[c(RGDfK)]$_2$, ^{111}In-DOTA-PEG$_4$-E-[c(RGDfK)]$_2$, ^{111}In-DOTA-E-E-[c(RGDfK)]$_2$, and ^{111}In-DOTA-K-E-[c(RGDfK)]$_2$ in the presence and absence of an excess of unlabeled DOTA-E-[c(RGDfK)]$_2$ (+ xs) in athymic mice with s.c. SK-RC-52 tumors 2 h after injection. The organ uptake is expressed as %ID/g.

	No linker	+ xs	PEG$_4$	+ xs	E	+ xs	K	+ xs
Blood	0.07 ± 0.01	0.02	0.10 ± 0.03	0.05	0.13 ± 0.30	0.07	0.13 ± 0.02	0.14
Muscle	0.48 ± 0.37	0.04	1.32 ± 1.40	0.61	0.29 ± 0.04	0.07	0.31 ± 0.04	1.78
Tumor	4.65 ± 0.33	0.58	5.15 ± 1.05	0.76	4.36 ± 0.95	0.53	4.04 ± 0.05	0.75
Lung	0.70 ± 0.04	0.17	1.43 ± 0.37	0.37	0.88 ± 0.05	0.19	0.92 ± 0.11	0.35
Spleen	1.56 ± 0.19	0.31	2.07 ± 0.50	0.62	1.78 ± 0.19	0.26	1.67 ± 0.16	0.47
Kidney	2.63 ± 0.19	1.86	3.23 ± 0.70	2.09	2.16 ± 0.21	1.86	4.05 ± 0.20	3.93
Liver	1.64 ± 0.10	0.30	1.75 ± 0.27	0.63	2.12 ± 0.09	0.29	1.52 ± 0.04	0.45
Intestine	4.87 ± 0.61	0.68	5.59 ± 0.49	0.78	3.99 ± 0.48	0.47	4.77 ± 0.14	0.78
Colon	1.89 ± 0.21	0.32	2.96 ± 0.52	0.29	3.10 ± 1.41	0.24	2.06 ± 0.29	0.55

At 2 h p.i. the blood activity of ^{111}In-DOTA-E-E-[c(RGDfK)]$_2$ and ^{111}In-DOTA-K-E-[c(RGDfK)]$_2$ was slightly higher compared to ^{111}In-DOTA-E-[c(RGDfK)]$_2$, resulting in a significantly higher tumor-to-blood ratio for ^{111}In-DOTA-E-[c(RGDfK)]$_2$ (71.9 ± 6.80) compared to ^{111}In-DOTA-E-E-[c(RGDfK)]$_2$

(34.3 ± 8.88, P<0.001) and ^{111}In-DOTA-K-E-[c(RGDfK)]$_2$ (31.2 ± 4.29, P<0.001). In addition, the tumor-to-blood ratio of ^{111}In-DOTA-PEG$_4$-E-[c(RGDfK)]$_2$ (54.5 ± 6.53) was significantly higher compared to ^{111}In-DOTA-E-E-[c(RGDfK)]$_2$ (P<0.05) and ^{111}In-DOTA-K-E-[c(RGDfK)]$_2$ (P<0.05).

The kidney uptake of ^{111}In-DOTA-K-E-[c(RGDfK)]$_2$ (4.05 ± 0.20 %ID/g) was significantly higher as compared to ^{111}In-DOTA-E-[c(RGDfK)]$_2$ (2.63 ± 0.19 %ID/g, P<0.05) and ^{111}In-DOTA-E-E-[c(RGDfK)]$_2$ (2.16 ± 0.21 %ID/g, P<0.01). The liver uptake of ^{111}In-DOTA-E-E-[c(RGDfK)]$_2$ (2.12 ± 0.09 %ID/g) was significantly higher as compared to ^{111}In-DOTA-E-[c(RGDfK)]$_2$ (1.64 ± 0.1 %ID/g, P<0.05) and ^{111}In-DOTA-K-E-[c(RGDfK)]$_2$ (1.52 ± 0.04 %ID/g, P<0.01).

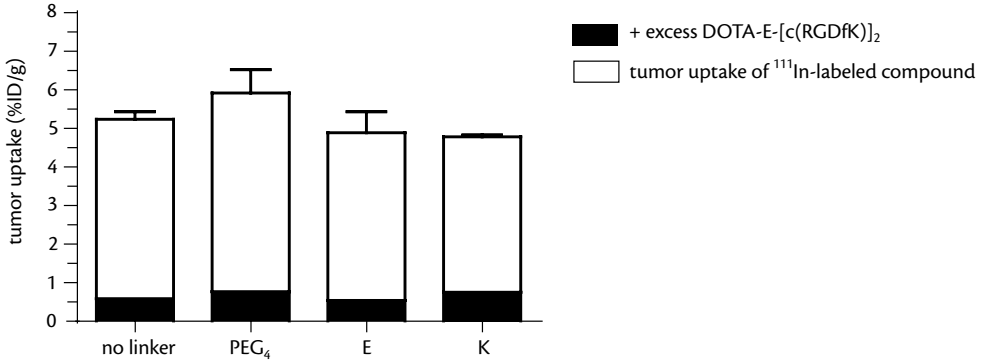

Figure 3A. Tumor uptake of ^{111}In-DOTA-E-[c(RGDfK)]$_2$, ^{111}In-DOTA-PEG$_4$-E-[c(RGDfK)]$_2$, ^{111}In-DOTA-E-E-[c(RGDfK)]$_2$, and ^{111}In-DOTA-K-E-[c(RGDfK)]$_2$ at 2 h p.i. in the presence (black bars) and absence (white bars) of an excess of non-radiolabeled DOTA-E-[c(RGDfK)]$_2$.

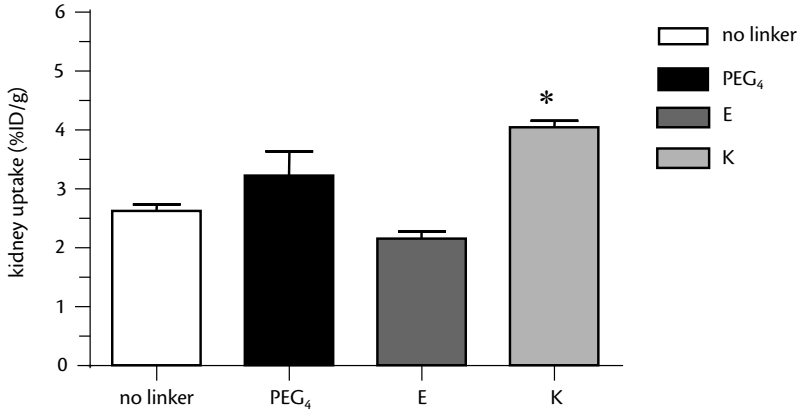

Figure 3B. Kidney uptake of ^{111}In-DOTA-E-[c(RGDfK)]$_2$, ^{111}In-DOTA-PEG$_4$-E-[c(RGDfK)]$_2$, ^{111}In-DOTA-E-E-[c(RGDfK)]$_2$, and ^{111}In-DOTA-K-E-[c(RGDfK)]$_2$ at 2 h p.i.. Results are reflected as mean %ID/g ± SD. Values were analyzed using One-way Analysis of Variance, * = P<0.05. P-value refers to difference in kidney uptake between ^{111}In-DOTA-E-[c(RGDfK)]$_2$ and ^{111}In-DOTA-K-E-[c(RGDfK)]$_2$.

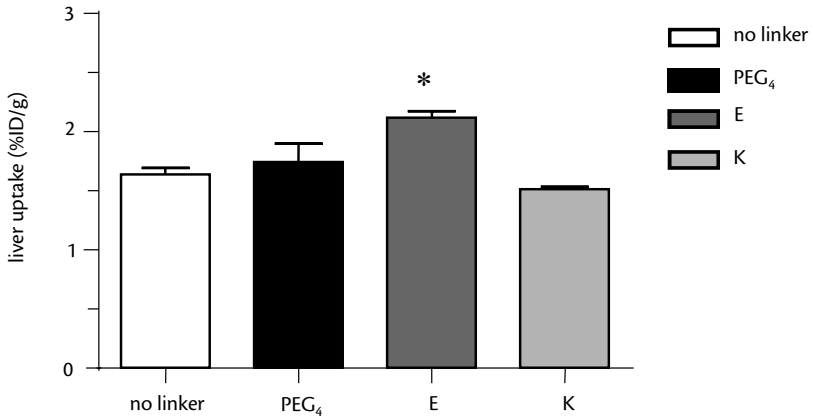

Figure 3C. Liver uptake of ^{111}In-DOTA-E-[c(RGDfK)]$_2$, ^{111}In-DOTA-PEG$_4$-E-[c(RGDfK)]$_2$, ^{111}In-DOTA-E-E-[c(RGDfK)]$_2$, and ^{111}In-DOTA-K-E-[c(RGDfK)]$_2$ at 2 h p.i.. Results are reflected as mean %ID/g ± SD. Values were analyzed using One-way Analysis of Variance, * = P<0.05. P-value refers to difference in liver uptake between ^{111}In-DOTA-E-[c(RGDfK)]$_2$ and ^{111}In-DOTA-E-E-[c(RGDfK)]$_2$.

Discussion

In this study the effect of the modification of the linker between a dimeric RGD peptide and the chelator DOTA on the in vitro and in vivo characteristics was investigated.

A prominent difference in renal handling between the RGD peptide containing the glutamic acid residue and the RGD peptide containing the lysine residue was observed in this study. The incorporation of a positively charged lysine residue between the DOTA-moiety and the dimeric RGD peptide E-[c(RGDfK)]$_2$, resulted in increased kidney uptake. This is in line with the reports that in general, positively charged peptides are more efficiently reabsorbed in the proximal renal tubular cells [18]. This would suggest that the uptake in the kidneys could be reduced by introducing negatively charged amino acids in the RGD peptide. However, in this study the RGD peptide containing the glutamic acid linker showed similar renal accumulation compared to the native dimeric RGD peptide E-[c(RGDfK)]$_2$. Recently, Béhé and coworkers demonstrated that removal of glutamic acid residues 2-5 could reduce the high renal uptake of ^{111}In-DTPA-D-Glu^1-minigastrin [19]. Apparently, the tubular reabsorption of a peptide is very subtle. However, it has been shown by Akiziwa and coworkers that the substitution of only one amino acid in ^{111}In-DTPA-octreotide derivatives significantly affected the renal accumulation of the peptides [20]. ^{111}In-DOTA-E-E-[c(RGDfK)]$_2$ had a significantly higher liver uptake compared to ^{111}In-DOTA-E-[c(RGDfK)]$_2$ and ^{111}In-DOTA-K-E-[c(RGDfK)]$_2$. However, ^{111}In-DOTA-E-E-[c(RGDfK)]$_2$ was more hydrophilic, as indicated from its octanol-water partition coefficient (logP = -3.55 ± 0.03). In this study, the accumulation in the kidneys of each of the RGD peptides is low compared to that of other ^{111}In-labeled peptides. For example, in mice the uptake of ^{111}In-DTPA-octreotide in the

kidney at 2 h p.i. exceeds 25 %ID/g [21]. Apparently, the RGD peptides used in our study are not efficiently reabsorbed in the renal tubular cells.

The peptides containing glutamic acid or lysine as a linker demonstrated a significantly higher blood activity and concomitant lower tumor-to-blood ratios compared to the native peptide. Introduction of the PEG_4 linker did not significantly affect the tumor-to-blood ratio compared to the native dimeric RGD peptide. Recently, Chen et al. showed similar blood clearance for a ^{64}Cu-labeled dimeric RGD peptide, ^{64}Cu-DOTA-E-$[c(RGDyK)]_2$ compared to its PEGylated counterpart, ^{64}Cu-DOTA-PEG-E-$[c(RGDyK)]_2$ [22]. However, for the monomeric RGD peptide, the PEGylated analog ^{64}Cu-DOTA-PEG-RGD showed a more rapid blood clearance than ^{64}Cu-DOTA-RGD [23]. Probably, the effect of PEGylation is more pronounced in a smaller molecule.

The binding affinity of DOTA-PEG_4-E-$[c(RGDfK)]_2$, DOTA-E-E-$[c(RGDfK)]_2$, and DOTA-K-E-$[c(RGDfK)]_2$ was similar to that of the lead compound DOTA-E-$[c(RGDfK)]_2$, indicating that introduction of a PEG_4 moiety, glutamic acid residue, or lysine residue did not affect the affinity for the $\alpha_v\beta_3$ integrin. The K_i values of all four compounds are in the single digit nanomolar range, indicating that these compounds have a relatively high affinity for the $\alpha_v\beta_3$ integrin.

In conclusion, this study demonstrates that optimization of a dimer RGD peptide for $\alpha_v\beta_3$ targeting by systematic linker variation can alter the in vivo kinetics of the tracers, without influencing the $\alpha_v\beta_3$ targeting potential. Results suggest that ^{111}In-DOTA-PEG_4-E-$[c(RGDfK)]_2$ and ^{111}In-DOTA-E-E-$[c(RGDfK)]_2$ are the most suitable ligands for $\alpha_v\beta_3$ targeting because of the highest tumor-to-blood ratio and the lowest uptake in kidney and liver.

References

1. Hynes RO. Integrins: versatility, modulation, and signaling in cell adhesion. Cell 1992;69:11-25.
2. Brooks PC. Role of integrins in angiogenesis. Eur J Cancer 1996;32A:2423-9.
3. Fiedler W, Graeven U, Ergun S, Verago S, Kilic N, Stockschlader M, et al. Vascular endothelial growth factor, a possible paracrine growth factor in human acute myeloid leukemia. Blood 1997;89:1870-5.
4. Foss HD, Araujo I, Demel G, Klotzbach H, Hummel M, Stein H. Expression of vascular endothelial growth factor in lymphomas and Castelman's disease. J Pathol 1997;183:44-50.
5. Perez-Atayde AR, Sallan SE, Tedrow U, Connors S, Allred E, Folkman J. Spectrum of tumor angiogenesis in the bone marrow of children with acute lymphoblastic leukemia. Am J Pathol 1997;150:815-21.
6. Folkman J. Angiogenesis in cancer, vascular, rheumatoid and other disease. Nat Med 1995;1:27-31.
7. Plow EF, Haas TA, Zhang L, Loftus J, Smith JW. Ligands binding to integrins. J Biol Chem 2000;275:21785-8.
8. Haubner R, Finsinger D, Kessler H. Stereoisomeric Peptide Libraries and Peptidomimetics for Designing Selective Inhibitors of the $\alpha_v\beta_3$ Integrin for a New Cancer Therapy. Angew Chem Int Ed Engl 1997;36:1374-89.
9. Haubner R, Wester HJ. Radiolabeled tracers for imaging of tumor angiogenesis and evaluation of anti-angiogenic therapies. Curr Pharm Des 2004;10:1439-55.

10. Chen X. Multimodality imaging of tumor integrin expression. Mini Rev Med Chem 2006;6:227-34.

11. Haubner R, Wester HJ, Reuning U, Senekowitsch-Schmidtke R, Diefenbach B, Kessler H, et al. Radiolabeled $\alpha_v\beta_3$ Integrin Antagonists: A New Class of Tracers for Tumor Targeting. J Nucl Med 1999;40:1061-71.

12. Haubner R, Wester HJ, Burkhart F, Senekowitsch-Schmidtke R, Weber W, Goodman SL, et al. Glycosylated RGD-containing peptides: tracer for tumor targeting and angiogenesis imaging with improved biokinetics. J Nucl Med 2001;42:326-36.

13. Okarvi SM. Peptide-Based Radiopharmaceuticals: Future Tools for Diagnostic Imaging of Cancer and Other Diseases. Medicinal Research Reviews 2004;24:357-97.

14. Janssen M, Oyen WJG, Massuger LFAG, Frielink C, Dijkgraaf I, Edwards DS, et al. Comparison of a monomeric and dimeric RGD-peptide for tumor targeting. Cancer Biother Radiopharm 2002;17:641-6.

15. Liu S, Cheung E, Ziegler M, Rajopadhye M, Edwards DS. ^{90}Y and ^{177}Lu labeling of a DOTA-conjugated vitronectin receptor antagonist useful for tumor therapy. Bioconjugate Chem 2001;12:559-68.

16. Cheng HC. The power issue: determination of K_B or K_I from IC_{50}. A closer look at the Cheng-Prusoff equation, the Schild plot and related power equations. J Pharmacol Toxicol Methods 2002;46:61-71.

17. Cheng HC. The influence of cooperativity on the determination of dissociation constants: examination of the Cheng-Prusoff equation, the Scatchard analysis, the Schild analysis and related power equations. Pharmacol Res 2004;50:21-40.

18. Behr TM, Goldenberg DM, Becker W. Reducing the renal uptake of radiolabeled antibody fragments and peptides for diagnosis and therapy: present status, future prospects and limitations. Eur J Nucl Med 1998;25:201-12.

19. Béhé M, Reubi J, Nock B, Mäcke H, Breeman WAP, Bernard HF, et al. Evaluation of a DOTA-minigastrin derivative for therapy and diagnosis for CCK-2 receptor positive tumours. Eur J Nucl Med Mol Imaging 2005;32(Suppl 1): S78.

20. Akiziwa H, Arano Y, Mifune M, Iwado A, Saito Y, Mukai T, et al. Effect of molecular charges on renal uptake of ^{111}In-DTPA-conjugated peptides. Nucl Med Biol 2001;28:761-8.

21. Schmitt A, Bernhardt P, Nilsson O, Ahlman H, Kölby L, Forssell-Aronsson E. Differences in Biodistribution Between ^{99m}Tc-Depreotide, ^{111}In-DTPA-Octreotide, and ^{177}Lu-DOTA-Tyr^3-Octreotate in a Small Cell Lung Cancer Animal Model. Cancer Biother Radiopharm 2005;20:231-6.

22. Chen X, Sievers E, Hou Y, Park R, Tohme M, Bart R, et al. Integrin $\alpha_v\beta_3$ targeted Imaging of Lung Cancer Neoplasia 2005;7:271-9.

23. Chen X, Hou Y, Tohme M, Park R, Khankaldyyan V, Gonzales-Gomez I, et al. Pegylated Arg-Gly-Asp Peptide: ^{64}Cu Labeling and PET Imaging of Brain Tumor $\alpha_v\beta_3$-Integrin Expression. J Nucl Med 2004;45:1776-83.

Chapter 6

$\alpha_v\beta_3$ Integrin targeting of intraperitoneally growing tumors with a radiolabeled RGD peptide

Ingrid Dijkgraaf
John A. W. Kruijtzer
Cathelijne Frielink
Frans H. M. Corstens
Wim J. G. Oyen
Rob M. J. Liskamp
Otto C. Boerman

Int J Cancer 2007:120;605-610

Abstract

Ovarian cancer is the fourth most common cause of cancer deaths among females in the Western world after cancer of the breast, colon and lung. The inability to control the disease within the peritoneal cavity is the major cause of treatment failure in patients with ovarian cancer. The majority of ovarian carcinomas express the $\alpha_v\beta_3$ integrin. Here we studied the tumor targeting potential of an ^{111}In-labeled cyclic RGD peptide in athymic BALB/c mice with intraperitoneally (i.p.) growing NIH:OVCAR-3 human ovarian carcinoma tumors.

Methods: The cyclic RGD peptide, c(RGDfK)E, was synthesized, conjugated with DOTA, and radiolabeled with ^{111}In. The targeting potential of ^{111}In-DOTA-E-c(RGDfK) was studied in athymic mice with i.p. growing NIH:OVCAR-3 xenografts and the optimal dose of this compound was determined (0.01 μg up to 10 μg). The biodistribution at optimal peptide dose was determined at various time points (0.5 up to 72 h). Furthermore, the therapeutic potential of ^{177}Lu-DOTA-E-c(RGDfK) was studied in this model.

Results: Two hours after i.p. administration, ^{111}In-DOTA-E-c(RGDfK) showed high and specific uptake in the i.p. growing tumors. Optimal uptake in the i.p. growing tumors was observed at a 0.03-0.1 μg dose range. Tumor uptake of ^{111}In-DOTA-E-c(RGDfK) peaked 4 h p.i. (38.8 ± 2.7 %ID/g), gradually decreasing at later time points (24.0 ± 4.1 %ID/g at 48 h p.i.).

Conclusions: I.p. growth of OVCAR-3 could be significantly delayed by injecting 37 MBq ^{177}Lu-labeled peptide i.p.. Radiolabeled DOTA-E-c(RGDfK) is suitable for targeting of i.p. growing tumors and potentially can be used for peptide-receptor radionuclide therapy of these tumors.

Introduction

Ovarian cancer remains the most lethal gynecological malignancy in the Western world [1]. About 90% of ovarian cancer originates from malignant transformation of the ovarian surface epithelium and in most patients the disease is diagnosed in an advanced stage [2]. Most patients with stage III and IV ovarian cancer achieve a clinical complete remission after cytoreductive surgery and combination chemotherapy. Unfortunately, in the majority of these patients the disease relapses [3]. Over the past 25 years the principal treatment of advanced ovarian cancer has been surgery followed by chemotherapy. At the moment, paclitaxel combined with cisplatin or carboplatin is the standard first-line treatment in most countries [4], resulting in response rates of 70 to 80%. In comparison with former regimens, response rates have ameliorated and tolerability has improved. However, only small improvements in overall survival have been achieved. Further progress will depend on new treatments that eradicate residual disease after surgery and chemotherapy. The use of radiolabeled antibodies to achieve this goal has been investigated in past decades. For example, Epenetos et al. found that patients who achieve complete remission with conventional therapy had a relatively long-mean survival when treated with intraperitoneal radioimmunotherapy using

^{90}Y-labeled anti MUC1 antibody [5]. However, the promising results of this phase I/II study were not confirmed in a recently completed phase III trial [6].

During the past decade radiolabeled receptor binding peptides have emerged as an important class of radiopharmaceuticals for diagnosis and therapy. Peptides used for tumor targeting offer considerable advantages over antibodies, as they are not immunogenic, accumulate rapidly in the target tissue, and clear rapidly from the blood and non-target tissues.

For peptide receptor-targeted radiotherapy (PRRT) peptides with specific affinity for tumor-associated receptors on cancer cells, labeled with cytotoxic radionuclides can be used. Due to the restricted expression of the $\alpha_v\beta_3$ integrin in tumors, $\alpha_v\beta_3$ is considered a suitable receptor for tumor targeting. RGD peptides contain the amino acid sequence Arg-Gly-Asp and preferentially bind to the $\alpha_v\beta_3$ integrin receptor. In previous studies we have shown that the radiolabeled cyclic RGD peptides specifically accumulated in subcutaneously (s.c.) growing $\alpha_v\beta_3$ expressing tumors in athymic mice [7]. Here we studied the tumor targeting potential of an ^{111}In-labeled cyclic RGD peptide in athymic BALB/c nude mice with intraperitoneally (i.p.) growing NIH:OVCAR-3 ovarian carcinoma tumors. Furthermore, in this mouse model, the therapeutic potential of the ^{177}Lu-labeled cyclic RGD peptide was investigated.

Material and methods

Radiolabeling of DOTA-E-c(RGDfK)

^{111}In-DOTA-E-c(RGDfK) was prepared by adding 18.5 MBq $^{111}InCl_3$ (Mallinckrodt, Petten, The Netherlands) to 5 µg (4.4 nmol) DOTA-E-c(RGDfK) (Figure 1) dissolved in 300 µL 0.5 M ammonium acetate buffer, pH 6, containing 0.6 mg/mL gentisic acid. ^{177}Lu-DOTA-E-c(RGDfK) was prepared by adding 1.3 GBq (35.5 mCi) $^{177}LuCl_3$ (NRG, Petten, The Netherlands) to 9 µg (8.0 nmol) DOTA-E-c(RGDfK) dissolved in 300 µL 0.5 M ammonium acetate buffer, pH 5, containing 0.6 mg/mL gentisic acid.

The reaction mixtures were degassed and the mixtures were heated at 100 °C for 15 minutes. The radiochemical purity was determined by reversed-phase high-performance liquid chromatography (RP-HPLC) (HP 1100 series, Hewlett Packard, Palo Alto, CA, USA) using a C18 column (RX-C18, 4.6 × 250 mm, Zorbax) eluted with a gradient mobile phase (8-20% B over 25 min, solvent A = 25 mM ammonium acetate buffer, solvent B = acetonitrile) at 1 mL/min. The radioactivity of the eluate was monitored using an in-line radiodetector (Flo-One Beta series, Radiomatic, Meriden, CT, USA).

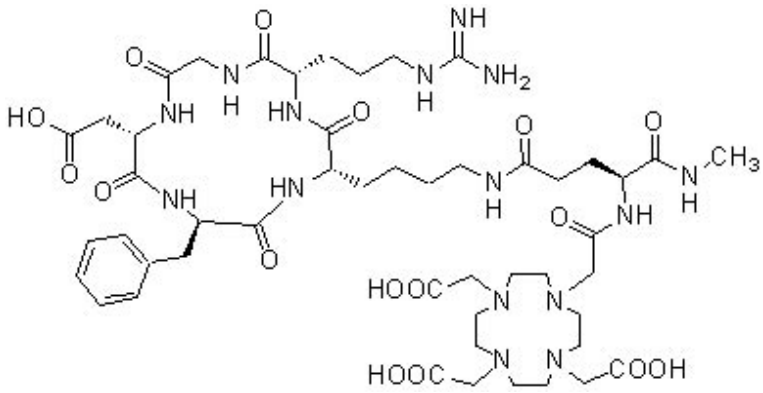

Figure 1. Structural formula of the DOTA-conjugated RGD peptide, DOTA-E-c(RGDfK).

Nude mouse tumor model

To ensure a reproducible growth of tumors in the mice, NIH:OVCAR-3 ovarian carcinoma cells were serially transplanted i.p. in female BALB/c nude mice. On day 0, OVCAR-3 cells were harvested from a mouse with ascitic tumor, and 6-8 weeks old mice were inoculated intraperitoneally with 0.2 mL of a cell suspension of NIH:OVCAR-3 cells (5×10^7 cells/mL). The radiolabeled DOTA-E-c(RGDfK) was administered 10 or 11 days after tumor inoculation.

Biodistribution studies

Ten or eleven days after tumor inoculation mice were randomly divided in seven groups and received 0.01, 0.03, 0.1, 0.3, 1, 3 (n=4-5) or 10 μg (n=2) DOTA-E-c(RGDfK) i.p.. Therefore, ^{111}In-labeled DOTA-E-c(RGDfK) was prepared as described above (140 kBq/nmol) and peptide dose was adjusted by adding non-radiolabeled DOTA-E-c(RGDfK). Mice were killed by CO_2 asphyxiation two hours postinjection (p.i.) and the OVCAR-3 cells were harvested by rinsing the abdominal cavity twice with 5 mL 0.9% NaCl. Cells were spun down (1200 rpm, 5 min), and the activity in pellet and the supernatant was determined. In addition, blood and the major organs and tissues were collected, weighed, and counted in a γ-counter (1480 Wizard, Wallac, Turku, Finland). The percentage injected dose per gram (%ID/g) was determined for each sample. At seven time points p.i. (0.5, 2, 4, 8, 24, 48 and 72 h) the biodistribution of the optimal dose of ^{111}In-DOTA-E-c(RGDfK) was determined in 5 mice/group. In addition, to investigate whether the localization of ^{111}In-DOTA-E-c(RGDfK) is receptor-mediated, the biodistribution of the optimal dose of ^{111}In-DOTA-E-c(RGDfK) in the presence of an excess of unlabeled RGD peptide was determined at each time point (2 mice/group). Furthermore, at 2 h p.i. the effect of the route of administration was studied in one group of mice (n=5). This group received 0.1 μg ^{111}In-DOTA-E-c(RGDfK) intravenously (i.v.).

Radionuclide therapy study

One group of mice with i.p. OVCAR-3 tumors (n=10) received 37 MBq ^{177}Lu-DOTA-E-c(RGDfK). A second group of mice with i.p. OVCAR-3 tumors (n=12) did not receive any treatment and served as control group. Twice a week the body weight of the mice in each group was recorded. When intraperitoneal ascitic tumor growth was apparent, mice were killed by CO_2 asphyxiation. Differences in survival between groups were compared using a logrank test for survival analysis. The level of significance was set at $P<0.05$.

Autoradiography

To study the intratumoral distribution, three mice with i.p. growing OVCAR-3 tumors received 1.1 MBq (0.3 µg) ^{111}In-DOTA-E-c(RGDfK) i.p.. Mice were killed by CO_2 asphyxiation two hours p.i.. One solid tumor deposit per mouse was removed and snap-frozen in liquid isopentane and cryofixed (OCT Tissue-Tek; SAKURA Finetek U.S.A. Inc.) The tumor was sectioned (5 µm) using a cryostatic microtome. After air drying, tumor sections were exposed to a storage phosphor imager screen overnight. The screen was scanned in a phosphor imaging system (Molecular Imager GS363, BioRad Laboratories, Hercules, CA) at a pixel size of 100 × 100 µm. Images were processed with Quantity One software (version 4.5.2, BioRad Laboratories, Hercules, CA).

Results

Radiolabeling of DOTA-E-c(RGDfK)

RP-HPLC analysis indicated that the radiochemical purity of ^{111}In-DOTA-E-c(RGDfK) and ^{177}Lu-DOTA-E-c(RGDfK) preparations used in these experiments was at least 93%. The elution profile of ^{111}In-DOTA-E-c(RGDfK) and ^{177}Lu-DOTA-E-c(RGDfK) showed a single peak for both compounds with an elution time of 14.0 min for the ^{111}In-labeled compound (Figure 2) and 14.2 min for the ^{177}Lu-labeled compound.

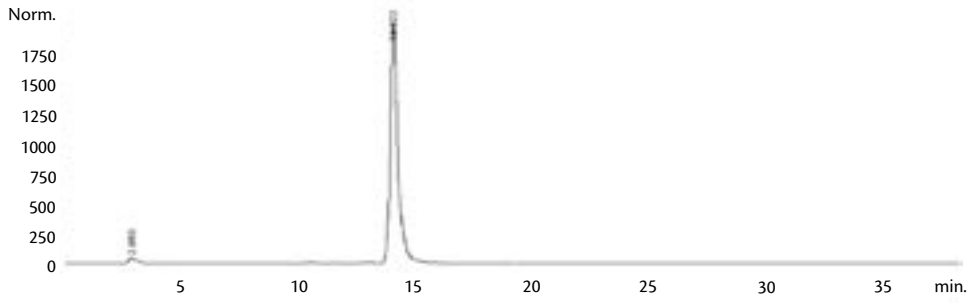

Figure 2. RP-HPLC elution profile of ^{111}In-DOTA-E-c(RGDfK).

Biodistribution studies

The results of the peptide dose escalation study of ^{111}In-DOTA-E-c(RGDfK) are summarized in Figure 3. The optimal tumor uptake was observed when a peptide dose of 0.03 µg and 0.1 µg was administered (20.6 ± 9.7 %ID/g and 18.5 ± 5.9 %ID/g, respectively). At 2 h p.i., the tumor-to-blood ratio at a peptide dose of 0.1 µg was 133 ± 46 (Figure 4). At higher peptide doses the uptake in the tumor was significantly lower, probably due to saturation of the $\alpha_v\beta_3$ integrin receptors in the tumor.

The optimal dose of 0.1 µg per mouse was used to study the biodistribution of the radiolabeled peptide at 0.5, 2, 4, 8, 24, 48, and 72 h p.i.. The results are shown in Figure 5. Tumor uptake peaked at 4 h p.i. (38.8 ± 2.7 %ID/g) and gradually decreased with time to 19.3 ± 1.9 %ID/g at 72 h p.i.. Blood levels were 0.98 ± 0.20 %ID/g 0.5 h p.i. and rapidly decreased to 0.006 ± 0.001 %ID/g at 72 h p.i.. Coinjection of an excess unlabeled RGD peptide (50 µg) along with 0.1 µg ^{111}In-DOTA-E-c(RGDfK) resulted in a significantly lower radioactivity concentration in the tumor, indicating that uptake of the major fraction of ^{111}In-DOTA-E-c(RGDfK) in the tumor is $\alpha_v\beta_3$-mediated (Figure 6).

The route of administration of ^{111}In-DOTA-E-c(RGDfK) in the i.p. OVCAR-3 model was clearly in favor of the i.p. route (Figure 7). At 2 h p.i. tumor uptake after i.p. administration of 0.1 µg ^{111}In-DOTA-Ec(RGDfK) was 35.2 ± 3.8 %ID/g whereas after i.v. administration, the tumor uptake was 0.98 ± 0.26 %ID/g.

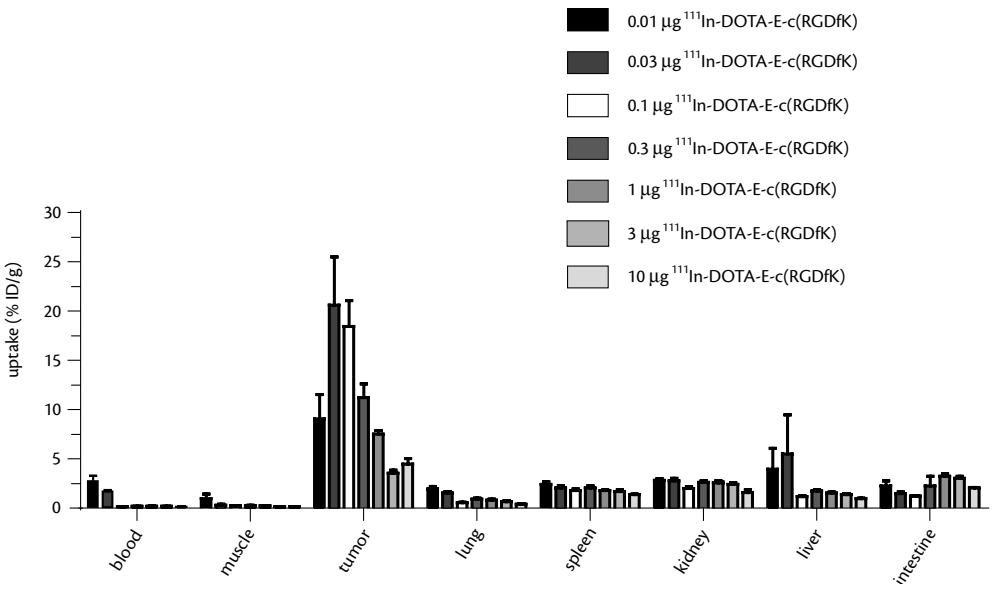

Figure 3. Biodistribution of ^{111}In-DOTA-E-c(RGDfK) in BALB/c nude mice with i.p. growing OVCAR-3 ovarian carcinoma at 2 h p.i. at various peptide doses.

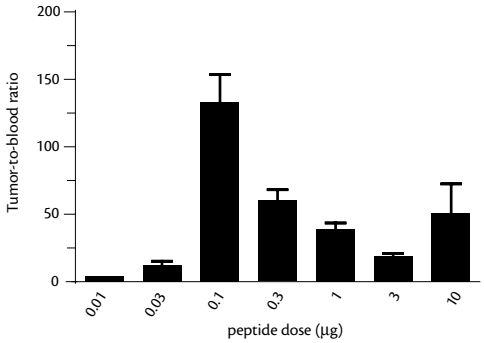

Figure 4. Tumor-to-blood ratios at various peptide doses at 2 h p.i. in BALB/c nude mice with i.p. growing OVCAR-3 ovarian carcinoma.

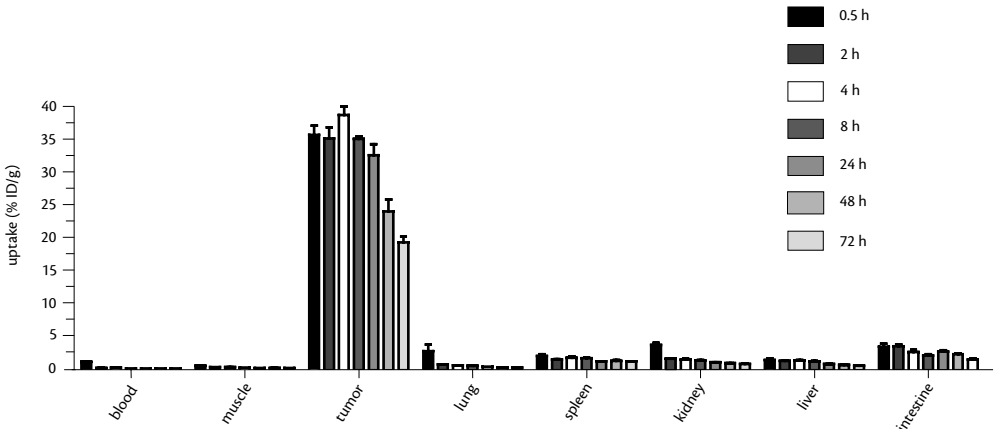

Figure 5. Biodistribution of 0.1 µg ^{111}In-DOTA-E-c(RGDfK) at different time points in BALB/c nude mice with i.p. growing OVCAR-3 ovarian carcinoma.

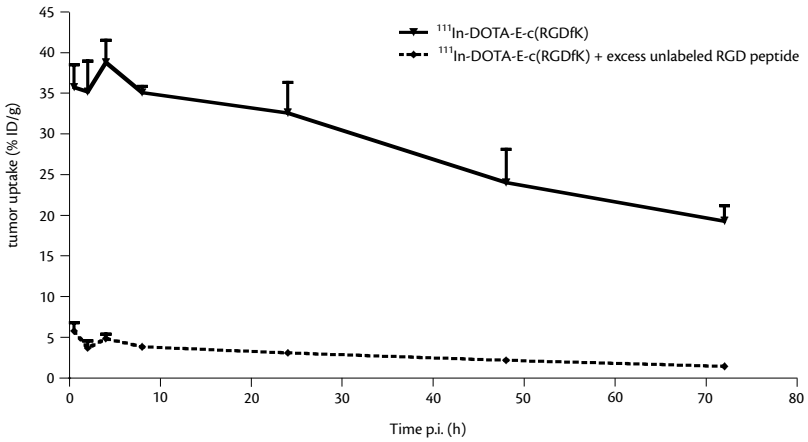

Figure 6. Tumor uptake of 0.1 µg ^{111}In-DOTA-E-c(RGDfK) at different time points in the presence (dotted line) and absence (solid line) of an excess of unlabeled RGD peptide.

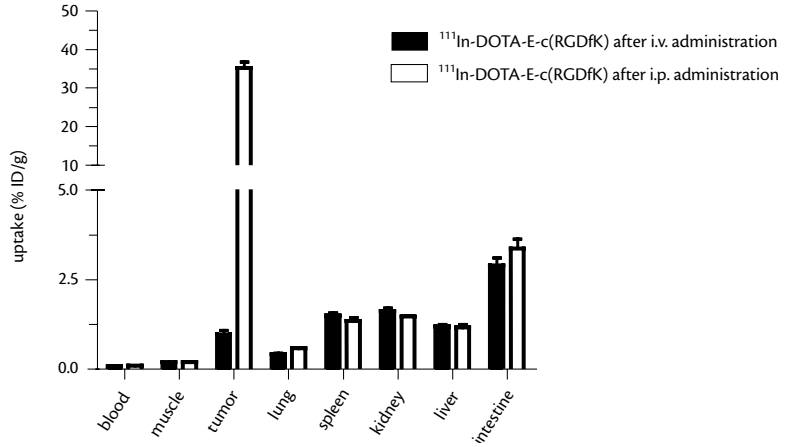

Figure 7. Biodistribution of ^{111}In-DOTA-E-c(RGDfK) in BALB/c nude mice with i.p. growing OVCAR-3 ovarian carcinoma 2 h after i.v. (black bars) and i.p. (white bars) administration.

Survival study

The results of the survival study are given in Figure 8. Mice that received 37 MBq ^{177}Lu-DOTA-E-c(RGDfK) i.p. showed a statistically significant longer survival than the mice that received no treatment (P=0.017). The median survival for the untreated mice was 5 weeks, whereas the median survival for the treated mice was 21 weeks.

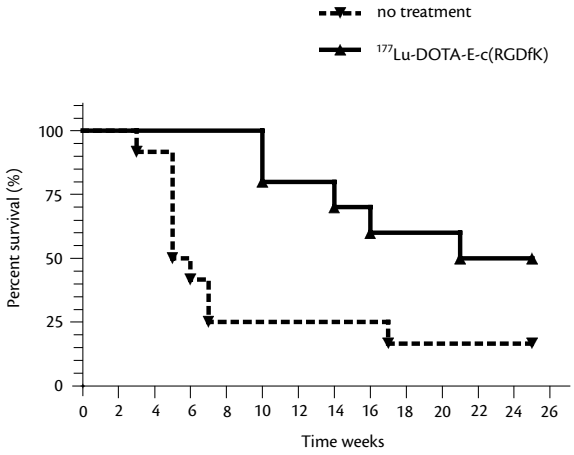

Figure 8. Kaplan-Meier survival plot of BALB/c nude mice with i.p. growing OVCAR-3 ovarian carcinoma. There is a significant increase in median survival between the treated and untreated group (21 weeks and 5 weeks, respectively; P=0.017).

Autoradiography

In Figure 9, tumor sections from 3 tumor deposits are shown. In all tumor sections, ^{111}In-DOTA-E-c(RGDfK) showed a heterogeneous distribution throughout the tumor 2 h p.i., mainly accumulating in the periphery of the tumor deposit.

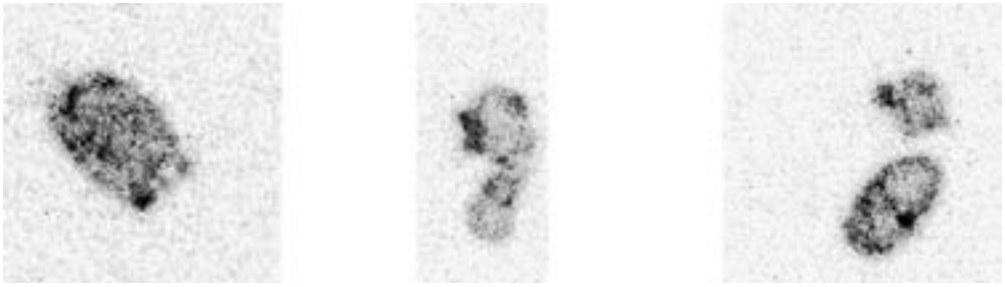

Figure 9. Autoradiographs showing the intratumoral distribution of ^{111}In-DOTA-E-c(RGDfK) 2 h after i.p. administration.

Discussion

The ^{111}In-labeled cyclic RGD peptide showed tumor targeting potential in i.p. growing ovarian carcinoma. Uptake of the peptide in the i.p. growing ascitic tumor was specific, dose dependent and saturable. Optimal tumor uptake of ^{111}In-DOTA-E-c(RGDfK) was achieved at a peptide dose in the range of 0.03 µg and 0.1 µg. At higher peptide dose the uptake in the tumor was reduced, due to saturation of the $\alpha_v\beta_3$ integrin receptors. At the lowest peptide dose, 0.01 µg, the blood levels were relatively high, which may be caused by a relevant fraction of the peptide associated with plasma proteins.

For peptide receptor-targeted radiotherapy, high uptake in the tumor is important, but retention of the radiolabel in the tumor is also crucial. With a peak in tumor uptake at 4 h p.i., followed by a slow decrease to 24.0 ± 4.1 %ID/g after 48 h, this cyclic RGD peptide fulfilled this requirement. The long retention of ^{111}In-DOTA-E-c(RGDfK) in the tumor deposits may be due to internalization of the radiolabeled ligand. The internalization of radiolabeled RGD peptides and RGD-containing macromolecular conjugates by $\alpha_v\beta_3$ expressing cells has been described [8, 9].

Coinjection of an excess of unlabeled RGD peptide resulted in a significant decrease of radioactivity in the tumor, clearly demonstrating that the uptake of ^{111}In-DOTA-E-c(RGDfK) in the tumor was $\alpha_v\beta_3$-mediated. It is noteworthy that the uptake of ^{111}In-DOTA-E-c(RGDfK) in the i.p. growing tumor after i.p. administration was much higher compared to the uptake in subcutaneously (s.c.) growing OVCAR-3 tumors after i.v. administration. The uptake of ^{111}In-DOTA-E-c(RGDfK) at 2 h p.i. in the i.p. growing tumor was 35.2 ± 3.8 %ID/g, which is more than 15-fold higher than the uptake in s.c. tumors (2.04 ± 0.3 %ID/g).

Radiolabeled antibodies directed against the mucin-1 antigen and other tumor-associated

glycoproteins, such as TAG-72 and gp-38 have been used to target ovarian cancer [10]. Several clinical trials on radioimmunotherapy (RIT) in patients with ovarian cancer have been published [11-18]. However, the use of monoclonal antibodies (MAbs) for tumor targeting show some disadvantages like the high molecular weight, which hinders rapid pharmacokinetics resulting in slow diffusion into the target tissue and comparatively high blood concentration. Another complicating factor for the application of radiolabeled antibodies is that MAbs are immunogenic. Although antibody fragments have been developed to overcome these problems, peptides have more favorable properties for tumor targeting. Peptides have a small size and a rapid clearance from blood and non-target tissues compared to proteins and antibodies. In addition, peptides have a low immunogenicity.

The effect of the route of administration has been the subject of various studies. These studies showed that for radiolabeled antibodies, the route of administration, i.v. *vs.* i.p. only has limited effect on the targeting of i.p. growing tumors [19-23]. Colcher et al. investigated the efficacy of intracavitary radiolabeled MAb administration and demonstrated the advantage of the concomitant use of intracavitary and i.v. administered MAbs for tumor targeting [19]. Furthermore, Koppe et al. showed that in nude mice with i.p. LS174T tumors the biodistribution of the monoclonal antibody MN-14 labeled with ^{131}I, ^{186}Re, and ^{88}Y after i.v. and i.p. administration was not significantly different [20]. In a study in patients suspected of having primary or recurrent ovarian carcinoma were simultaneously injected i.v. and i.p. with ^{125}I/^{131}I-labeled chimeric antibody MOv18 [21]. In this study antibody uptake in i.p. tumor deposits was independent of the route of administration. The present study demonstrates that for radiolabeled peptides, the route of administration has a marked influence on tumor targeting. Tumor uptake after i.v. administration of 0.1 µg ^{111}In-DOTA-E-c(RGDfK) at 2 h p.i. was 0.98 ± 0.26 %ID/g, whereas after i.p. administration tumor uptake was 35.2 ± 3.8 %ID/g (Figure 7). Due to the fast blood clearance of peptides compared to antibodies, the i.p. route of administration is preferred for peptides.

Compared to other studies investigating the tumor targeting potential of peptides, the i.p. tumor model showed excellent tumor uptake of ^{111}In-DOTA-E-c(RGDfK) and low uptake in non-target tissues. Especially, the kidney concentration of ^{111}In-DOTA-E-c(RGDfK) is low compared to that of other ^{111}In-labeled peptides. Apparently, this peptide is not efficiently reabsorbed in the renal tubular cells.

In this mouse model of ovarian cancer the therapeutic potential of the cyclic RGD peptide was also determined. In this i.p. OVCAR-3 model the tumor burden consisted of cell clusters in ascitic fluid and small omental solid tumor depositions. High energy particles such as ^{90}Y (β_{max} 2.3 MeV, $t_{1/2}$ 64 h) and ^{188}Re (β_{max} 2.1 MeV, $t_{1/2}$ 17 h) are considered more appropriate for the treatment of larger tumors whereas low energy particles such as ^{177}Lu (β_{max} 0.5 MeV, $t_{1/2}$ 161 h) and ^{131}I (β_{max} 0.6 MeV, $t_{1/2}$ 192 h) could be more effective for the treatment of tumor cell clusters and small tumor lesions [24]. Therefore, DOTA-E-c(RGDfK) was radiolabeled with the β-emitting radionuclide ^{177}Lu. In mice with i.p. growing OVCAR-3 tumors i.p. treatment with ^{177}Lu-DOTA-E-c(RGDfK) resulted in

a statistically significant better survival as compared to untreated controls (P=0.017).
In conclusion, we demonstrated that ^{111}In-DOTA-E-c(RGDfK) has high and specific uptake in nude mice with intraperitoneally growing OVCAR-3 tumors. PRRT experiments in this model of ovarian cancer indicated that i.p. tumor growth can be inhibited significantly by a therapeutic dose of ^{177}Lu-DOTA-E-c(RGDfK).

References

1. Ozols RF. Treatment goals in ovarian cancer. Int J Gynecol Cancer 2005;15:3-11.
2. Ozols RF, Bookman MA, Connolly DC, Daly MB, Godwin AK, Schilder RJ, Xu X, Hamilton TC. Focus on epithelial ovarian cancer. Cancer Cell 2004;5:19-24.
3. Ozols RF. Maintenance Therapy in Advanced Ovarian Cancer: Progression-Free Survival and Clinical Benefit. J Clin Oncol 2003;21:2451-3.
4. Neder Kalil NG, McGuire WP. Chemotherapy for advanced epithelial ovarian carcinoma. Best Pract Res Clin Obstet Gynaecol 2002;16:553-71.
5. Epenetos AA, Hird V, Lambert H, Mason P, Coulter C. Long term survival of patients with advanced ovarian cancer treated with intraperitoneal radioimmunotherapy. Int J Gynecol Cancer 2000;10:44-6.
6. Verheijen RH, Massuger LF, Benigno BB, Epenetos AA, Lopes A, Soper JT, Markowska J, Vyzula R, Jobling T, Stamp G, Spiegel G, Thurston D, et al. A phase III trial of intraperitoneal therapy with yttrium-90-labeled HMFG1 murine monoclonal antibody in patients with epithelial ovarian cancer after a surgically defined complete remission. J Clin Oncol 2006;24:571-8.
7. Janssen ML, Oyen WJ, Dijkgraaf I, Massuger LF, Frielink C, Edwards DS, Rajopadhye M, Boonstra H, Corstens FH, Boerman OC. Tumor targeting with radiolabeled alpha-v-beta-3 integrin binding peptides in a nude mouse model. Cancer Res 2002;62:6146-51.
8. Van Hagen PM, Breeman WAP, Bernard HF, Schaar M, Mooij CM, Srinivasan A, Schmidt MA, Krenning EP, De Jong M. Evaluation of a Radiolabelled Cyclic DTPA-RGD Analogue for Tumour Imaging and Radionuclide Therapy. Int J Cancer 2000;90:186-98.
9. Schraa AJ, Kok RJ, Berendsen AD, Moorlag HE, Bos EJ, Meijer DKF, De Leij LFMH, Molema G. Endothelial cells internalize and degrade RGD-modified proteins developed for tumor vasculature targeting. J Control Release 2002;83:241-51.
10. Bombardieri E, Ferrari L, Spinelli A, Maffioli L, Seregni E, Braggi G. Radioimmunotherapy of ovarian cancer with radiolabelled monoclonal antibodies: Biological basis, present status and future perspectives. Anticancer Res 1997;17:1719-29.
11. Epenetos AA, Munro AJ, Stewart S, Rampling R, Lambert HE, McKenzie CG, Soutter P, Rahemtulla A, Hooker G, Sivolapenko GB. Antibody-guided irradiation of advanced ovarian cancer with intraperitoneally administered radiolabeled monoclonal antibodies. J Clin Oncol 1987;5:1890-99.
12. Nicholson S, Gooden CS, Hird V, Maraveyas A, Mason P, Lambert HE, Meares CF, Epenetos AA Radioimmunotherapy after chemotherapy compared to chemotherapy alone in the treatment of advanced ovarian cancer: A matched analysis. Oncol Rep 1998;5:223-6.
13. Rosenblum MG, Verschraegen CF, Murray JL, Kudelka AP, Gano J, Cheung L, Kavanagh JJ. Phase I study of

90Y-labeled B72.3 intraperitoneal administration in patients with ovarian cancer: Effect of dose and EDTA coadministration on pharmacokinetics and toxicity. Clin Cancer Res 1999;5:953-61.

14. Alvarez RD, Partridge EE, Khazaeli MB, Plott G, Austin M, Kilgore L, Russell CD, Liu T, Grizzle WE, Schlom J, LoBuglio AF, Meredith RF. Intraperitoneal radioimmunotherapy of ovarian cancer with 177Lu-CC49: a phase I/II study. Gynecol Oncol 1997;65:94-101.

15. Meredith RF, Alvarez RD, Partridge EE, Khazaeli MB, Lin CY, Macey DJ, Austin JM Jr., Kilgore LC, Grizzle WE, Schlom J, LoBuglio AF. Intraperitoneal radioimmunochemotherapy of ovarian cancer: A phase I study. Cancer Biother Radiopharm 2001;16:305-315.

16. Alvarez RD, Huh WK, Khazaeli MB, Meredith RF, Partridge EE, Kilgore LC, Grizzle WE, Shen S, Austin JM, Barnes MN, Carey D, Schlom J, LoBuglio AF. A phase I study of combined modality (90)Yttrium-CC49 intraperitoneal radioimmunotherapy for ovarian cancer. Clin Cancer Res 2002;8:2806-11.

17. Crippa F, Bolis G, Seregni E, Gavoni N, Scarfone G, Ferraris C, Buraggi GL, Bombardieri E. Single-dose intraperitoneal radioimmunotherapy with the murine monoclonal antibody I-131 MOv18: clinical results in patients with minimal residual disease of ovarian cancer. Eur J Cancer 1995:31A:686-90.

18. Zanten-Przybysz I, Molthoff CF, Roos JC, Plaizier MA, Visser GW, Pijpers R, Kenemans P, Verheijen RH. Radioimmunotherapy with intravenously administered 131I-labeled chimeric monoclonal antibody MOv18 in patients with ovarian cancer. J Nucl Med 2000;41:1168-76.

19. Colcher D, Esteban J, Carrasquillo JA, Sugarbaker P, Reynolds JC, Bryant G, Larson SM, Schlom J. Complementation of Intracavitary and Intravenous Administration of a Monoclonal Antibody (B72.3) in Patients with Carcinoma. Cancer Res 1987;47:4218-24.

20. Koppe MJ, Bleichrodt RP, Soede AC, Verhofstad AA, Goldenberg DM, Oyen WJG, Boerman OC. Biodistribution and Therapeutic Efficacy of $^{125/131}$I-, ^{186}Re-, $^{88/90}$Y-, ^{177}Lu-labeled Monoclonal Antibody MN-14 to Carcinoembryonic Antigen in Mice with Small Peritoneal Metastases of Colorectal Origin. J Nucl Med 2004;45:1224-32.

21. Van Zanten-Przybysz I, Moltoff CF, Roos JC, Verheijen RH, Van Hof A, Buist MR, Prinssen HM, Den Hollander W, Kenemans P. Influence of the route of administration on targeting of ovarian cancer with the chimeric monoclonal antibody MOv18: i.v. vs. i.p.. Int J Cancer 2001;92:106-14.

22. Griffin TM, Collins J, Bokhari F, Stochl M, Brill AB, Ito T, Emond G, Sands H. Intraperitoneal immunoconjugates. Cancer Res 1990;50(Suppl):1031s-8s.

23. Tibben JG, Massuger LFAG, Boerman OC, Borm GF, Claessens RAMJ, Corstens FHM. Effect of the route of administration on the biodistribution of radioiodinated OV-TL 3 F(ab')2 in experimental ovarian cancer. Eur J Nucl Med 1994;21:1183-90.

24. O'Donoghue JA, Bardies M, Wheldon TE. Relationships between tumor size and curability for uniformly targeted therapy with β-emitting radionuclides. J Nucl Med 1995;36:1902-9.

Chapter 7

Summary and general discussion

Samenvatting

Summary and general discussion

Radiolabeled receptor binding peptides have emerged as a new class of radiopharmaceuticals for tumor diagnosis and therapy. Several malignant tumors overexpress particular types of receptors on their cell surface, which can be targeted with radiolabeled peptides.

The $\alpha_v\beta_3$ integrin receptor is an interesting candidate for tumor targeting, as it is expressed on the cell membrane of various tumor cell types such as ovarian cancer, neuroblastoma, breast cancer, melanoma, and others. Furthermore, for growth beyond the size of 1-2 mm in diameter, tumors require the formation of new blood vessels. The $\alpha_v\beta_3$ integrin receptor is overexpressed on the endothelium of newly formed bloodvessels. $\alpha_v\beta_3$ Integrin receptors expressed on endothelial cells modulate cell migration and survival during angiogenesis, while $\alpha_v\beta_3$ integrin receptors expressed on carcinoma cells potentiate metastasis by facilitating invasion and movement across blood vessels. Radiolabeled ligands for this integrin receptor could be used as tracers to non-invasively visualize $\alpha_v\beta_3$ expression in tumors. Non-invasive determination of $\alpha_v\beta_3$ expression potentially can be used to monitor treatment response to antiangiogenic drugs or even to select patients likely to respond to treatment with antiangiogenic drugs.

The $\alpha_v\beta_3$ integrin specifically interacts with the arginine-glycine-aspartic acid (RGD) amino acid sequence present in extracellular matrix proteins such as vitronectin, fibrinogen, and laminin [1]. Based on the RGD tripeptide sequence, a series of small peptides has been designed to antagonize the function of the $\alpha_v\beta_3$ integrin.

A few groups have systematically tested RGD containing peptides for their ability to bind the $\alpha_v\beta_3$ integrin. It was shown that linear RGD peptides have a relatively low affinity for $\alpha_v\beta_3$ compared to cyclic RGD peptides. In addition, linear RGD peptides are often degraded rapidly in serum by proteases. Therefore, linear RGD peptides are considered suboptimal for $\alpha_v\beta_3$ targeting. It appeared that cyclization of RGD peptides resulted in increased selectivity and affinity for the $\alpha_v\beta_3$ integrin. Especially cyclic RGD peptides consisting of five amino acids have a high and selective affinity for $\alpha_v\beta_3$. Furthermore, it was shown that besides the essential RGD sequence, a hydrophobic amino acid in position 4 increases the affinity, whereas the amino acid in position 5 had no influence on the affinity [2]. The *cyclo*[Arg-Gly-Asp-D-Phe-Val] (c[RGDfV]), as developed by Kessler and coworkers, is one of the most active and selective antagonists for the $\alpha_v\beta_3$ integrin [3]. Structure-activity relationship studies on this cyclic pentapeptide showed that the exchange of the valine amino acid (V) by lysine (K) did not significantly influence activity and selectivity. Because the ε-amino moiety of the lysine residue can easily be modified, numerous applications of c[RGDfK] are presented in the literature for tumor targeting and imaging.

In **chapter 1**, the criteria of peptide ligand development, the selection of radioisotopes, chelators, and chemical aspects of radiopeptide development are described. In addition, the current state of clinical use of radiopeptides for diagnosis and therapy of tumors is discussed.

In **chapter 2**, we developed RGD analogs with improved in vivo $\alpha_v\beta_3$ targeting characteristics. Therefore, we synthesized apart from our lead compound c(RGDfK), three analogs: (I) a cyclic peptoid-

peptide hybrid in which the arginine residue is replaced by the corresponding peptoid residue, (II) an all-peptoid in which all the amino acid residues are replaced by their corresponding peptoid residues, and (III) a peptidomimetic $\alpha_v\beta_3$ receptor antagonist. The compounds were conjugated with 1,4,7,10-tetraazacyclododecane-N,N',N'',N'''-tetaacetic acid (DOTA) and then radiolabeled with ^{111}In. Subsequently, the in vitro and in vivo $\alpha_v\beta_3$ binding characteristics were determined. The study demonstrated that modification of the cyclic RGD peptide to a peptoid-peptide hybrid resulted in reduced affinity for $\alpha_v\beta_3$ and concomitant lower tumor uptake. The all-peptoid analog had no affinity for $\alpha_v\beta_3$ and did not show any specific tumor uptake in vivo. In contrast, in vivo $\alpha_v\beta_3$ targeting of the non-amino acid containing peptidomimetic was as high as that of the native DOTA-conjugated cyclic RGD peptide. The native cyclic RGD peptide and the non-amino acid containing peptidomimetic had the best characteristics for $\alpha_v\beta_3$ targeting in tumors. Both compounds showed high uptake in non-target tissues such as intestine, colon, liver and spleen. Coinjection of an excess of non-radioactive compound resulted in a significantly lower uptake in these organs, indicating that the uptake is $\alpha_v\beta_3$-mediated. In contrast, the accumulation of these two ^{111}In-labeled compounds in the kidneys was apparently not $\alpha_v\beta_3$-mediated, as the kidney uptake of both compounds was not significantly lower in the presence of an excess of non-radioactive compound. Compared to other radiolabeled receptor binding peptides (e.g. octreotide, minigastrin), the kidney concentration of these two ^{111}In-labeled compounds was low, indicating that these compounds apparently are not efficiently reabsorbed in the renal tubular cells.

Multivalent interactions could increase the affinity of ligand-receptor interactions. Potentially, multivalent RGD peptides could have a higher affinity for $\alpha_v\beta_3$ and could target $\alpha_v\beta_3$ expressing tumors more efficiently. Therefore, we aimed to improve the tumor targeting properties of RGD peptides by multimerization (**chapter 3**). A DOTA-conjugated monomeric, dimeric, and tetrameric peptide were synthesized and radiolabeled with ^{111}In. It was shown that multimerization of c(RGDfK) resulted in enhanced affinity for $\alpha_v\beta_3$ as determined in vitro. Tumor uptake of the tetrameric RGD peptide was significantly higher compared to that of the monomeric and dimeric analogs. It is unlikely that the multivalent RGD peptides used in this study could bind multiple $\alpha_v\beta_3$ integrins simultaneously, as the distance between the RGD units is very short (~20 bond distances). Therefore, statistical rebinding appears the most likely explanation for the enhanced affinity of the multimeric RGD peptides: the receptor binding of one RGD unit will significantly enhance the local concentration of the other RGD unit in the vicinity of the receptor. This will lead to a higher "on rate" of receptor binding and/or a lower "off rate" of the RGD multimer.

An alternative way to synthesize multimeric RGD peptides was studied by using dendrimers. Dendrimers are macromolecules consisting of multiple perfectly branched monomers and this architecture makes them versatile constructs for the simultaneous presentation of especially biologically relevant molecules.

In our study, a monomeric, dimeric, and tetrameric c(RGDfK) dendrimer was synthesized via a microwave-assisted 1,3-dipolar cycloaddition - denoted as "click reaction" - of dendrimeric alkynes

with the *N*-ε-azido derivative of c(RGDfK) (**chapter 4**). In this chapter, the enhanced affinity of the tetrameric dendrimer compared to its monomeric and dimeric analogs was demonstrated in vitro in a competitive binding assay. In athymic mice with subcutaneous SK-RC-52 tumors, the tetrameric RGD dendrimer showed a significantly higher tumor uptake compared to its monomeric and dimeric analog at 24 h p.i..

Currently, hexameric and octameric RGD peptides have been synthesized and tested in vitro for their $\alpha_v\beta_3$ affinity. It appeared that the receptor binding affinity was not only dependent on the number of RGD moieties, but also on the spatial alignments of the RGD moieties [4]. Most likely, there is an upper limit on multimerization for in vivo tumor targeting. By multimerization of a compound, the molecular size will increase resulting in longer circulation times, which could lead to reduced tumor-to-background ratios.

An important aspect of the research on $\alpha_v\beta_3$ targeted radiotracers is to improve tumor-to-background ratios by modifying excretion kinetics of RGD peptides. Cyclic RGD peptides are generally composed of five amino acids. Apart from the RGD sequence, a variety of two additional amino acids have been used for different purposes such as radioiodination or linkage of chelators. These two amino acids may affect the three dimensional structure of the cyclic peptide and may thus affect the affinity and the in vivo behaviour of the peptide. It was shown that - besides the essential RGD sequence - a hydrophobic amino acid in position 4 increased the affinity, whereas the amino acid in position 5 had no influence on the affinity. The nature of these two amino acids can affect charge and hydrophilicity of the cyclic peptide. Apart from the two amino acids, a chelator and a linker between chelator and RGD peptide could also affect in vivo dynamics. It has been shown that introduction of a sugar moiety in a monomeric RGD peptide resulted not only in enhanced renal excretion, but also in enhanced tumor uptake of the radiotracer [5, 6].

In the study described in **chapter 5**, the effect of modification of the linker between the two cyclic RGD sequences and the DOTA chelator on the in vitro and in vivo characteristics was systematically investigated. A dimeric (E-[c(RGDfK)]$_2$) RGD peptide was synthesized and conjugated either directly with DOTA or via different linkers: PEG_4, glutamic acid, and lysine. It was demonstrated that optimization of the dimeric RGD peptide for $\alpha_v\beta_3$ targeting by systemetic linker variation, affected the in vivo kinetics of the tracers without influencing the affinity for $\alpha_v\beta_3$ and the $\alpha_v\beta_3$ targeting potential. The RGD peptide containing lysine as a linker showed a significantly higher uptake in the kidneys compared to the native RGD peptide and the RGD peptide containing the glutamic acid residue in the linkage. The latter showed a significant higher uptake in the liver compared to the native RGD peptide and the RGD peptide containing lysine as a linker.

For peptide-receptor radionuclide therapy (PRRT), high tumor uptake is crucial, but a low kidney retention of the radiotracer is also very important. By incorporation of a linker, the retention in non-target organs can be modified. This study showed that the native dimeric RGD peptide and the RGD peptide containing the PEG_4 linker appeared to be the optimal radiotracers. The native dimeric RGD peptide could not be improved by introduction of glutamic acid or lysine as a linker.

Ovarian cancer remains the most lethal gynecological malignancy in the Western world. Over the past 25 years the principal treatment of advanced ovarian cancer has been surgery followed by chemotherapy. Despite improvements in surgical management and advances in cytotoxic therapy, only small improvements in overall survival have been achieved. Further progress will depend on new treatments that eradicate residual disease after surgery and chemotherapy. The use of radiolabeled antibodies to achieve this goal has been investigated in the past decades.

In **chapter 6**, we studied the tumor targeting potential of the ^{111}In-labeled cyclic RGD peptide in athymic BALB/c mice with intraperitoneally (i.p.) growing NIH:OVCAR-3 ovarian carcinoma tumors.

In mice with i.p. growing ovarian carcinoma the ^{111}In-labeled cyclic RGD peptide showed excellent tumor targeting and tumor retention after i.p. administration. Several studies showed that for radiolabeled antibodies, the route of administration - meaning intravenous (i.v.) *vs*. intraperitoneal (i.p.) - had only limited effect on the targeting of intraperitoneally growing tumors. In contrast, for radiolabeled peptides the route of administration appeared to have a marked influence on the targeting of the i.p. tumor. At 2 h p.i. the tumor uptake after i.p. administration was more than 30-fold higher than the tumor uptake after i.v. administration. In addition, the tumor uptake of the radiolabeled RGD peptide in the i.p. growing tumor after i.p. administration was more than 15-fold higher compared to the uptake in subcutaneously (s.c.) growing OVCAR-3 tumors after i.v. administration. In view of the efficient targeting of the i.p. tumor with this RGD peptide, we studied whether this could be applied therapeutically. I.p. treatment of mice with i.p. growing ovarian carcinoma xenografts with the ^{177}Lu-labeled RGD peptide resulted in a statistically significant better survival as compared to untreated controls. Peptides used for tumor targeting offer considerable advantages over antibodies, as they are not immunogenic, accumulate far more rapidly in the target tissue, and clear faster from the blood and non-target tissues. The faster clearance of peptides from the blood and non-target tissues compared to antibodies leads to higher tumor-to-background ratios. Therefore, peptide-receptor radionuclide therapy (PRRT) with $\alpha_v\beta_3$ targeting peptides might be an alternative for antibody-based radioimmunotherapy (RIT) for the treatment of patients with i.p. tumors. However, $\alpha_v\beta_3$ expression in non-target tissues such as lung, spleen and intestine might lead to unwanted radiation to normal organs and thus hamper PRRT.

In the last few years, significant progress has been made on the development of $\alpha_v\beta_3$ targeting radiotracers for the visualization of $\alpha_v\beta_3$ expression in tumors by single photon emission computed tomography (SPECT) or positron emission tomography (PET). [^{18}F]Galacto-RGD has been under clinical investigations as the first $\alpha_v\beta_3$ targeted radiotracer for non-invasive visualization of $\alpha_v\beta_3$ in cancer patients. Radiolabeled $\alpha_v\beta_3$ binding ligands are radiotracers with the potential for visualization of angiogenesis in tumors and early detection of rapidly growing and metastatic tumors. These tracers might have the potential to select patients who might benefit from treatment with antiangiogenic drugs and these tracers might also be used to monitor the therapeutic effect with $\alpha_v\beta_3$ targeted drugs.

The studies described in this thesis demonstrate that the $\alpha_v\beta_3$ antagonists c(RGDfK) and a non-amino acid containing peptidomimetic had the best characteristics for $\alpha_v\beta_3$ targeting in tumors. The former showed high and specific uptake in i.p. growing tumors. It appeared that i.p. tumor growth can be inhibited with a therapeutic dose of ^{177}Lu-labeled c(RGDfK). The tetrameric analog of c(RGDfK), DOTA-E{E[c(RGDfK)]$_2$}$_2$, has optimal characteristics for the visualization of $\alpha_v\beta_3$ expression in tumors. Further studies should aim to radiolabel this compound with positron emitting nuclides such as ^{18}F or ^{68}Ga in order to image $\alpha_v\beta_3$ expression in tumors using the best imaging technique, being PET. Furthermore, when labeled with a β-emitting radionuclide this compound might particularly be used for PRRT of i.p. growing tumors.

References

1. Plow EF, Haas TA, Zhang L, Loftus J, Smith JW. Ligands binding to integrins. J Biol Chem 2000; 275:21785-8.
2. Haubner R, Gratias R, Diefenbach B, Goodman SL, Jonczyk A, Kessler H. Structural and functional aspects of RGD-containing cyclic pentapeptides as highly potent and selective integrin $\alpha_v\beta_3$ antagonists. J Am Chem Soc 1996;118: 7461-72.
3. Aumailley M, Gurrath M, Muller G, Calvete J, Timpl R, Kessler H. Arg-Gly-Asp constrained within cyclic pentapeptides. Strong and selective inhibitors of cell adhesion to vitronectin and laminin fragment P1. FEBS Lett 1991;291:50-4.
4. Ye Y, Bloch S, Xu B, Achilefu S. Design, Synthesis, and Evaluation of Near Infrared Fluorescent Multimeric RGD Peptides for Targeting Tumors. J Med Chem 2006;49:2268-75.
5. Haubner R, Wester HJ, Weber WA, Mang C, Ziegler SI, Goodman SL, et al. Noninvasive imaging of $\alpha_v\beta_3$ integrin expression using ^{18}F-labeled RGD-containing glycopeptide and positron emission tomography. Cancer Res 2001;61:1781-5.
6. Haubner R, Wester HJ, Burkhart F, Senekowitsch-Schmidtke R, Weber W, Goodman SL, et al. Glycosylated RGD-containing peptides: tracer for tumor targeting and angiogenesis imaging with improved biokinetics. J Nucl Med 2001;42:326-36.

Samenvatting

Radioactief gelabelde peptiden, die met hoge affiniteit binden aan receptoren op het celoppervlak van tumorcellen, vormen een nieuwe groep van radiofarmaca die gebruikt kan worden voor detectie en behandeling van tumoren. De $\alpha_v\beta_3$ integrine receptor komt tot expressie op de celmembraan van tumorcellen van verschillende typen tumoren, zoals bijvoorbeeld eierstokkanker, neuroblastoom, borstkanker en melanoom. Bovendien komt de $\alpha_v\beta_3$ integrine receptor tot expressie op de endotheelcellen van nieuw gevormde bloedvaten. Om te kunnen groeien, moeten in een tumor constant nieuwe bloedvaten worden aangemaakt, ook wel angiogenese genoemd. De $\alpha_v\beta_3$ integrine receptor *op endotheelcellen*, regelt tijdens angiogenese de celmigratie en overleving van de endotheelcellen. De $\alpha_v\beta_3$ integrine receptor die tot expressie komt *op tumorcellen* speelt een belangrijke rol bij invasie en de migratie (metastasering). Radioactief gelabelde liganden voor deze integrine receptor kunnen gebruikt worden om de expressie van $\alpha_v\beta_3$ in tumoren zichtbaar te maken. Het bepalen van $\alpha_v\beta_3$-expressie zou gebruikt kunnen worden voor het bepalen van het effect van angiogenese remmende stoffen en mogelijk het selecteren van patiënten voor behandeling met geneesmiddelen die de angiogenese remmen.

Het $\alpha_v\beta_3$ integrine gaat een specifieke interactie aan met de aminozuursequentie arginine-glycine-asparaginezuur, afgekort RGD. Deze RGD sequentie is aanwezig in extracellulaire matrixeiwitten zoals bijvoorbeeld vitronectine, fibrinogeen en laminine [1]. Er zijn verschillende kleine, RGD bevattende peptiden gesynthetiseerd die specifiek en met hoge affiniteit binden aan de $\alpha_v\beta_3$ integrine receptor.

Enkele onderzoeksgroepen hebben op systematische wijze de $\alpha_v\beta_3$-bindende eigenschappen van peptiden met de RGD sequentie getest. Het bleek dat lineaire RGD peptiden een relatief lage affiniteit voor $\alpha_v\beta_3$ hebben in vergelijking met cyclische RGD peptiden. Bovendien worden lineaire RGD peptiden in serum relatief snel door proteases afgebroken. Daarom zijn lineaire RGD peptiden niet optimaal voor targeting van $\alpha_v\beta_3$. Cyclische RGD peptiden daarentegen hebben over het algemeen een hogere selectiviteit en affiniteit voor het $\alpha_v\beta_3$ integrine. Met name de cyclische RGD peptiden die bestaan uit vijf aminozuren hebben een hoge en selectieve affiniteit voor $\alpha_v\beta_3$. Verder is gebleken dat naast de essentiële RGD sequentie, een hydrofoob aminozuur op positie 4 leidt tot een verhoogde affiniteit [2]. Het door Kessler en medewerkers ontwikkelde *cyclo*[Arg-Gly-Asp-D-Phe-Val] (c[RGDfV]) is één van de meest actieve en selectieve $\alpha_v\beta_3$ integrine antagonisten (Figuur 1) [3]. Structuur-activiteit relatie studies van dit cyclische pentapeptide toonden aan dat vervanging van het aminozuur valine (V) door lysine (K), geen significante invloed had op de activiteit en selectiviteit. Aangezien de ε-amino groep van c[RGDfK] gemakkelijk gemodificeerd kan worden, is het cyclische pentapeptide c[RGDfK] een veel bestudeerd RGD peptide.

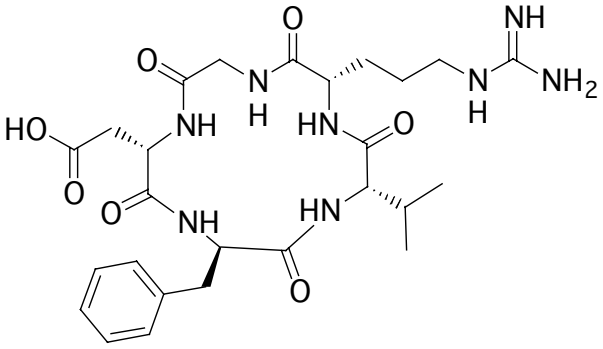

Figuur 1. Structuurformule van het cyclische RGD peptide c(RGDfV).

In **hoofdstuk 1** van dit proefschrift wordt een overzicht gegeven van verschillende gelabelde peptiden die ontwikkeld zijn voor medische toepassing. De volgende aspecten die van belang zijn bij het ontwikkelen van een radiopeptide worden besproken: de noodzakelijke eigenschappen van het peptide ligand, de selectie van het radionuclide en de chelator en de chemische aspecten die van belang zijn bij het ontwikkelen van een radiopeptide. Daarnaast wordt in dit hoofdstuk de klinische toepassing van enkele radiopeptiden voor diagnose en therapie van tumoren beschreven.

In **hoofdstuk 2** is geprobeerd om RGD analoga met verbeterde $\alpha_v\beta_3$-bindende eigenschappen te ontwikkelen. Daarvoor zijn, naast de referentie stof c(RGDfK), drie verschillende analoga gesynthetiseerd: (I) een cyclisch hybride van een peptoïde en een peptide waarvan het arginine residu is vervangen door het overeenkomstige peptoïde residu, (II) een peptoïde waarin alle aminozuur residuen zijn vervangen door de overeenkomstige peptoïde residuen, en (III) een peptidomimeticum. Alle verbindingen werden geconjugeerd met DOTA en radioactief gelabeld met ^{111}In. Vervolgens werden in vitro en in vivo de $\alpha_v\beta_3$-bindende eigenschappen van de gelabelde liganden bepaald.

In deze studie bleek het omzetten van het cyclische RGD peptide in een hybride te leiden tot een sterk verlaagde affiniteit voor het $\alpha_v\beta_3$ integrine en een lagere opname van de verbinding in de tumor. Het peptoïde had geen affiniteit voor het $\alpha_v\beta_3$ integrine en vertoonde dan ook geen specifieke opname in de tumor. In vitro vertoonden het peptidomimeticum en het cyclische RGD peptide de hoogste affiniteit voor het $\alpha_v\beta_3$ integrine. Het natieve cyclische RGD peptide en het peptidomimeticum vertoonden ook in het muizenmodel de hoogste opname in de tumor. Beide verbindingen vertoonden echter ook een hoge opname in verschillende normale weefsels zoals dunne darm, dikke darm, lever en milt. Coinjectie van de radioactief gelabelde stof met een overmaat niet-radioactief gelabelde stof resulteerde in een significant lagere opname van het betreffende ligand in deze normale weefsels, waaruit blijkt dat de opname van deze liganden in deze weefsels $\alpha_v\beta_3$-gemedieerd is. De nieropname van het ^{111}In-gelabelde natieve RGD peptide en het peptidomimeticum bleek niet $\alpha_v\beta_3$-gemedieerd.

Multivalente interacties zouden de affiniteit van een ligand voor zijn receptor kunnen verhogen. Mogelijk zouden multivalente RGD peptiden een hogere affiniteit voor het $\alpha_v\beta_3$ integrine kunnen hebben en daardoor $\alpha_v\beta_3$-expresserende tumoren efficiënter kunnen targeten. Het doel van de studies beschreven in **hoofdstuk 3** was door multimerisatie van RGD peptiden de tumoropname van RGD peptiden te verbeteren. Daarvoor werden een DOTA-geconjugeerd monomeer, dimeer en tetrameer RGD peptide gesynthetiseerd en radioactief gelabeld met ^{111}In. In vitro bleek dat multimerisatie van c(RGDfK) resulteerde in een verhoogde affiniteit voor het $\alpha_v\beta_3$ integrine. In naakte muizen met subcutane $\alpha_v\beta_3$-positieve tumoren was de opname van het tetramere RGD peptide in de tumor hoger dan dat van het dimere en monomere RGD peptide. De afstand tussen de RGD eenheden is te kort om te veronderstellen dat meerdere RGD eenheden van een multivalent construct gelijktijdig aan verschillende $\alpha_v\beta_3$ integrine receptoren binden. De meest voor de hand liggende verklaring voor de verhoogde affiniteit van multimere RGD peptiden voor $\alpha_v\beta_3$ is derhalve dat de multivalente constructen een verhoogde kans hebben dat het ligand opnieuw bindt aan de $\alpha_v\beta_3$ receptor. Met andere woorden: de binding aan de $\alpha_v\beta_3$ receptor van één RGD eenheid zal de locale concentratie van RGD eenheden aan het celoppervlak verhogen. Dit resulteert in een hogere associatiesnelheid van het RGD multimeer.

Multimere RGD peptiden kunnen ook op een andere manier gesynthetiseerd worden. In **hoofdstuk 4** wordt de synthese van een serie multimere RGD peptiden op basis van dendrimeren beschreven. Dendrimeren zijn macromoleculen die opgebouwd zijn uit volledig vertakte monomeren.

In dit hoofdstuk wordt de synthese van een monomeer, dimeer en een tetrameer c(RGDfK) dendrimeer beschreven. Deze dendrimeren zijn gesynthetiseerd via een magnetron-geïnduceerde 1,3-dipolaire cycloadditie reactie van dendrimere alkynen met het *N*-ε-azido derivaat van c(RGDfK). Deze reactie wordt ook wel een „click reactie" genoemd. In vitro vertoonde de tetramere dendrimeer een verhoogde affiniteit voor $\alpha_v\beta_3$ integrine ten opzichte van het monomere en dimere dendrimeer. Zowel 2 als 24 uur na injectie vertoonde het tetramere RGD dendrimeer in muizen met subcutane SK-RC-52 tumoren een significant hogere opname in de tumor dan het monomere en dimere dendrimeer.

In **hoofdstuk 5** is op systematische wijze het effect van de linker tussen de twee RGD eenheden en de DOTA chelator op de in vitro en in vivo eigenschappen van een dimeer RGD peptide onderzocht. Het dimere RGD peptide werd óf direct met DOTA (natieve ligand) óf via verschillende linkers (PEG_4, glutaminezuur of lysine) geconjugeerd (Figuur 2). De in vivo kinetiek van het dimere RGD peptide bleek afhankelijk van de aard van de linker, terwijl de affiniteit voor $\alpha_v\beta_3$ niet afhankelijk bleek van de linker. Het RGD peptide met de lysine linker had een significant hogere opname in de nieren vergeleken met het natieve ligand en het RGD peptide met de glutaminezuur linker. Deze laatste vertoonde echter een significant hogere opname in de lever vergeleken met het natieve ligand en het RGD peptide met de lysine linker.

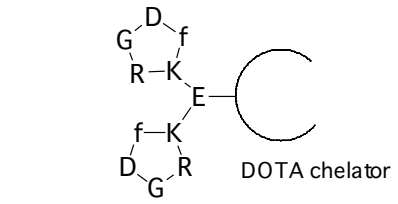

dimeer RGD peptide

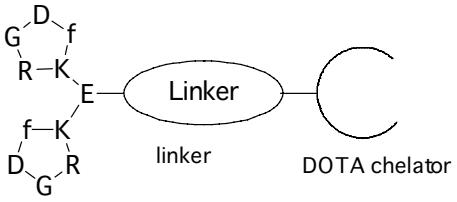

dimeer RGD peptide

Figuur 2. Schematische weergave van het dimere RGD peptide geconjugeerd met de DOTA chelator (boven) en het dimere RGD peptide geconjugeerd met de DOTA chelator via een linker (onder).

De linker tussen het peptide en de chelator, kan de retentie van het radiofarmacon in de normale organen beïnvloeden, hetgeen belangrijk is voor peptide receptor radionuclide therapie. Hierbij is niet alleen een hoge opname van het radiofarmacon in de tumor essentieel, maar is ook van belang dat het radiofarmacon weinig retentie in de nieren vertoont. In deze studie hadden het natieve peptide en het peptide met de PEG_4 linker de meest gunstige eigenschappen.

In **hoofdstuk 6** werd de tumortargeting van een ^{111}In-gelabeld cyclisch RGD peptide bestudeerd in een model van intraperitoneaal (i.p.) groeiende ovariumtumoren in naakte muizen. Het ^{111}In-gelabelde RGD peptide bleek na i.p. toediening zeer efficiënt te accumuleren in i.p. groeiende OVCAR-3 tumoren.

Uit deze studies bleek dat de toedieningsroute van radioactief gelabelde peptiden een belangrijke invloed heeft op het targeten van i.p. groeiende tumoren. Twee uur na i.p. injectie was de accumulatie van het peptide in de tumor meer dan 30 keer hoger dan na intraveneuze (i.v.) toediening. Bovendien accumuleerde het peptide efficiënter in i.p. groeiende tumoren dan in subcutaan (s.c.) groeiende tumoren: na i.p. toediening van het peptide was de accumulatie in i.p. groeiende tumoren meer dan 15 keer hoger dan in s.c. groeiende tumoren. Vanwege de efficiënte tumortargeting door dit peptide, zijn de therapeutische mogelijkheden van dit peptide

onderzocht. De overleving van de muizen met het i.p. groeiende ovariumcarcinoom verbeterde inderdaad door behandeling met het ^{177}Lu-gelabelde RGD peptide.

Peptide receptor radionuclide therapie (PRRT) met $\alpha_v\beta_3$-bindende peptiden zou een alternatief kunnen zijn voor radioimmunotherapie (RIT) met behulp van antilichamen, omdat peptiden voor het targeten van tumoren betere eigenschappen hebben dan antilichamen: ze zijn over het algemeen niet immunogeen, accumuleren snel in tumoren en klaren snel uit de circulatie en normale weefsels.

In de afgelopen jaren zijn een aantal goede radiofarmaca voor de visualisatie van $\alpha_v\beta_3$-expressie in tumoren met behulp van SPECT (single photon emission computed tomography) of PET (positron emission tomography) ontwikkeld. [^{18}F]Galacto-RGD was het eerste $\alpha_v\beta_3$-bindende radiofarmacon dat in klinische studies is toegepast.

Potentiële toepassingsgebieden van radioactief gelabelde $\alpha_v\beta_3$-bindende liganden zijn het visualiseren van angiogenese in tumoren, het detecteren van snel groeiende en metastaserende tumoren en wellicht ook het selecteren van patiënten die baat zouden kunnen hebben bij de behandeling met antiangiogene geneesmiddelen.

Referenties

1. Plow EF, Haas TA, Zhang L, Loftus J, Smith JW. Ligands binding to integrins. J Biol Chem 2000; 275:21785-8.
2. Haubner R, Gratias R, Diefenbach B, Goodman SL, Jonczyk A, Kessler H. Structural and functional aspects of RGD-containing cyclic pentapeptides as highly potent and selective integrin $\alpha_v\beta_3$ antagonists. J Am Chem Soc 1996;118: 7461-7472.
3. Aumailley M, Gurrath M, Muller G, Calvete J, Timpl R, Kessler H. Arg-Gly-Asp constrained within cyclic pentapeptides. Strong and selective inhibitors of cell adhesion to vitronectin and laminin fragment P1. FEBS Lett 1991;291:50-4.

Curriculum vitae

Curriculum vitae

Ingrid Dijkgraaf werd geboren op 22 mei 1979 te Epe. Na het behalen van het VWO diploma aan RSG De Springborn te Epe begon zij in 1997 met de studie Moleculaire Wetenschappen aan Wageningen Universiteit. In 1998 werd het propaedeutisch examen gehaald. Het doctoraal examen werd in 2002 gehaald met als hoofdrichting Organische Chemie in de werkgroep van Prof. dr. Æ. de Groot. Na deze hoofdrichting werd een onderzoeksstage uitgevoerd bij de afdeling Organische Chemie aan de Katholieke Universiteit Nijmegen in de werkgroep van Dr. J.W. Scheeren.

In 2002 werd zij aangesteld als junior onderzoeker bij de afdeling Nucleaire Geneeskunde (Prof. dr. F.H.M. Corstens) van het Universitair Medisch Centrum Sint Radboud te Nijmegen in samenwerking met de afdeling Medicinal Chemistry and Chemical Biology (Prof. dr. R.M.J. Liskamp) van Universiteit Utrecht. Tijdens deze onderzoeksperiode zijn verschillende RGD peptiden en peptidomimetica gesynthetiseerd, radioactief gelabeld en in vitro en in vivo geëvalueerd. De resultaten van het onderzoek zijn beschreven in dit proefschrift.

List of publications

List of publications

Dijkgraaf I, Rijnders AY, Soede A, Dechesne AC, van Esse GW, Brouwer AJ, Corstens FHM, Boerman OC, Rijkers DTS, Liskamp RMJ. Synthesis of DOTA-conjugated multivalent cyclic-RGD peptide dendrimers via 1,3-dipolar cycloaddition and their biological evaluation: implications for tumor targeting and tumor imaging purposes. *Org Biomol Chem* 2007; in press.

Dijkgraaf I, Boerman OC, Oyen WJ, Corstens FH, Gotthardt M. Development and application of peptide-based radiopharmaceuticals. *Anticancer Agents Med Chem* 2007; in press.

Dijkgraaf I, Kruijtzer JA, Liu S, Soede AC, Oyen WJ, Corstens FH, Liskamp RM, Boerman OC. Improved targeting of the $\alpha_v\beta_3$ integrin by multimerization of RGD peptides. *Eur J Nucl Med Mol Imaging* 2007;34:267-273.

Dijkgraaf I, Kruijtzer JA, Frielink C, Corstens FH, Oyen WJ, Liskamp RM, Boerman OC.$\alpha_v\beta_3$ Integrin targeting of intraperitoneally growing tumors with a radiolabeled RGD peptide. *Int J Cancer* 2007;120:605-610.

Dijkgraaf I, Liu S, Kruijtzer JA, Soede AC, Oyen WJ, Liskamp RM, Corstens FH, Boerman OC. Effects of linker variation on the in vitro and in vivo characteristics of an ^{111}In-labeled RGD peptide. *Nucl Med Biol* 2007;34:29-35.

Dijkgraaf I, Kruijtzer JA, Frielink C, Soede AC, Hilbers HW, Oyen WJ, Corstens FH, Liskamp RM, Boerman OC. Synthesis and biological evaluation of potent $\alpha_v\beta_3$ integrin receptor antagonists. *Nucl Med Biol* 2006;33:953-961.

Gotthardt M, Dijkgraaf I, Boerman OC, Oyen WJ. Nuclear medicine imaging and therapy of neuroendocrine tumours. *Cancer Imaging* 2006;6:S178-184.

Janssen ML, Frielink C, Dijkgraaf I, Oyen W, Edwards DS, Rajopadhye M, Massuger L, Corstens F, Boerman O. Improved tumor targeting of radiolabeled RGD peptides using rapid dose fractionation. *Cancer Biother Radiopharm* 2004;19:399-404.

Janssen M, Oyen WJ, Massuger LF, Frielink C, Dijkgraaf I, Edwards DS, Radjopadhye M, Corstens FH, Boerman OC. Comparison of a monomeric and a dimeric radiolabeled RGD-peptide for tumor targeting. *Cancer Biother Radiopharm* 2002;17:641-646.

Janssen ML, Oyen WJ, Dijkgraaf I, Massuger LF, Frielink C, Edwards DS, Rajopadhye M, Boonstra H, Corstens FH, Boerman OC. Tumor targeting with radiolabeled alpha(v)beta(3) integrin binding peptides in a nude mouse model. *Cancer Res* 2002;62:6146-6151.

Dankwoord

Dankwoord

De mensen die aan de totstandkoming van dit proefschrift hebben bijgedragen zou ik graag willen bedanken:

Als eerste wil ik mijn copromotor Dr. O.C. Boerman en mijn promotores Prof. dr. R.M.J. Liskamp, Prof. dr. F.H.M. Corstens en Prof. dr. W.J.G. Oyen bedanken voor de mogelijkheid die zij mij hebben gegeven om aan dit multidisciplinaire promotieonderzoek te kunnen beginnen.

Beste Otto, jouw enthousiasme, gedrevenheid en positieve instelling zijn onmisbaar voor een promovendus. Het meerdere malen luisteren naar een oefenpresentatie, de snelle correcties van manuscripten en het altijd binnen kunnen lopen voor vragen heb ik altijd zeer gewaardeerd. Hartelijk dank daarvoor.

Beste Rob, door u kon ik op gesprek komen toen er een samenwerkingsproject Nijmegen-Utrecht op tafel lag. Uw enthousiasme en nieuwe ideeën voor de synthese van liganden zijn zeer gemotiverend, bedankt voor alle hulp en begeleiding.

Beste Frans, door uw steun en het vertrouwen dat u in mij stelde, kon ik dit proefschrift afronden. Hartelijk dank voor uw begeleiding en adviezen.

Beste Wim, uw snelle correcties van manuscripten zorgden ervoor dat de vaart erin bleef, bedankt voor het vertrouwen en de begeleiding.

Verder wil ik graag de collega's bedanken die mij geholpen hebben op het laboratorium.
John Kruijtzer, je bijdrage aan dit proefschrift is groot. Dankzij jouw begeleiding en adviezen heb ik verschillende peptiden en peptidomimetica kunnen synthetiseren. Hartelijk dank daarvoor.

Dirk Rijkers, jouw idee om cyclische RGD peptiden aan de dendrimeren te koppelen heeft in een prachtig hoofdstuk geresulteerd. Bedankt voor al je hulp en vriendschap.

Hans Hilbers, Johan Kemmink, Hans Ippel en Annemarie Dechesne bedankt voor de molecular modelling en het meten en analyseren van de diverse NMR- en massaspectra.

Cathelijne Frielink jouw "coupe werk" is fenomenaal, bedankt voor je inzet en hulp. Annemieke Soede, hartelijk dank voor al je hulp bij menig experiment. Anneloes Rijnders, ook jouw bijdrage aan dit proefschrift is aanzienlijk, bedankt.

In addition, I would like to thank Prof. dr. Shuang Liu for his contribution to this project.

De in dit proefschrift beschreven dierexperimenten waren niet mogelijk geweest zonder de deskundige assistentie van de mensen van het centraal dierenlaboratorium. Gerry Grutters, Hennie Eikholt, Bianca Lemmers, Iris Lamers, Maarten Blom en Connie Verbaas bedankt voor al jullie hulp en flexibiliteit wanneer ik weer eens wat later dan het afsproken tijdstip op het CDL was, fantastisch!

Sandra Dahm, Natatia Lobato, Paula Pereira en Jacqueline van Rens bedankt voor jullie secretariële bijdrage!

De collega's van de afdeling Medicinal Chemistry wil ik bedanken voor de collegialiteit, hulp en plezier op de afdeling en daarbuiten. Het was altijd weer gezellig om in het Went werkzaam te zijn, ook nadat ik weer een lange tijd in Nijmegen werkzaam was geweest.

Mede-aquariumbewoners van de afdeling Nucleaire Geneeskunde, Huub Rennen, Peter Laverman, Julliëtte van Eerd, Martin Gotthardt, Frits Aarts, Manuel Koppe en Frank van Schaijk, bedankt voor de prettige samenwerking en gezelligheid op de werkvloer en erbuiten. De collega's van de afdeling Nucleaire Geneeskunde, hartelijk dank voor de prettige werksfeer, behulpzaamheid en gezelligheid.

Maaike Joerink en Jolanda Lambert, het is altijd erg gezellig als we samen zijn. Jullie zorgen voor de nodige ontspanning en plezier, bedankt voor alles.

Lieve pa en ma, jullie staan altijd voor me klaar en hebben me altijd vrijgelaten in mijn keuzes, bedankt voor jullie goede zorgen en onvoorwaardelijke steun.

Lieve Vasco, bedankt voor alles wat je voor me bent en voor me doet.